NOVEL APPLICATIONS OF ZEIN NANOPARTICLES

by

Christopher J. Cheng

A Dissertation

Submitted to the Faculty of Purdue University

In Partial Fulfillment of the Requirements for the degree of

Doctor of Philosophy

Department of Food Science

West Lafayette, Indiana

December 2018

THE PURDUE UNIVERSITY GRADUATE SCHOOL
STATEMENT OF COMMITTEE APPROVAL

Dr. Owen Jones, Chair
Department of Food Science
Dr. Bruce Hamaker
Department of Food Science
Dr. Mario Ferruzzi
Department of Food Science
Dr. Brian Degner
Research Fellow of ConAgra
Dr. Jen-Yi Huang
Department of Food Science

Approved by:

Dr. Arun Bhunia
Head of the Graduate Program

To My Parents

For their Unconditional Love and Support

ACKNOWLEDGMENTS

I would like to acknowledge Dr. Owen Jones for his guidance and advice throughout my graduate career. I have learned a great deal from him about what it is to be a true scientist. Next, I would like to thank my committee members: Dr. Bruce Hamaker, Dr. Mario Ferruzzi, Dr. Brian Degner, and Dr. Jen-Yi Huang. Their insight and support were much appreciated. I am thankful for my friends and lab mates who created a fun enjoyable atmosphere in graduate school. Finally, I would like to thank my family for their unwavering support and showing me while growing up the value of dedication for the unending pursuit of greater knowledge.

TABLE OF CONTENTS

LIST OF TABLES

LIST OF FIGURES

ABSTRACT

Author: Cheng, Christopher, J. PhD
Institution: Purdue University
Degree Received: December 2018
Title: Novel Applications for Zein Nanoparticles
Committee Chair: Owen Jones

Zein is major nitrogen storage protein that accounts for nearly half of the protein content of the corn grain. As a byproduct of starch and ethanol processing, it is generally recognized as safe (GRAS) and soluble in up to 70% ethanol. Historically, zein has been used for films and coatings. However, usage of the corn protein has diminished in recent years. New advances in food nanotechnology has renewed interest in zein. By forming the protein into stable nanoparticles capable of being dispersed in aqueous solution, zein can be used in many applications ranging from improving stability and digestion of functional ingredients or active biodegradable packaging. Developing novel applications for this protein would then add value to a waste product during the processing of corn.

The formation of hydrophobic zein nanoparticles (ZNPs) would allow for easier dispersion in aqueous systems without further modification to increase hydrophilicity. However, their dispersibility and subsequent stability in aqueous systems is important for its functionality in food. Addition of sufficient ι-carrageenan (ι-CGN) prevented aggregation in the pH range of 5.25 to 6.75 and limited aggregation at pH 7.0. Enhanced stability was attributed to the adhesion of ι-CGN to the nanoparticle surface, as the ZNPs surface charge became significantly negative with introduction of ι-CGN. These particles remained stable for up to 30 days with significantly lower turbidity and greater resistance to gravitational separation when compared to ZNPs alone.

Lutein was encapsulated in zein nanoparticles, and the bioaccessibility was determined by quantifying lutein content after exposure to *in vitro* gastric and intestinal conditions. It was found that ZNPs provided a protective environment for lutein in aqueous dispersions and would release the carotenoid into the small intestine by rapid breakdown of ZNP structure during intestinal digestion. However, the process or residual components must have limited uptake of lutein into mixed micelles. ZNPs can be a promising encapsulating agent to improve the digestive stability of lutein.

Composite films composed of methylcellulose (MC) and zein nanoparticles (ZNPs) were prepared as a potential biodegradable alternative for synthetic packaging. The effects of ZNP aggregation on mechanical and moisture barrier properties as affected by drying temperature, pH, and stabilizers were tested. The phase separation of composite films was determined to be detrimental to both its mechanical and moisture barrier properties. The drying temperature, pH, and composition of the solvent casting solution all affected the distribution of ZNPs dispersed in MC films. Drying films at 23°C or setting the pH to 6.5 resulted in ZNP aggregation and weaker, brittle films that were poor moisture barriers. The presence of CGN was able to provide stability to ZNPs at both pH 4 and 6.5, thus improving its mechanical and moisture barrier properties.

CHAPTER 1 BACKGROUND AND OBJECTIVES

1.1 Zein

Zein is a protein found in corn that is used to store nitrogen for the seedling. The protein content for corn ranges from 6-12% on a dry weight basis, half of which is zein (Shukla and Cheryan 2001; Patel and Velikov 2014b). It is a water insoluble protein and classified as generally recognized as safe (GRAS) by the Food and Drug Administration (Patel and Velikov 2014b). This protein is hydrophobic and only soluble in up to 70% ethanol, some organic acids like acetic acid, or high alkaline (pH >11) solutions.

1.1.1 Production

About 560 million tons of corn is produced in the world in a year, half of which is grown in the United States (Shukla and Cheryan 2001). Harvested corn is processed to separate the components into starch, oil, and gluten meal. The starch from the endosperm is largely used for producing food sweeteners and ethanol. Oil extracted from the germ can be used for cooking oil (Anderson and Lamsal 2011). Nearly all of zein will be found in the gluten meal which is currently used as animal feed in the United States (Shukla and Cheryan 2001). After corn is milled, zein is extracted from corn gluten meal typically with a polar solvent like ethanol or isopropanol. A non-polar solvent like hexane is then used to extract any impurities such as pigments and residual lipids (Shukla and Cheryan 2001). Developing applications for this prolamin would add value to these processing waste streams.

1.1.2 Structure

There are four types of zein found in corn: alpha, beta, gamma, and delta (Shukla and Cheryan 2001). Alpha zein is the most abundant form at about 35% of total zein and is most soluble in 95% ethanol. Beta zein is most soluble in 60% ethanol and is less stable (Shukla and Cheryan 2001). SDS-PAGE analysis of alpha zein shows 2 distinct bands at 24 and 22 kDa, while beta-zein reveals three bands at 24 kDa, 22kDa and 14 kDa (Shukla and Cheryan 2001). SDS-PAGE of gamma zein typically shows an additional band at 9.6 kDa (Paulis 1981). Gamma zein only constitutes 5-10% of the total zein content, and it is unique in that over a quarter (25.8%) of its amino acid composition is proline.

The structure of zein in corn has been described by Argos (Shukla and Cheryan 2001; Argos and others 1982) as an aggregated structure stabilized by disulfide bonds with an average molecular weight of 44 kDa. The secondary structure of zein also changes in various solvents. It was found that in aqueous ethanol, the protein is not completely soluble and behaves like a swollen colloid in solution, which indicates that zein still isn't completely soluble in typical good prolamin solvents (Li and others 2012b). The amino acid sequence of zein is high in glutamic acid, leucine, proline, and alanine, which contributes to its overall hydrophobicity. It is also deficient in the essential amino acids lysine and tryptophan, making it a poor nutrient source, by itself.

1.2 Applications

1.2.1 Historic Commercial Applications of Zein

Historically, zein has been mainly used as a coating and binding agent (Lawton 2002). During World War II, zein was mainly used as a replacement for shellac, a material used in many coatings and varnishes. After the war, zein in combination with rosin and fatty acids was coated onto paper packaging to improve its grease and moisture barrier properties (Anderson and Lamsal 2011). The corn prolamin has also been used as a binding agent, particularly for adhering pigments and inks to paper. In addition to binding ink, the corn protein was used as an adhesive for composition cork and chewing gum (Lawton 2002). In the pharmaceutical industry, zein was an alternative to sugar as a tablet coating (Shukla and Cheryan 2001). Similar coatings were also used in the food industry to coat products like rice, confectionary, and nuts.

In the 1950's the creation of cheaper synthetic materials largely replaced zein in many applications (Lawton 2002). In the 1990's zein usage was mostly limited to pharmaceutical coatings or feed for livestock (Shukla and Cheryan 2001; Reiners and others 1972). However, the recent rapid growth of the nanotechnology sector in the food industry has renewed interest in using zein in new potential applications. In 2004, the nanotechnology sector of the food industry was valued at $860 million (Sozer and Kokini 2009). By forming the corn protein into stable nanoparticles capable of being dispersed in aqueous solution, zein can be used in many applications ranging from active biodegradable packaging or improving stability and digestion of functional ingredients.

1.2.2 Zein Nanotechnology

Nanoparticles are colloidal structures with dimensions ranging from 1 to 100 nm in diameter. In food, these are typically assembled from proteins, polysaccharides, or lipids (He and Hwang 2016). Biopolymer nanoparticles typically have unique properties that differ from the same bulk polymer (Sekhon 2010). For example, bulk zein is insoluble in water, but forming them into zein nanoparticles (ZNPs) allows the protein to be dispersed in water. Although the protein is still insoluble, ZNPs can remain small enough that it remains evenly dispersed and to provide functionality.

1.2.3 Applications of Zein Nanoparticles (ZNPs)

The formation of hydrophobic zein into nanoparticles would allow for easier dispersion in aqueous systems without further modification to increase hydrophilicity. One application for zein nanoparticles would be to incorporate them into solvent cast packaging material to make nanocomposites. Nanocomposite materials can be stronger, have better barrier properties, or have active properties like deliver antimicrobials (Akbari and others 2007; Rhim and others 2013). Another application for ZNPs would be to encapsulate functional or bioactive compounds such as flavors, nutraceuticals, and antimicrobials. The encapsulating agent can then improve the stability or target the delivery of the functional ingredient. The hydrophobic nature of zein allows it to associate with lipophilic functional ingredients such as resveratrol (Davidov-Pardo and others 2015c), curcumin (Gomez-Estaca and others 2012; Hu and others 2015), and various antimicrobial essential oils (Chen and Zhong 2015b; Wu and others 2012). Encapsulating these bioactive compounds into zein nanoparticles can effectively allow for easy dispersion in water while controlling their release into the digestive system once consumed.

1.2.4 Producing Zein Nanoparticles

Formation of ZNPs can be done by dispersing the hydrophobic zein in water. It can also increase the protein content in a dispersion without increasing viscosity. ZNPs are formed from the antisolvent precipitation method as outlined by Zhong et al (Zhong and Jin 2009). The protein is first solubilized in an 80% ethanol solution. It is then homogenized into water where the zein/ethanol solution is sheared into small droplets. Once the water to ethanol ratio of the solution reaches a critical limit, the solubility of zein plummets and it precipitate to form spherical nanoparticles. Factors such as the starting concentration of zein, ethanol, or the shear rate of the

homogenizer would affect the final size of the nanoparticles (Zhong and Jin 2009). Higher concentrations of ethanol results in a smaller final particle size. It is thought that the greater ethanol concentration allows the homogenizer to shear the solution into smaller droplets before the concentration of ethanol drops below the critical point where zein precipitates into nanoparticles (Zhong and Jin 2009). Increasing starting zein concentration has the opposite effect of increasing final particle size by increasing the viscosity of the mixture. Ideally, the antisolvent precipitation method should produce zein nanoparticles of similar size. It has been found that the ideal concentration of zein is 2-5% (Patel and others 2010a).

Another developed antisolvent precipitation method used propylene glycol as the solvent and low shear dispersion into the antisolvent. This replacement of ethanol is beneficial because it cannot be used in non-alcoholic food products (Chen and Zhong 2015b).There have been other methods of synthesizing zein nanoparticles. Electrohydrodyanmic atomization has been used to create spherical particles of relatively uniform size that were stable for up to 3 months (Gomez-Estaca and others 2012).

1.2.5 Challenges of Using Zein in the Food Industry

There are many challenges in utilizing zein in food systems. Zein nanoparticles are susceptible to flocculation, which is a destabilizing mechanism that is driven by random Brownian motion. When particles remain small, random motion and the viscosity of the continuous phase can respectively prevent and slow the settling of particles. However, attractive van der Waal forces of particles in a dispersion can cause these particles in the dispersed phase randomly collide and adhere together forming a larger particle (Dickinson 2003). If this process continues, the particles become large enough to overcome Brownian forces and form a sediment that gets pulled out of dispersion through gravity. There are many approaches to prevent or slow down flocculation. One way is to increase the surface viscosity of the system to slow down the movement of particles. Another way is to coat the particles with charged or large soluble molecules. Electrostatic repulsion and steric hindrance would prevent two particles from moving close enough together to aggregate and maintain a small particle size (Dickinson 2003). Carbohydrates are a good candidate to provide both steric and electrostatic stability.

Zein has an isoelectric point at about pH 6.2 so it is more likely to aggregate at neutral pH ranges. The nanoparticle form of the protein is susceptible to aggregation by simply changing the pH or the ionic strength of the solvent (Patel and others 2010b). Another major challenge is that

due to their hydrophobic properties, lyophilizing these particles will cause them to agglomerate and are poorly redispersed into water (Patel and Velikov 2014b). One way to overcome these issues is to stabilize the system electrosterically with other biopolymers.

1.3 Protein and Polysaccharides Interactions

1.3.1 Intermolecular Forces

Polymers in solution can interact with each other with a variety of different attractive and repulsive forces. The weakest force are Van der Waal forces which are weak attractive forces between two non-polar molecules (Liang and others 2007). The next weakest interaction are hydrophobic forces. This association of hydrophobic polymers is driven by entropy. In solution, all hydrophobic molecules would associate together in order to minimize the interfacial area of a hydrophobic and hydrophilic molecule (Liang and others 2007). Hydrogen bonding interactions are the next strongest force. Hydrophillic molecules contain highly electronegative atoms which creates asymmetry in the electron clouds called dipoles such as a hydroxyl or amine group. This asymmetry allows hydrogen bond donors to form weak bonds with hydrogen bond acceptors. Finally, ionic interactions occur when molecules electrostatically attract or repel due to charged atoms (Hu and others 2012b). Polysaccharides contain many hydroxyl groups and are typically hydrophilic. Some varieties such as carrageenan contained charged groups and can bind electrostatically (Galazka and others 1999). Proteins can participate in all types of interactions depending on its amino acid composition.

1.3.2 Protein Polysaccharide Interactions

A protein and polysaccharide in solution can interact by multiple mechanisms. Segregative phase separation occurs when there is a lack of intermolecular interactions between protein and polysaccharides (Figure 1). They subsequently partition into two separate phases with each phase containing one of the two of polymers (Dickinson 1998). Associative phase separation occurs when intermolecular interactions are so strong they form insoluble complexes and precipitate out of solution. Phase separation then occurs where one phase contains the majority of both the polymers in the solution. When there are intermediate levels of interactions, between both proteins and polysaccharides both polymers remain dispersed in the solvent and a relatively stable sol forms

in a single phase in the system. The polymers can be either cosoluble or associate together and form soluble complexes (Dickinson 2003).

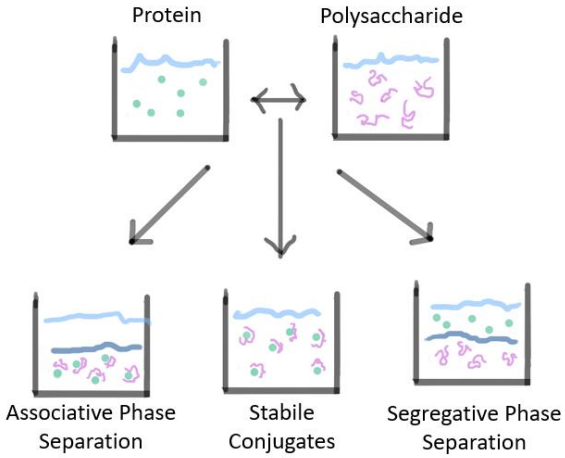

Figure 1 Protein Polysaccharide interactions

1.3.3 Stabilizing ZNPs with Polysaccharides

Biopolymers such as carbohydrates and proteins are commonly used to stabilize colloidal particles in dispersion. ZNPs stabilized by caseinate and maillard conjugates of casein and dextran were both able to provide stability in both various pH ranges and at high ionic strength (Davidov-Pardo and others 2015a; Patel and others 2010b). However, a major drawback is that the ZNPs would still be unstable at the stabilizer protein's isoelectric point and at low pH when it denatures (Chen and Zhong 2015b). Carbohydrates can potentially overcome the limitations of proteins by complexing ZNP with carbohydrates through electrostatic or polar interactions (Cheng and Jones 2017; Hu and others 2015). The polysaccharide coating can cause electrostatic and/or steric repulsion of ZNPs.

It has been found that addition of polymers like alginate, sodium caseinate, carboxymethyl-chitosan, gum Arabic, and pectin are effective stabilizers (Liang and others 2015; Luo and others 2012; Davidov-Pardo and others 2015b; Hu and McClements 2015). Gum Arabic, an anionic polysaccharide that is naturally conjugated with hydrophobic proteins, has been found to improve the stability of ZNP from pH 4-8 and in salt concentrations up to 50 mM (Chen and Zhong 2015b). Pectin, an anionic polysaccharide has improved stability at lower pH levels and in salt concentrations up to 200 mM, but failed to stabilize ZNPs at the isoelectric point of the prolamin (Huang and others 2016). This was attributed to pectin's relatively low charge density, so alginate another anionic polysaccharide with higher charge density was used in a follow up study. A

mixture of alginate and pectin was found to improve stability at pH 5-7 and better salt stability up to 2M, but alginate alone caused immediate precipitation of ZNPs due to its strong interactions with the protein (Huang and others 2016). Chitosan, a positively charged polymer has also been used as a stabilizing agent. Various modified chitosan ingredients have been used to improve encapsulation efficiency of bioactive compounds and improve stability to UV light at an even wider pH range at levels from 2-11 (Liang and others 2015; Park and others 2015) When compared to proteins, carbohydrates generally can provide better stability at low pH levels, but they do not provide as much stability in high salt conditions.

Carrageenan is a sulfonated anionic polysaccharide derived from seaweed (Campo and others 2009). This polysaccharide has been shown to electrostatically interact with various proteins and form complex coacervates (Dickinson 2003; Galazka and others 1999; Stone and Nickerson 2012). Because the sulfate groups on carrageenan have a pKa of ~2 (Gu and others 2004), it has the potential to stabilize ZNPs by interacting with cationic residues on the ZNP surface and forming a negatively charged outer layer. Carrageenan has a relatively high charge density so it could potentially stabilize protein nanoparticles at a lower usage rate and over a wider pH range when compared to other anionic polysaccharides such as pectin (Dickinson 1998).

1.4 Improving Bioaccessibility of Bioactive Compounds with ZNPs

1.4.1 Encapsulation of Bioactive Compounds in Functional Foods

Functional foods are defined as foods that are consumed to provide health benefits outside of providing nutrition (Espin and others 2007). For example, ingesting bioactive carotenoids has been found in epidemiological studies to reduce the risk of cancer, heart disease, and degradation in eye health (Alves-Rodrigues and Shao 2004; Espin and others 2007; Maiani and others 2009). Other bioactive compounds include phenolic acids, flavonoids, and isoflavones (Espin and others 2007).

Encapsulation of bioactive compounds can be used to improve their functional properties such as improved resistance to environmental degradation, improved physical stability, controlled release into the environment, and masking undesirable flavors (Shahidi and Han 1993; McClements and others 2009; Zou and others 2017; Chuacharoen and Sabliov 2016a) Generally, encapsulation is done by complexing the desired bioactive with another compound such as a protein, a polysaccharide, a lipid, or a combination of the three (Shahidi and Han 1993;

McClements and others 2009). A variety of encapsulation structures can be created. Lipids can form many types of emulsions, micellar structures, or solid lipid particle dispersions (McClements and others 2009; Salvia-Trujillo and others 2013). Proteins and polysaccharides can form core shell particles and hydrogels (Luo and others 2012). These polymers can also be combined to form more complex particles, gels, or even covalently linked conjugates (Luo and others 2012; Davidov-Pardo and others 2015a). The type of encapsulating agent and structure to choose depends on the goals of the delivery system which can include loading efficiency, delivery efficiency, environmental protection, food matrix compatibility, and cost (McClements and others 2009).

Zein is a good candidate for encapsulating lipophilic bioactive compounds. The hydrophobic nature of zein allows it to encapsulate compounds that are not normally soluble in water. Zein has already been found to be able to encapsulate ingredients like resveratrol (Davidov-Pardo and others 2015c), tangeretin (Chen and others 2014b), curcumin (Gomez-Estaca and others 2012; Hu and others 2015), Lutein (Hu and others 2012b), and various antimicrobial essential oils (Chen and Zhong 2015b; Wu and others 2012).

1.4.2 Lutein

Lutein belongs to a class of compounds called carotenoids which are typically yellow, orange, and red organic pigments produced by plants, bacteria, and fungi. In the diet, lutein is commonly found in leafy green vegetables and corn. The molecular structure of lutein contains a long stretch of conjugated double bonds, which gives it the ability to absorb light and quench free radicals. Among the carotenoids, it is classified as a xanthophyll which contains two extra hydroxyl groups at the ends of the molecule resulting in a relatively more polar molecule (Reboul and others 2006). When consumed, lutein has many health benefits. It is thought to be an antioxidant in the human eye that helps prevent the formation of cataracts. It has also been found to lower the risk of coronary heart disease and stroke (Arnal and others 2009; Granado and others 2003). Despite the known health benefits for the consumption of lutein, the average daily intake in the United States is approximately 1.7 mg/day. The USDA and HHS recommend about 3.8 mg lutein intake per day (estimated from 5 servings of fruit and vegetables). An intake of 6-14 mg/day is associated with improved eye health (Alves-Rodrigues and Shao 2004).

In 2010, there were 2 million cases of age related macular degeneration in the United States, and that number is projected to increase to over 6.3 million by 2030 (NIH 2015). Additionally,

nearly 50% of Americans older than 75 years suffer from cataracts (Granado and others 2003). Increased consumption of lutein is associated with lower risk of these eye disorders as well as decreased risk of cardiovascular disease and many types of cancer (Granado and others 2003). However, the average daily intake in the United States is approximately half of the USDA and Department of Health and Human Services recommendation of about 3.8 mg lutein intake per day (Granado and others 2003).

There are two major challenges with increasing dietary lutein intake. Carotenoids in general are known to be susceptible to degradation in the presence of heat, oxygen, and light under processing, storage, and digestive conditions (Lin and Chen 2005; Tang and Chen 2000). The other major challenge is that carotenoids are poorly absorbed during digestion. It has been found that lutein in vegetables has fairly low bioaccessibility ranging from 14-55%, and much of it was passed through the digestive tract and unavailable for absorption (Serrano and others 2005).

Bioaccessibility is defined as the amount of nutrient present in the small intestine that is ready to be absorbed into epithelial cells. In contrast, bioavailability is the amount of a consumed nutrient absorbed by enterocytes, transported into the bloodstream, and available for physiological function (Garrett and others 1999; Yonekura and Nagao 2007). Bioaccessibility is typically measured using *in vitro* methods, and it is used as a screening method to predict bioavailability of a nutrient which is typically measured *in vivo* (Fernandez-Garcia and others 2009). *In vitro* methods are typically done in artificial vessals where the digesta is mixed with enzyme solution at a set pH. The vessal is then submerged in a shaking water bath for a set amount of time and temperature (Garrett and others 1999). Previous studies have suggested that bioaccessibility of carotenoids may be influenced by food matrix, amount of lipids consumed with carotenoids, size of lipid droplets, and lipase in the intestine (Hof and others 2000; Yonekura and Nagao 2007).

1.4.3 Zein Nanoparticle (ZNP) Encapsulation

Encapsulation of lutein into ZNPs is a promising technique to improve bioaccessibility, which may potentially help fortified foods achieve the desired health benefits with relatively lower carotenoid usage rate. It would simultaneously add value to zein, a waste product of corn processing. There is an inherent affinity of zein towards carotenoids. Yellow corn meal naturally contains lutein and other xanthophylls which have a bioaccessibility ranging from 50-60% (Kean and others 2008). Zein nanoparticles (ZNPs) can be formed by solubilizing zein in 80% aqueous

ethanol and then promoting their aggregation into nanoparticles by sudden exposure to large quantities of water (Zhong and Jin 2009). Developing an application for this protein byproduct would add value to a byproduct of starch and ethanol production thus reducing food waste.

Encapsulation of carotenoids into ZNPS has been shown to improve its digestive, photo oxidative, and storage stability (Chuacharoen and Sabliov 2016b; Chuacharoen and Sabliov 2016a). In addition to improving stability of carotenoids, ZNPs have been used to improve the bioaccessibility of other hydrophobic bioactive compounds. Curcumin was found to have a bioaccessibility of 33%, but it increased to 84% after encapsulation in ZNPs which was attributed to increased digestive stability (Wang and others 2016). Another study found that resveratrol micellarization was increased from ~60% to ~70% when encapsulated in ZNPs that have been conjugated with dextran in the presence of lecithin (Davidov-Pardo and others 2015c). To improve bioaccessibility of encapsulated lutein, it is necessary to investigate how ZNPs influence the digestion and absorption process.

1.4.4 Zein Digestibility

Zein is susceptible to enzymatic breakdown by both gastric and intestinal proteolytic enzymes. Pepsin has a broad specificity, but it prefers cleaving the peptide bonds of aromatic amino acids. It will also cleave the carboxyl side of leucine and glutamic acid but ignores alanine, valine, and glycine (Sweeney and Walker 1993). If a molecule of zein is cleaved at those sites, it is theoretically broken down into 55 different individual peptides and amino acids with molecular weights ranging from 131 Da to 1500 Da.

There is no prior evidence to indicate that zein is resistant to enzymatic digestion in intestinal conditions. A previous study has found that the fraction alpha zein in 100 mM NaCl was digested by pepsin within 30 minutes whereas gamma zein was not digested (Lee and Hamaker 2006). However, another study found that limited digestion of unstructured zein in gastric conditions was observed even after 60 min if 0.03 M sodium chloride was included (Fu and others 2002). Another study found that unstructured zein dispersions were digested within 5 min of intestinal conditions (Fu and others 2002). Other studies have shown that structuring of the zein may be important during gastric conditions, as zein nanoparticles formed in the presence of tween 20 and polyvinyl pyrrolidone, which aided their dispersion in the aqueous phase, were completely

digested within 60 minutes (Pepi Hurtado-López and Sudax) while digestibility among films of zein was reduced by ~25% (Matthews and others 2011).

There has been little research on the digestibility of protein nanoparticles. However, it is known that a protein's primary and quaternary structure affect its digestibility. It has been found that the presence of cysteine and disulphide bond formation in gamma zein significantly decreased pepsin digestibility when compared to alpha zein (Lee and Hamaker 2006). Protein solubility is also a significant factor. Cooked kafirin, the prolamin from sorghum, became less water soluble than uncooked kafirin and consequently decreased digestibility (Duodu and others 2003). The size of lipid colloidal structures has been found to affect digestibility. When the radius of lipid nanoparticles decreased, digestibility increased (Salvia-Trujillo and others 2017; Salvia-Trujillo and others 2013).

When evaluating the nutrition of zein, the prolamin has low protein quality compared to lactalbumin, gelatin, gliadin, casein, and soy protein. A greater amount of fecal nitrogen was recovered from rats with a diet high in zein which suggested less of the protein was absorbed (Keith and Bell 1988). This was attributed to low palatability and low dietary amino acid levels like lysine and tryptophan. However, *in vitro* studies have shown that the protein is susceptible to breakdown by both gastric and pancreatic enzymes (Pepi Hurtado-López and Sudax ; Duodu and others 2003).

1.4.5 Digestion and Bioaccessibility of Lutein

The digestion process of lutein is similar to lipids due to the lipophilic nature of carotenoids (Figure 2). Once food containing lutein is ingested, it passes through the mouth and stomach where it is physically broken down. To be bioaccessible, the carotenoids in the food must remain intact in the oral and gastric phase of the digestive process. In the small intestine, the lutein must then be released from the food matrix, and solubilized by accompanying lipids from the food and bile salts secreted from the gall bladder. Carotenoids are considered bioaccessible once they are incorporated into mixed micelles in the intestinal aqueous phase (Garrett and others 1999). When these mixed micelles are absorbed by enterocytes, they are considered bioavailable.

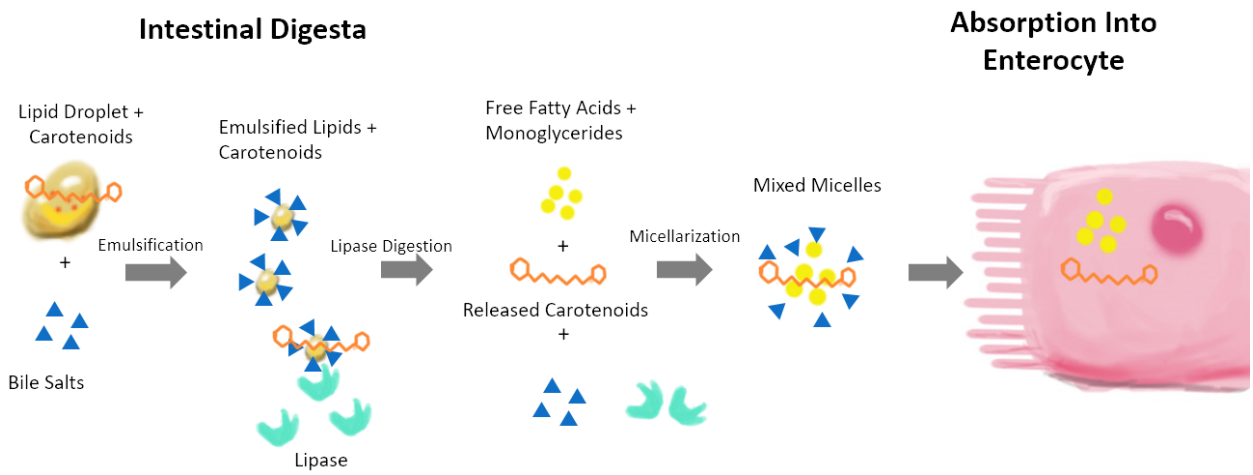

Figure 2: Digestion of Lipids Containing Carotenoids

1.4.5.1 Effect of the Food Matrix on Carotenoid Bioaccessibility

During the digestive process carotenoids must first be released from the surrounding matrix into the aqueous phase in the intestine (Yonekura and Nagao 2007). Undigested fractions of food like caroteno-protein complexes have been found to contain significant amounts of lutein and beta carotene which would not be utilized by the body (Rich and others 2003; Vishnevetsky and others 1999; Serrano and others 2005). Food processing such as heat or mechanical treatments can release carotenoids from the food matrix and improve availability (Stahl and Sies 1992). If the carotenoids are not released from the digested food matrix in the small intestines, it is passed to the large intestine where it is effectively unavailable (Serrano and others 2005).

1.4.5.2 Effect of Lipase Activity on Carotenoid Bioaccessibility

Lipids consumed in conjunction with carotenoids have been found to improve carotenoid bioavailability by solubilizing and delivering them into mixed micelles in the small intestine (Hof and others 2000; Yonekura and Nagao 2007). It has been found that incorporating at least 5g of dietary fat into test meals significantly improved vitamin A bioavailability (Jalal and others 1998). The transfer of carotenoids from lipid droplets into the mixed micelle is affected by lipase activity in the intestine (Borel and others 1996; Tyssandier and others 2001). The amount of lipid digestion products like monoglycerides and free fatty acids is directly correlated with increased bioaccessibility of carotenoids (Mutsokoti and others 2017; Salvia-Trujillo and others 2017).

Enzymatic digestion of lipid droplets would also release the solubilized carotenoids and improve their uptake into the mixed micelle (Yi and others 2014).

Lipase, which is water soluble, must adsorb onto the oil-water phase interface of oil droplets to hydrolyze lipids (Delorme and others 2011). Surface-active compounds such as gum Arabic, phospholipids, and surface-active peptides can decrease lipase activity by competitively adsorbing onto the interfacial layer and limiting exposure between lipids and lipase (Delorme and others 2011; Tiss and others 2001). Digested zein peptides may have surface-active properties and inhibit lipase through the same mechanism.

1.5 Formation of Biopolymer Films

Food packaging is an important material for preventing the chemical, microbiological, and physical degradation of food. Petroleum based plastic packaging is an excellent material as it can be a physically durable that can prevent microbes, gas, and moisture pass through it to contaminate or alter the food. Its properties can be modified to suit a given application. However, the accumulation of non-degradable synthetic packaging waste is a major environmental and sustainability concern. (Hammer and others 2012; Geyer and others 2017) From 1950 to 2015, approximately 6300 million metric tons of plastic waste has been generated. Of that amount, only 9% was recycled and 79% of plastic waste was disposed in landfills or polluted the environment (Geyer and others 2017). As of 2015 in Europe, nearly 40% of plastic is used for packaging (Kaiser and others 2018). Because of their physical and chemical stability, plastic packaging waste remains in the environment for long periods of time and has a detrimental effect on natural ecosystems, such as marine life in the oceans (Hammer and others 2012). Biodegradable films made from renewable natural polymers, such as carbohydrates, proteins, and lipids can be used as replacements for synthetic and poorly degradable polymers to create a smaller environmental footprint (Rhim and others 2013). However, these materials typically display poor water vapor barrier properties when compared to petroleum-based materials, as well as a reduced mechanical strength and extensibility (Rhim and others 2013; Siracusa and others 2008).

1.5.1 Film Formation

There are two main ways to form biopolymer films. The first method used is the solvent cast method where a biopolymer solution is cast onto a flat surface and the solvent is evaporated (Navarro-Tarazaga and others 2008; Xu and others 2012; Jimenez and others 2010). This process

is highly affected by the composition of the casting solution as well as the drying rate (Rhim and Ng 2007). Another method of creating biopolymer films is to utilize the dry process method. This is done by creating a liquid melt of the polymer with low moisture content and then heating it above its glass transition temperature. The liquid is then kneaded, blown, or extruded into a desired shape. This method has the advantage of having higher throughput but requires costly equipment such as an extruder (Rhim and Ng 2007).

There are many factors that affect a film's properties during the drying process such as temperature, airflow, differences in relative humidity, and the composition of the solvent casting solution. There are two main phases during the drying process (Guerrier and others 1998). In the first phase, known as the constant rate, the solvent of the casting solution is high, and the polymer concentration is fairly dilute. The rate dehydration is largely dictated by the environment, and the evaporation behavior of the solvent is rapid and like pure solvent. In the second phase known as the falling rate, once the polymer concentration reaches a critical point, the evaporation of the solvent slows (Guerrier and others 1998). The rate of drying in this step is limited by the migration of moisture from the interior of the film to the surface.

The drying conditions of a solvent cast film affects the physical state of the dissolved polymers which, in turn, affect the final film's mechanical properties. However, it can have positive or negative impacts on the mechanical properties of biopolymer films depending on the choice of polymer used. High temperature drying was determined to increase the tensile strength of whey protein isolate films while decreasing the elongation (Alcantara and others 1998). However, oven drying chitosan films at 80°C decreased its elongation and tensile strength compared to films dried at ambient temperatures which was attributed to over drying the films (Srinivasa and others 2004). Higher drying temperature has also been found to significantly decrease the elasticity of alginate films from 20%-30% (Mariana Altenhofen da Silva and Andréa Cristiane Krause Bierhalz and Theo Guenter). Finally, when gelatin films were dried below the gelation temperature, the film had higher mechanical strength due to greater amounts of ordered helical structure when compared to films dried above its gelation temperature (Chiou and others 2009).

The glass transition temperature (Tg) of a material both affects the film forming properties of a solvent cast film as well as the mechanical properties of the resulting dried film. It is a transition point where when the temperature of an amorphous material is below Tg, it is rigid and

stiff. When the temperature rises above Tg, then the material becomes rubbery. When examining the solvent casting solution for a film, the solvent lowers the Tg of the dissolved polymer as it enables a greater free form movement allowing the polymers in the film to easily rearrange its configuration. However, as the solvent evaporates, less is available to plasticize the solute so Tg increases. Eventually as the moisture content drops during drying, the polymer transitions from a rubbery state into a glassy state (Harnkarnsujarit 2017). At that point, the polymer has little ability to rearrange to form a different type of network. Consequently, the structure it forms would depend on its conditions during its drying process such as heat denaturation, cross linking, or disulfide bond formation in proteins (Aguirre-Alvarez and others 2011; Harnkarnsujarit 2017). The water vapor permeability is also greatly influenced by the Tg of a material. If a polymer is in the rubbery state, the greater mobility would allow for easier diffusion of moisture through the cross section of the film (Harnkarnsujarit 2017).

The Tg of a material can be affected by plasticizers. These are molecules ranging from 300-600 Da with a high boiling point that can be used to improve the flexibility of films and polymers. Plasticizers associate with polymers in a film, which would prevent tight association between chains allowing for greater molecular mobility. This results in a reduction in the glass transition temperature of a polymer allowing it to remain in the rubbery state at lower temperatures (Vieira and others 2011). It has been found that addition of polyols at up to 30% into starch/MC composite films increased elongation by 20-30% while decreasing the tensile strength by about 20 MPa (1999).

1.5.2 Zein Films

Zein is known to have film forming capabilities. Its hydrophobicity has made it an alternative material for coatings on packaging and pharmaceuticals (Patel and Velikov 2014b). These films are typically prepared with the solvent casting method by dissolving zein in aqueous ethanol. However, zein films alone are extremely brittle (Park and others 1994; Xu and others 2012). The incorporation of plasticizers such as polyethylene glycol, glycerol, and oleic acid had been used to increase the elasticity of zein (Xu and others 2012; Corradini and others 2014). Dry zein has a glass transition temperature of 150 - 180°C, but the addition of plasticizers can significantly decrease that temperature. Fatty acids have been shown to decrease it to 47-50°C (de Almeida and others 2018) while a 12% moisture content can decrease it to as low as 30°C (Madeka and Kokini 1996). Glycerol was able to increase elongation of zein films from ~1.5% to 2.5%

while oleic acid was able to increase it by 0.5%. These plasticizers were also able to increase the tensile strength by 4-5 MPa (Xu and others 2012).

1.5.3 Methylcellulose (MC) Films

Methylcellulose (MC) has been utilized for its cold water solubility, emulsification, and film forming properties (BeMiller and Huber 2008). Similar to other polysaccharide-based films, MC films are moderately stiff, brittle, and highly hygroscopic with a young's modulus of about 2 GPa, a tensile strength of over 50-100 MPa, and an elongation of 10-20% (Donhowe and Fennema 1993; Peressini and others 2003; Debeaufort and Voilley 1997; CHEN and others 1996; Rimdusit and others 2008). In comparison, chitosan films have been found to have a tensile strength of ~7 MPa and an elongation up to 80%; while starch films have been found to have a tensile strength ranging from 2-5 MPa with an elongation of 15-30% (Zhang and others 2015; Torres and others 2011). While the mechanical properties can be improved with addition of various plasticizers, the excessive hygroscopicity and water vapor permeability of MC films limits their utility in food systems where water is ubiquitous. Lipids, such as lauric and palmitic acid, have been used as coatings and additives to help lower moisture migration of MC films by up to ~90% (Park and others 1994). Others have attempted to incorporate structured polysaccharide assembles in cellulose films to increase film strength, provide antimicrobial activity, or decrease water vapor permeability (Sebti 2007; de Moura and others 2009; Maftoonazad and others 2008; Tunç and Duman 2011).

MC is a carbohydrate that exhibits thermo-gelling properties, upon heating to 54°C, a thermo-reversible gel forms. It has been found that MC film casting solutions dried at higher temperatures exhibited more crystalline structure, but it had no effect on its mechanical properties (Donhowe).

1.5.4 Nanocomposite Films

One promising strategy to improve barrier functions of biopolymer films is to reinforce them with biopolymer-based nanoparticles, and the resultant bio-nanocomposites could then serve as replacements for synthetic plastic films (Rhim and others 2013; Arora and Padua 2010; Akbari and others 2007). If the incorporated nanoparticles possessed affinity for entrapment and delivery of active molecules, such as antimicrobial agents, then the nanocomposites would possess further value as active films (Abdollahi and others 2012; Persico and others 2009). Many types of

materials have been used as nanofillers in nanocomposite films such as clay, chitosan, silver, zinc oxide, and titanium dioxide (Othman 2014; Abdollahi and others 2012; Escamilla-Garcia and others 2013). Nanocomposite films incorporating these particles have been found to improve the mechanical and water barrier properties of biopolymer films (Honarvar and others 2016). The improved barrier properties of nanocomposite films are attributed to the increase of the tortuous path that water vapor or gas must take to traverse through the film (Honarvar and others 2016). Biopolymer-based nanoparticles formed from either chitosan/tripolyphosphate or microcrystalline cellulose were found to moderately improve water barrier properties (40-50% improvement) of cellulose-based films by increasing the density of the interstitial matrix (de Moura and others 2009; Bilbao-Sáinz and others 2010). It then logically follows that nanoparticles with hydrophobic properties would improve water barrier properties of films by altering the hydrophobicity of the film and also increasing the density of the matrix.

Nanoparticles are thought to improve mechanical strength of composite films when any exterior stress on the film transfers efficiently from the matrix to the nanoparticle (Fu and others 2008). There are two theories on how particles reinforce the surrounding matrix: coupling and particle jamming. For coupling, the nanoparticles are thought to fill gaps between the polymer matrix and reduce mobility. In particle jamming, the particles are thought to interact with each other to form a reinforcing structure (Hassanabadi and Rodrigue 2014). The particle size, interfacial adhesion of the particle and matrix, and loading of the particle are all factors that affect mechanical properties of composite films (Fu and others 2008). For nanocomposites containing clay nanoparticles, the dispersion of the nanoparticle through the continuous phase can result changes in the film's mechanical and water barrier properties. It is commonly thought that exfoliated nanocomposites where the nanoparticle is well dispersed in the continuous phase leads to the greatest improvements in functionality (Rhim and Ng 2007).

Zein is poorly soluble in water and, therefore, may improve the water barrier properties of biopolymer films. The hydrophobicity of ZNP, as well as its peptide-based composition that permits greater affinity with bioactive molecules, provide unique advantages as a nanoparticle for film preparation over relatively-hygroscopic carbohydrate-based particles. ZNP are then promising materials for preparation of biopolymer-based nanocomposite films because of their physical properties, natural source, and potential for encapsulation and controlled-delivery of high-valued compounds for active film applications. Unlike globular zein, the dispersibility of ZNPs

in aqueous dispersions also allows them to be incorporated into hydrophilic biopolymer films like MC with minimal phase separation. ZNP have the potential to increase the hydrophobicity and decrease water vapor permeability of MC films.

1.6 Colloidal Characterization Techniques

A scientist has many techniques to determine various properties of biopolymers in colloidal systems. The sizes and stability of particles in aqueous dispersion can be measured with dynamic light scattering and turbidity. The surface charge can be measured with zeta potential. These measurements can provide information on the state of aggregation of nanoparticles and their stability. The mechanical and water vapor barrier properties of biopolymer films can be determined with the extension test and a dynamic vapor sorption analyzer respectively. These measurements can help determine the viability of these materials for normal use as a packaging material. Finally, these systems can be imaged using microscopy techniques such as atomic force microscopy, scanning electron microscopy, and confocal laser microscopy. These techniques can provide into the micro and nanostructure of various colloidal systems.

1.6.1 Dynamic Light Scattering

There are many experimental techniques that can be used to characterize colloidal particles in dispersions including dynamic light scattering (DLS), zeta potential, and turbidity. DLS is a technique used to determine the size of particles in a liquid dispersion. It does this by emitting a monochromatic light source like a laser through a dispersion (Finsy 1994). Once the laser beam contacts a particle with a radius less than 10 nm, the light scatters in all directions called Rayleigh scattering. The scattered light is detected at a known angle in relation to the incident ray. Due to Brownian motion of the dispersed particles, constructive or destructive interference of the scattered light will occur due to overlapping waves of neighboring particles, which creates a distinctive scattering pattern. Larger particles have a lower rate of Brownian motion, and the resulting scattering pattern will change slower compared to those of smaller particles (Finsy 1994).

The changing intensity of this pattern over time can be mathematically modeled to calculate the particle size distribution of a dispersion. A normalized intensity time correlation function is used to predict the position of particles (Goldburg 1999). Over short periods of time, the function has high correlation between a particle's scattered intensity, but it decays exponentially over time. This exponential decay function directly relates to the motion of the particles and their diffusion

coefficient. From the determined diffusion coefficient, the hydrodynamic radius of a suspended particle can be calculated using the Stokes-Einstein equation with a given temperature and viscosity of the solvent.

$$D = \frac{k_B T}{6\pi\eta R_h}$$

Where k_B is the Botzmann constant, T is the temperature, and η is the viscosity of the solvent. The hydrodynamic radius of a polymer can be described as the radius of an equivalent hard sphere that has the same diffusion behavior as the polymer of interest. This is best used to describe non-spherical free moving polymers or colloidal structures that can adopt many conformations in a solution (Finsy 1994).

1.6.2 Turbidity

The turbidity describes the cloudiness of a solution and can be used to assess the stability of a colloidal dispersion. Particles in a suspension or solution can scatter or absorb light that passes through a sample, thus decreasing the intensity of the light beam. The larger or more numerous a particle is in solution, the more light it scatters. For example, the opacity of milk is attributed to casein micelles, which have an average diameter of 200 nm. Some molecules absorb light at specific wavelengths. Proteins specifically can absorb light at 280 nm if it contains aromatic amino acids, and the peptide bond can absorb light at 205 nm. Whereas the carotenoid lutein can absorb light at 475 nm. The turbidity of a solution is typically measured with a spectrophotometer. This piece of equipment emits a beam of monochromatic light through a solution in a cuvette with a known path length.

1.6.3 Zeta Potential

The zeta potential is the difference in electrostatic potential of the surface of a material and the layer of solvent surrounding it (Clogston and Patri 2011). A charged particle in solution will form a double layer of solvent surrounding it. The inner layer, called the Stern Layer, will be composed of tightly adsorbed counterions. The outer layer called the Diffuse Layer will be composed of an equilibrium ion concentration dictated by the electrostatic force of the particle and random browning motion of the solvent ions. The main factors that affect the zeta potential of a particle are the pH of the solution as well as the ionic strength. The composition of a material will

also affect its surface charge density. For example, proteins with many charged amino acids and charged carbohydrates such as carrageenan will have a greater magnitude of zeta potential.

Although the zeta potential of a system cannot be directly measured, it is typically determined in colloidal dispersions through electrophoretic mobility. Experimentally, an electric field is applied to a colloidal dispersion, which results in charged particles migrating to either the anode or cathode. Dynamic light scattering can be performed during this process to measure the movement of the particles. The greater the magnitude of the particle charge, the faster the movement. The zeta potential is a reliable predictor for electrostatic stabilization of dispersed particles. Highly positive or negative zeta potential would indicate strong electrostatic repulsion between particles, which would result in lower levels of destabilizing forces such as aggregation or coalescence.

1.6.4 Microscopy

1.6.4.1 Atomic Force Microscopy (AFM)

Atomic Force Microscopy is a robust method for producing topographical images and nanomechanical properties of materials at a nanometer scale. This is done by bringing a nanoscale cantilever close to the surface of the sample. A laser is then deflected off the cantilever into a photodetector in order to measure positional changes of the cantilever. The tip of the cantilever is then moved across the sample where it responds to changes in the height of the sample. During the scan, depending on the imaging technique, the height of the tip is (Rugar and Hansma 1990) constantly adjusted to maintain either a constant deflection or oscillatory amplitude. There are multiple ways that an AFM can detect these height changes in the sample through the tip. The main techniques are static mode and intermittent contact mode.

In static mode, the tip of the cantilever is in constant contact with the sample. As the tip moves across the surface, height changes in the sample have varying repulsive Van der Waal forces that are detected by the AFM. The instrument then adjusts the height of the tip to maintain a constant force (Carter and Shieh 2015). In general, scanning samples in static mode is not ideal for biological samples because the constant contact with the tip can damage the sample.

For intermittent contact mode, the cantilever is oscillated at its resonant frequency and brought to the sample surface. As the tip is moved across the surface of the sample, the oscillating tip taps the sample Figure 3. Height variations in the sample would cause changes in the amplitude

of the vibrating cantilever that would cause the AFM to adjust the height of the tip to maintain a constant amplitude. This technique is much less damaging to samples due to less direct contact with the instrument (Rugar and Hansma 1990). However, the major disadvantage is that it is difficult to perform this technique in liquid environments as the oscillations may cause shear forces in the liquid, which may disrupt measurements.

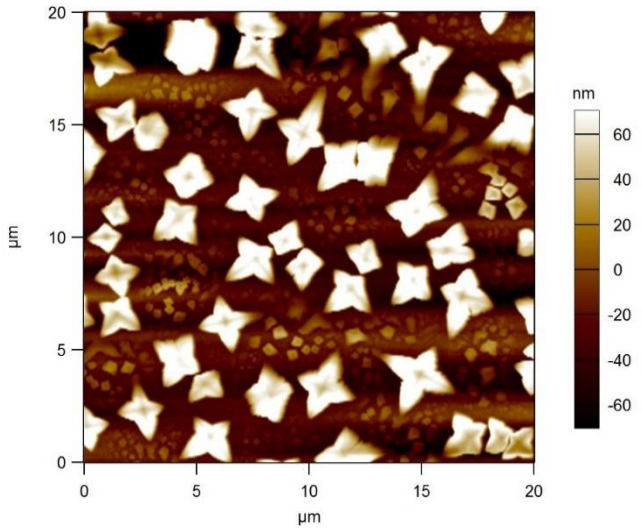

Figure 3. AFM Topographical Image in Intermittent Tapping Mode of NaCl Crystals

The nanomechanical properties of biopolymers can also be measured with two AFM techniques called force spectroscopy and bimodal force spectroscopy (BFS). Force spectroscopy is done by using the cantilever of an AFM to indent into the material. The force of the cantilever that is exerted onto the surface of the material is measured from the deflection of the laser on the tip. After the tip of the AFM is extended a known distance, it retracts away from the surface. The measured compression force of the sample is then plotted against the indentation distance. From these resulting force distance curves, mathematical models such as the Hertz or the Oliver-Pharr model can be used to calculate the Young's modulus (Oliver and Pharr 1992). The Hertz model is derived from Hook's law of elasticity and is suitable for measuring the Young's modulus of a linearly elastic material. The Oliver-Pharr method utilizes the real indentation area of the material caused by the indenter. This method is more suitable for materials that exhibit plasticity such as softer biological materials.

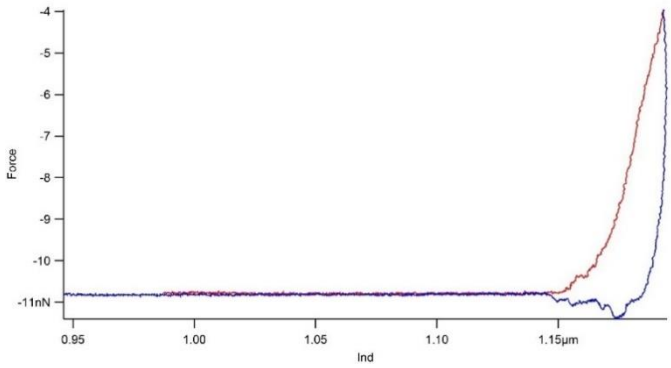

Figure 4. Force Indentation Plot Gathered from Force Spectroscopy. The red line illustrates the approach of the tip, and the blue illustrates the retract.

BFS, also known as Amplitude-Modulation Frequency-Modulation (AMFM), is performed by vibrating an AFM cantilever at two simultaneous frequency and using it to scan the surface of a sample. It allows for the simultaneous measurement of a material's surface morphology as well as its mechanical properties. The topography of the sample is measured from the changes in amplitude of the tip's lower frequency as in traditional tapping AFM. The higher frequency is used for measuring the mechanical properties of the sample. This is done when the oscillating cantilever deforms the surface of the material, and the resulting viscoelastic response will cause shifts in the higher frequency (Gilbert and others 2017). The topography of the sample can be detected most accurately with the probe's lower frequency, and its young's modulus can be measured most accurately with the cantilever's higher frequency (Garcia and Proksch 2013).

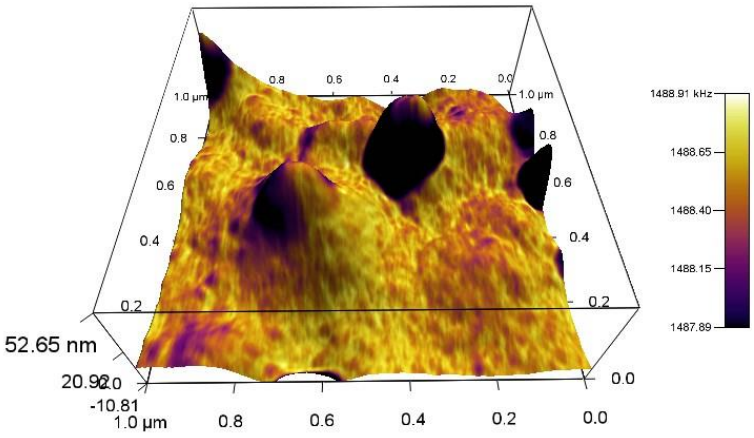

Figure 5. BFS Topographical Image of ZNP/MC Film. Lighter Colors indicate Higher Young's Modulus

1.6.4.2 Scanning Electron Microscopy (SEM)

SEM is an imaging technique that can have resolutions as low as 1nm. Samples are imaged by bombarding its surface with an electron gun. The electrons emitted from the gun are focused through a variety of different lenses and apertures and directed at the sample. At that point, the original focused beam can interact with the sample and produce backscattered electrons, secondary electrons, and x-rays which can all be detected with various pieces of equipment to form an image. Based on the morphology of the sample and the position of the electron beam, the detected signal can be used to form an image (Kulkarni and Shaw 2016). The biggest advantage of imaging with SEM is its ability to measure samples at a large range of magnification ranging from nanometer scale to mm scale. However, samples must be fixed and dried (Carter and Shieh 2015). In order to image many biological samples, the moisture must be removed by sublimation after cryogenic freezing. Another disadvantage of SEM is that because images only show the intensity of detected electrons, it cannot naturally produce colored images, and they must be added in artificially as a post processing effect.

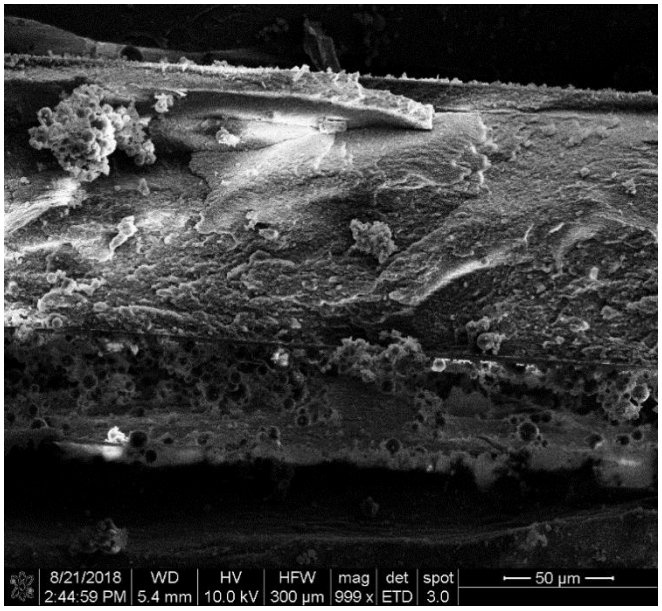

Figure 6. SEM image of a Cross Section of a ZNP/MC Composite Film

1.6.4.3 Confocal Laser Scanning Microscopy (CLSM)

CLSM uses optical light to image samples. A spatial pinhole is used to filter out light that is outside of the plane of focus to increase the instrument's resolving power. The resulting image

thus focuses on a specific thin slice at a given depth inside a sample (Carter and Shieh 2015). Optical sectioning can be done by capturing multiple two-dimensional images at different depths in the sample can be formed into a three-dimensional image called a z-stack. Samples imaged by CLSM are also typically tagged with various fluorescent dyes and scanned with different laser sources to differentiate the components of a sample. For example, Nile Red can be used to dye lipids and other hydrophobic molecules, and FITC can be used to dye proteins to produce an image with a color corresponding to each type of molecule.

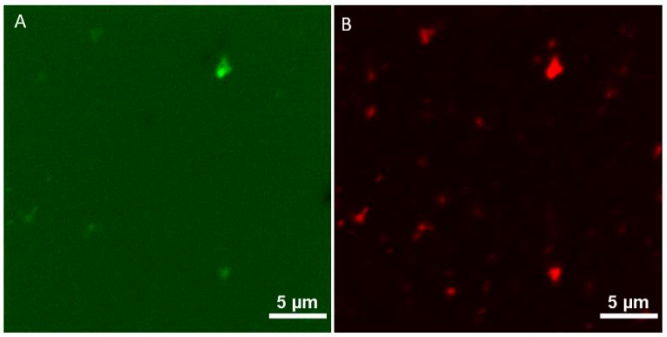

Figure 7. Confocal microscopy images of ZNP Encapsulating Lutein with fluorescence labelling by (A) Fluorescein Isothiocyanate and (B) Nile Red

1.6.5 Biopolymer Film Mechanical Properties

The mechanical properties of polymer films can be evaluated by measuring its tensile strength. A tensile test is performed by stretching a sample until it breaks and calculating its Young's modulus (E) which is defined as the following equation.

$$E = \frac{\sigma}{\varepsilon} = \frac{F/A}{L/\Delta L_0}$$

Where σ is the tensile stress on the sample calculated by dividing the tensile force (F) by the cross sectional area (A). The extensional strain (ε) is calculated by dividing the original length of the object (L) by the change in length from extension (ΔL_0). The tensile test is also used to determine the material's elongation until break and its ultimate tensile strength. These parameters indicate its deformability as well as the force required to break the sample.

1.6.6 Water Vapor Barrier Properties

An important desirable property of food packaging is for it to be a good moisture barrier. Without such a barrier, the relative humidity in the environment can often alter the desired water

activity of food which may cause quality issues or enable growth of pathogenic microbes (Slade and Levine 1991). Water Vapor Permeability (WVP) is a measure of the ability for water to pass through a material. Films with lower WVP will be a better moisture barrier as water will slowly pass through it. There are many factors that might affect the WVP of a material. These factors include thickness, hydrophobicity of the material, and homogeneity of its composition (Grewal and others 2012). The WVP of a film can be measured with the method outlined by the ASTM E96/E96M-16. First a container with a known relative humidity is placed in a chamber of a different relative humidity. The relative humidity of both the container and the outer chamber is separated by the sample in question. The movement of the moisture between the container and the chamber is then typically measured gravimetrically. The slope of the weight change of the sample container is measured to determine the water vapor transmission rate which is converted. WVP is calculated from WVTR using the following equation:

$$WVP = \frac{WVTR}{\Delta P} L_{film}$$

where ΔP is the difference in the partial pressure on either side of the film and L_{film} is the film thickness. The partial pressure can be derived from the relative humidity, RH with the following equation where P_s is saturation vapor pressure of water at a given temperature.

$$P_w = \frac{RH}{100} P_s$$

1.7 References

1999. Physical properties of polyol-plasticized edible blends made of methyl cellulose and soluble starch. Carbohydrate Polymers 38(1):47 - 58.

Abdollahi M, Rezaei M, Farzi G. 2012. A novel active bionanocomposite film incorporating rosemary essential oil and nanoclay into chitosan. Journal of Food Engineering 111(2):343-50.

Aguirre-Alvarez G, Pimentel-Gonzalez DJ, Campos-Montiel RG, Foster T, Hill SE. 2011. The effect of drying temperature on mechanical properties of pig skin gelatin films. Cyta-Journal of Food 9(3):243-9.

Akbari Z, Ghomashchi T, Moghadam S. 2007. Improvement in Food Packaging Industry with Biobased Nanocomposites. International Journal of Food Engineering 3(4).

Alcantara CR, Rumsey TR, Krochta AM. 1998. Drying rate effect on the properties of whey protein films. Journal of Food Process Engineering 21(5):387-405.

Alves-Rodrigues A, Shao A. 2004. The science behind lutein. Toxicology Letters 150(1):57-83.

Anderson TJ, Lamsal BP. 2011. Zein Extraction from Corn, Corn Products, and Coproducts and Modifications for Various Applications: A Review. Cereal Chemistry 88(2):159-73.

Argos P, Pedersen K, Marks MD, Larkins BA. 1982. A STRUCTURAL MODEL FOR MAIZE ZEIN PROTEINS. Journal of Biological Chemistry 257(17):9984-90.

Arnal E, Miranda M, Almansa I, Muriach M, Barcia JM, Romero FJ, Diaz-Llopis M, Bosch-Morell F. 2009. Lutein prevents cataract development and progression in diabetic rats. Graefes Archive for Clinical and Experimental Ophthalmology 247(1):115-20.

Arora A, Padua GW. 2010. Review: Nanocomposites in Food Packaging. Journal of Food Science 75(1):R43-R9.

BeMiller JN, Huber KC. 2008. Chapter 3: Carbohydrates, Fourth ed. Boca Raton, FL: CRC Press.

Bilbao-Sáinz C, Avena-Bustillos RJ, Wood DF, Williams TG, McHugh TH. 2010. Composite Edible Films Based on Hydroxypropyl Methylcellulose Reinforced with Microcrystalline Cellulose Nanoparticles. Journal of Agricultural and Food Chemistry 58(6):3753-60.

Borel P, Grolier P, Armand M, Partier A, Lafont H, Lairon D, AzaisBraesco V. 1996. Carotenoids in biological emulsions: Solubility, surface-to-core distribution, and release from lipid droplets. Journal of Lipid Research 37(2):250-61.

Campo VL, Kawano DF, da Silva DB, Carvalho I. 2009. Carrageenans: Biological properties, chemical modifications and structural analysis - A review. Carbohydrate Polymers 77(2):167-80.

Carter M, Shieh J. 2015. Chapter 5 - Microscopy.117 - 44.

Chen HQ, Zhong QX. 2015. A novel method of preparing stable zein nanoparticle dispersions for encapsulation of peppermint oil. Food Hydrocolloids 43:593-602.

Chen JJ, Zheng JK, McClements DJ, Xiao H. 2014. Tangeretin-loaded protein nanoparticles fabricated from zein/beta-lactoglobulin: Preparation, characterization, and functional performance. Food Chemistry 158:466-72.

CHEN MC, YEH GHC, CHIANG BH. 1996. Antimicrobial and physicochemical properties of methylcellulose and chitosan films containing a preservative. Journal of Food Processing and Preservation 20(5):379-90.

Cheng CJ, Jones OG. 2017. Stabilizing zein nanoparticle dispersions with ι-carrageenan. 69:28-35.

Chiou BS, Avena-Bustillos RJ, Bechtel PJ, Imam SH, Glenn GM, Orts WJ. 2009. Effects of drying temperature on barrier and mechanical properties of cold-water fish gelatin films. Journal of Food Engineering 95(2):327-31.

Chuacharoen T, Sabliov CM. 2016a. Stability and controlled release of lutein loaded in zein nanoparticles with and without lecithin and pluronic F127 surfactants. Colloids and Surfaces a-Physicochemical and Engineering Aspects 503:11-8.

Chuacharoen T, Sabliov CM. 2016b. The potential of zein nanoparticles to protect entrapped beta-carotene in the presence of milk under simulated gastrointestinal (GI) conditions. Lwt-Food Science and Technology 72:302-9.

Corradini E, Curti PS, Meniqueti AB, Martins AF, Rubira AF, Muniz EC. 2014. Recent Advances in Food-Packing, Pharmaceutical and Biomedical Applications of Zein and Zein-Based Materials. International Journal of Molecular Sciences 15(12):22438-70.

Davidov-Pardo G, Joye IJ, Espinal-Ruiz M, McClements DJ. 2015a. Effect of Maillard Conjugates on the Physical Stability of Zein Nanoparticles Prepared by Liquid Antisolvent Coprecipitation. Journal of Agricultural and Food Chemistry 63(38):8510-8.

Davidov-Pardo G, Joye IJ, McClements DJ. 2015b. Encapsulation of resveratrol in biopolymer particles produced using liquid antisolvent precipitation. Part 1: Preparation and characterization. Food Hydrocolloids 45:309-16.

Davidov-Pardo G, Perez-Ciordia S, Marin-Arroyo MR, McClements DJ. 2015c. Improving Resveratrol Bioaccessibility Using Biopolymer Nanoparticles and Complexes: Impact of Protein-Carbohydrate Maillard Conjugation. Journal of Agricultural and Food Chemistry 63(15):3915-23.

de Almeida CB, Corradini E, Forato LA, Fujihara R, Lopes JF. 2018. Microstructure and thermal and functional properties of biodegradable films produced using zein. Polimeros-Ciencia E Tecnologia 28(1):30-7.

de Moura MR, Aouada FA, Avena-Bustillos RJ, McHugh TH, Krochta JM, Mattoso LHC. 2009. Improved barrier and mechanical properties of novel hydroxypropyl methylcellulose edible films with chitosan/tripolyphosphate nanoparticles. Journal of Food Engineering 92(4):448-53.

Debeaufort F, Voilley A. 1997. Methylcellulose-based edible films and coatings: 2. Mechanical and thermal properties as a function of plasticizer content. Journal of Agricultural and food chemistry 45(3):685-9.

Delorme V, Dhouib R, Canaan S, Fotiadu F, Carriere F, Cavalier JF. 2011. Effects of Surfactants on Lipase Structure, Activity, and Inhibition. Pharmaceutical Research 28(8):1831-42.

Dickinson E. 1998. Stability and rheological implications of electrostatic milk protein-polysaccharide interactions. Trends in Food Science & Technology 9(10):347-54.

Dickinson E. 2003. Hydrocolloids at interfaces and the influence on the properties of dispersed systems. Food Hydrocolloids 17(1):25-39.

Donhowe IG, Fennema O. 1993. The effects of plasticizers on crystallinity, permeability, and mechanical properties of methylcellulose films. Journal of Food Processing and Preservation 17(4):247-57.

Donhowe IGaFO. THE EFFECTS of SOLUTION COMPOSITION and DRYING TEMPERATURE ON CRYSTALLINITY, PERMEABILITY and MECHANICAL PROPERTIES of METHYLCELLULOSE FILMS. Journal of Food Processing and Preservation 17(4):231-46.

Duodu KG, Taylor JRN, Belton PS, Hamaker BR. 2003. Factors affecting sorghum protein digestibility. Journal of Cereal Science 38(2):117-31.

Escamilla-Garcia M, Calderon-Dominguez G, Chanona-Perez JJ, Farrera-Rebollo RR, Andraca-Adame JA, Arzate-Vazquez I, Mendez-Mendez JV, Moreno-Ruiz LA. 2013. Physical and structural characterisation of zein and chitosan edible films using nanotechnology tools. International Journal of Biological Macromolecules 61:196-203.

Espin JC, Garcia-Conesa MT, Tomas-Barberan FA. 2007. Nutraceuticals: Facts and fiction. Phytochemistry 68(22-24):2986-3008.

Fernandez-Garcia E, Carvajal-Lerida I, Perez-Galvez A. 2009. In vitro bioaccessibility assessment as a prediction tool of nutritional efficiency. Nutrition Research 29(11):751-60.

Finsy R. 1994. Particle sizing by quasi-elastic light scattering. Advances in Colloid and Interface Science 52:79 - 143.

Fu SY, Feng XQ, Lauke B, Mai YW. 2008. Effects of particle size, particle/matrix interface adhesion and particle loading on mechanical properties of particulate-polymer composites. Composites Part B-Engineering 39(6):933-61.

Fu TT, Abbott UR, Hatzos C. 2002. Digestibility of food allergens and nonallergenic proteins in simulated gastric fluid and simulated intestinal fluid - A comparative study. Journal of Agricultural and Food Chemistry 50(24):7154-60.

Galazka VB, Smith D, Ledward DA, Dickinson E. 1999. Complexes of bovine serum albumin with sulphated polysaccharides: effects of pH, ionic strength and high pressure treatment. Food Chemistry 64(3):303-10.

Garcia R, Proksch R. 2013. Nanomechanical mapping of soft matter by bimodal force microscopy. European Polymer Journal 49(8):1897-906.

Garrett DA, Failla ML, Sarama RJ. 1999. Development of an in vitro digestion method to assess carotenoid bioavailability from meals. Journal of Agricultural and Food Chemistry 47(10):4301-9.

Geyer R, Jambeck JR, Law KL. 2017. Production, use, and fate of all plastics ever made. Science Advances 3(7).

Gilbert J, Charnley M, Cheng C, Reynolds NP, Jones OG. 2017. Quantifying Young's moduli of protein fibrils and particles with bimodal force spectroscopy. Biointerphases 12(4).

Goldburg WI. 1999. Dynamic light scattering. American Journal of Physics 67(12):1152-60.

Gomez-Estaca J, Balaguer MP, Gavara R, Hernandez-Munoz P. 2012. Formation of zein nanoparticles by electrohydrodynamic atomization: Effect of the main processing variables and suitability for encapsulating the food coloring and active ingredient curcumin. Food Hydrocolloids 28(1):82-91.

Granado F, Olmedilla B, Blanco I. 2003. Nutritional and clinical relevance of lutein in human health. British Journal of Nutrition 90(3):487-502.

Grewal R, Sweesy W, Jur JS, Willoughby J. 2012. Moisture Vapor Barrier Properties of Biopolymers for Packaging Materials. Functional Materials from Renewable Sources: American Chemical Society. p. 271-96.

Gu YS, Decker EA, McClements DJ. 2004. Influence of pH and ι-Carrageenan Concentration on Physicochemical Properties and Stability of β-Lactoglobulin-Stabilized Oil-in-Water Emulsions. Journal of Agricultural and Food Chemistry 52(11):3626-32.

Guerrier B, Bouchard C, Allain C, Benard CJAJ. 1998. Drying kinetics of polymer films. 44(4):791-8.

Hammer J, Kraak MHS, Parsons JR. 2012. Plastics in the Marine Environment: The Dark Side of a Modern Gift. Reviews of Environmental Contamination and Toxicology, Vol 220 220:1-44.

Harnkarnsujarit N. 2017. Glass-Transition and Non-equilibrium States of Edible Films and Barriers. Non-Equilibrium States and Glass Transitions in Foods: Processing Effects and Product-Specific Implications:349-77.

Hassanabadi HM, Rodrigue D. 2014. Effect of Particle Size and Shape on the Reinforcing Efficiency of Nanoparticles in Polymer Nanocomposites. Macromolecular Materials and Engineering 299(10):1220-31.

He XJ, Hwang HM. 2016. Nanotechnology in food science: Functionality, applicability, and safety assessment. Journal of Food and Drug Analysis 24(4):671-81.

Hof KHV, West CE, Weststrate JA, Hautvast J. 2000. Dietary factors that affect the bioavailability of carotenoids. Journal of Nutrition 130(3):503-6.

Honarvar Z, Hadian Z, Mashayekh M. 2016. Nanocomposites in food packaging applications and their risk assessment for health. Electronic Physician 8(6):2531-8.

Hu D, Lin C, Liu L, Li S, Zhao Y. 2012. Preparation, characterization, and in vitro release investigation of lutein/zein nanoparticles via solution enhanced dispersion by supercritical fluids. 109(3):545-52.

Hu K, Huang X, Gao Y, Huang X, Xiao H, McClements DJ. 2015. Core-shell biopolymer nanoparticle delivery systems: Synthesis and characterization of curcumin fortified zein-pectin nanoparticles. Food Chemistry 182:275-81.

Hu K, McClements DJ. 2015. Fabrication of biopolymer nanoparticles by antisolvent precipitation and electrostatic deposition: Zein-alginate core/shell nanoparticles. Food Hydrocolloids 44:101-8.

Huang XX, Huang XL, Gong YS, Xiao H, McClements DJ, Hu K. 2016. Enhancement of curcumin water dispersibility and antioxidant activity using core-shell protein-polysaccharide nanoparticles. Food Research International 87:1-9.

Jalal F, Nesheim MC, Agus Z, Sanjur D, Habicht JP. 1998. Serum retinol concentrations in children are affected by food sources of beta-carotene, fat intake, and anthelmintic drug treatment. American Journal of Clinical Nutrition 68(3):623-9.

Jimenez A, Fabra MJ, Talens P, Chiralt A. 2010. Effect of lipid self-association on the microstructure and physical properties of hydroxypropyl-methylcellulose edible films containing fatty acids. Carbohydrate Polymers 82(3):585-93.

Kaiser K, Schmid M, Schlummer M. 2018. Recycling of Polymer-Based Multilayer Packaging: A Review. Recycling 3(1):1.

Kean EG, Hamaker BR, Ferruzzi MG. 2008. Carotenoid Bioaccessibility from Whole Grain and Degermed Maize Meal Products. Journal of Agricultural and Food Chemistry 56(21):9918-26.

Keith MO, Bell JM. 1988. DIGESTIBILITY OF NITROGEN AND AMINO-ACIDS IN SELECTED PROTEIN-SOURCES FED TO MICE. Journal of Nutrition 118(5):561-8.

Kulkarni V, Shaw C. 2016. Chapter 10 - Microscopy Techniques.183 - 92.

Lawton JW. 2002. Zein: A history of processing and use. Cereal Chemistry 79(1):1-18.

Lee SH, Hamaker BR. 2006. Cys155 of 27 kDa maize gamma-zein is a key amino acid to improve its in vitro digestibility. Febs Letters 580(25):5803-6.

Li YQ, Li J, Xia QY, Zhang B, Wang Q, Huang QR. 2012. Understanding the Dissolution of alpha-Zein in Aqueous Ethanol and Acetic Acid Solutions. Journal of Physical Chemistry B 116(39):12057-64.

Liang H, Zhou B, He L, An Y, Lin L, Li Y, Liu S, Chen Y, Li B. 2015. Fabrication of zein/quaternized chitosan nanoparticles for the encapsulation and protection of curcumin. Rsc Advances 5(18):13891-900.

Liang Y, Hilal N, Langston P, Starov V. 2007. Interaction forces between colloidal particles in liquid: Theory and experiment. Advances in Colloid and Interface Science 134-35:151-66.

Lin CH, Chen BH. 2005. Stability of carotenoids in tomato juice during storage. Food Chemistry 90(4):837-46.

Luo YC, Teng Z, Wang Q. 2012. Development of Zein Nanoparticles Coated with Carboxymethyl Chitosn for Encapsulation and Controlled Release of Vitamin D3. Journal of Agricultural and Food Chemistry 60(3):836-43.

Madeka H, Kokini JL. 1996. Effect of glass transition and cross-linking on rheological properties of zein: Development of a preliminary state diagram. Cereal Chemistry 73(4):433-8.

Maftoonazad N, Ramaswamy HS, Marcotte M. 2008. Shelf- life extension of peaches through sodium alginate and methyl cellulose edible coatings. International journal of food science & technology 43(6):951-7.

Maiani G, Caston MJP, Catasta G, Toti E, Cambrodon IG, Bysted A, Granado-Lorencio F, Olmedilla-Alonso B, Knuthsen P, Valoti M, Bohm V, Mayer-Miebach E, Behsnilian D, Schlemmer U. 2009. Carotenoids: Actual knowledge on food sources, intakes, stability and bioavailability and their protective role in humans. Molecular Nutrition & Food Research 53:S194-S218.

Mariana Altenhofen da Silva and Andréa Cristiane Krause Bierhalz and Theo Guenter K. Influence of Drying Conditions on Physical Properties of Alginate Films. Drying Technology 30(1):72-9.

Matthews L, Kunkel J, Action A, Ogale, Dawson P. 2011. Bioavailability of Soy Protein and Corn Zein Films. Food and Nutrition Sciences. p. 1105-13.

McClements DJ, Decker EA, Park Y, Weiss J. 2009. Structural Design Principles for Delivery of Bioactive Components in Nutraceuticals and Functional Foods. Critical Reviews in Food Science and Nutrition 49(6):577-606.

Mutsokoti L, Panozzo A, Pallares AP, Jaiswal S, Van Loey A, Grauwet T, Hendrickx M. 2017. Carotenoid bioaccessibility and the relation to lipid digestion: A kinetic study. Food Chemistry 232:124-34.

Navarro-Tarazaga ML, Sothornvit R, Perez-Gago MB. 2008. Effect of Plasticizer Type and Amount on Hydroxypropyl Methylcellulose-Beeswax Edible Film Properties and Postharvest Quality of Coated Plums (Cv. Angeleno). Journal of Agricultural and Food Chemistry 56(20):9502-9.

Facts About Age-Related Macular Degeneration. National Eye Institute; 2015 [Accessed 2017 November 2] Available from: https://nei.nih.gov/health/maculardegen.

Oliver WC, Pharr GM. 1992. An improved technique for determining hardness and elastic modulus using load and displacement sensing indentation experiments. Journal of Materials Research 7(6):1564-83.

Othman SH. 2014. Bio-nanocomposite Materials for Food Packaging Applications: Types of Biopolymer and Nano-sized Filler. 2nd International Conference on Agricultural and Food Engineering (Cafe 2014) - New Trends Forward 2:296-303.
Park C-E, Park D-J, Kim B-K. 2015. Effects of a chitosan coating on properties of retinol-encapsulated zein nanoparticles. Food Science and Biotechnology 24(5):1725-33.
Park JW, Testin RF, Park HJ, Vergano PJ, Weller CL. 1994. FATTY-ACID CONCENTRATION-EFFECT ON TENSILE-STRENGTH, ELONGATION, AND WATER-VAPOR PERMEABILITY OF LAMINATED EDIBLE FILMS. Journal of Food Science 59(4):916-9.
Patel A, Hu Y, Tiwari JK, Velikov KP. 2010a. Synthesis and characterisation of zein-curcumin colloidal particles. Soft Matter 6(24):6192-9.
Patel AR, Bouwens ECM, Velikov KP. 2010b. Sodium Caseinate Stabilized Zein Colloidal Particles. Journal of Agricultural and Food Chemistry 58(23):12497-503.
Patel AR, Velikov KP. 2014. Zein as a source of functional colloidal nano- and microstructures. Current Opinion in Colloid & Interface Science 19(5):450-8.
Paulis JW. 1981. DISULFIDE STRUCTURES OF ZEIN PROTEINS FROM CORN ENDOSPERM. Cereal Chemistry 58(6):542-6.
Pepi Hurtado-López and Sudax M. Zein microspheres as drug/antigen carriers: A study of their degradation and erosion, in the presence and absence of enzymes. Journal of Microencapsulation 23(3):303-14.
Peressini D, Bravin B, Lapasin R, Rizzotti C, Sensidoni A. 2003. Starch–methylcellulose based edible films: rheological properties of film-forming dispersions. Journal of Food Engineering 59(1):25-32.
Persico P, Ambrogi V, Carfagna C, Cerruti P, Ferrocino I, Mauriello G. 2009. Nanocomposite polymer films containing carvacrol for antimicrobial active packaging. Polymer Engineering & Science 49(7):1447-55.
Reboul E, Richelle M, Perrot E, Desmoulins-Malezet C, Pirisi V, Borel P. 2006. Bioaccessibility of carotenoids and vitamin E from their main dietary sources. Journal of Agricultural and Food Chemistry 54(23):8749-55.
Reiners R, Pressick J, Morris L, inventors; Unilever Bestfoods North America Inc, assignee. 1972. Method of Treating Gluten. United States patent.
Rhim JW, Ng PKW. 2007. Natural biopolymer-based nanocomposite films for packaging applications. Critical Reviews in Food Science and Nutrition 47(4):411-33.
Rhim JW, Park HM, Ha CS. 2013. Bio-nanocomposites for food packaging applications. Progress in Polymer Science 38(10-11):1629-52.
Rich GT, Faulks RM, Wickham MSJ, Fillery-Travis A. 2003. Solubilization of carotenoids from carrot juice and spinach in lipid phases: II. Modeling the duodenal environment. Lipids 38(9):947-56.
Rimdusit S, Jingjid S, Damrongsakkul S, Tiptipakorn S, Takeichi T. 2008. Biodegradability and property characterizations of Methyl Cellulose: Effect of nanocompositing and chemical crosslinking. Carbohydrate Polymers 72(3):444-55.
Rugar D, Hansma P. 1990. Atomic force microscopy. Physics today 43(10):23-30.
Salvia-Trujillo L, Qian C, Martin-Belloso O, McClements DJ. 2013. Influence of particle size on lipid digestion and beta-carotene bioaccessibility in emulsions and nanoemulsions. Food Chemistry 141(2):1472-80.

Salvia-Trujillo L, Verkempinck SHE, Sun L, Van Loey AM, Grauwet T, Hendrickx ME. 2017. Lipid digestion, micelle formation and carotenoid bioaccessibility kinetics: Influence of emulsion droplet size. Food Chemistry 229:653-62.

Sebti I, Chollet, E., Degraeve, P., Noel, C., Pyrol, E. 2007. Water sensitivity, antimicrobial, and physicochemical analysis of edible films based on HPMC and/or chitosan. Journal of Agriculture and Food Chemistry 55(3):693-9.

Sekhon BS. 2010. Food nanotechnology – an overview. Nanotechnology, Science and Applications 3:1-15.

Serrano J, Goni I, Saura-Calixto F. 2005. Determination of ss-carotene and lutein available from green leafy vegetables by an in vitro digestion and colonic fermentation method. Journal of Agricultural and Food Chemistry 53(8):2936-40.

Shahidi F, Han XQ. 1993. ENCAPSULATION OF FOOD INGREDIENTS. Critical Reviews in Food Science and Nutrition 33(6):501-47.

Shukla R, Cheryan M. 2001. Zein: the industrial protein from corn. Industrial Crops and Products 13(3):171-92.

Siracusa V, Rocculi P, Romani S, Dalla Rosa M. 2008. Biodegradable polymers for food packaging: a review. Trends in Food Science & Technology 19(12):634-43.

Sozer N, Kokini JL. 2009. Nanotechnology and its applications in the food sector. Trends in Biotechnology 27(2):82-9.

Srinivasa P, Ramesh M, Kumar K, Tharanathan R. 2004. Properties of chitosan films prepared under different drying conditions. Journal of Food Engineering 63(1):79 - 85.

Stahl W, Sies H. 1992. UPTAKE OF LYCOPENE AND ITS GEOMETRICAL-ISOMERS IS GREATER FROM HEAT-PROCESSED THAN FROM UNPROCESSED TOMATO JUICE IN HUMANS. Journal of Nutrition 122(11):2161-6.

Stone AK, Nickerson MT. 2012. Formation and functionality of whey protein isolate-(kappa-, iota-, and lambda-type) carrageenan electrostatic complexes. Food Hydrocolloids 27(2):271-7.

Sweeney PJ, Walker JM. 1993. Enzymes of Molecular Biology: Humana Press

Tang YC, Chen BH. 2000. Pigment change of freeze-dried carotenoid powder during storage. Food Chemistry 69(1):11-7.

Tiss A, Carriere F, Verger R. 2001. Effects of gum Arabic on lipase interfacial binding and activity. Analytical Biochemistry 294(1):36-43.

Torres FG, Troncoso OP, Torres C, Diaz DA, Amaya E. 2011. Biodegradability and mechanical properties of starch films from Andean crops. International Journal of Biological Macromolecules 48(4):603-6.

Tunç S, Duman O. 2011. Preparation of active antimicrobial methyl cellulose/carvacrol/montmorillonite nanocomposite films and investigation of carvacrol release. LWT-Food Science and Technology 44(2):465-72.

Tyssandier V, Lyan B, Borel P. 2001. Main factors governing the transfer of carotenoids from emulsion lipid droplets to micelles. Biochimica Et Biophysica Acta-Molecular and Cell Biology of Lipids 1533(3):285-92.

Vieira MGA, da Silva MA, dos Santos LO, Beppu MM. 2011. Natural-based plasticizers and biopolymer films: A review. European Polymer Journal 47(3):254-63.

Vishnevetsky M, Ovadis M, Vainstein A. 1999. Carotenoid sequestration in plants: the role of carotenoid-associated proteins. Trends in Plant Science 4(6):232-5.

Wang YH, Yuan Y, Yang XQ, Wang JM, Guo J, Lin Y. 2016. Comparison of the colloidal stability, bioaccessibility and antioxidant activity of corn protein hydrolysate and sodium caseinate stabilized curcumin nanoparticles. Journal of Food Science and Technology-Mysore 53(7):2923-32.

Wu Y, Luo Y, Wang Q. 2012. Antioxidant and antimicrobial properties of essential oils encapsulated in zein nanoparticles prepared by liquid-liquid dispersion method. Lwt-Food Science and Technology 48(2):283-90.

Xu H, Chai YW, Zhang GY. 2012. Synergistic Effect of Oleic Acid and Glycerol on Zein Film Plasticization. Journal of Agricultural and Food Chemistry 60(40):10075-81.

Yi J, Li Y, Zhong F, Yokoyama W. 2014. The physicochemical stability and in vitro bioaccessibility of beta-carotene in oil-in-water sodium caseinate emulsions. Food Hydrocolloids 35:19-27.

Yonekura L, Nagao A. 2007. Intestinal absorption of dietary carotenoids. Molecular Nutrition & Food Research 51(1):107-15.

Zhang ZH, Han Z, Zeng XA, Xiong XY, Liu YJ. 2015. Enhancing mechanical properties of chitosan films via modification with vanillin. International Journal of Biological Macromolecules 81:638-43.

Zhong QX, Jin MF. 2009. Zein nanoparticles produced by liquid-liquid dispersion. Food Hydrocolloids 23(8):2380-7.

Zou Y, Zhong JJ, Pan RT, Wan ZL, Guo J, Wang JM, Yin SW, Yang XQ. 2017. Zein/tannic acid complex nanoparticles-stabilised emulsion as a novel delivery system for controlled release of curcumin. International Journal of Food Science and Technology 52(5):1221-8.

CHAPTER 2 STABILIZING ZEIN NANOPARTICLE DISPERSIONS WITH I-CARRAGEENAN

Reprinted from Food Hydrocolloids, Volume 69, Author: Chris Cheng, Owen Jones, "Stabilizing Zein Nanoparticle Dispersions with i-Carrageenan", p 28-35, Copyright 2017, with permission from Elsevier

2.1 Abstract

Zein nanoparticles (ZNPs) suspended in water were produced by the antisolvent precipitation method and combined with ι-carrageenan (ι-CGN) suspended in sodium phosphate buffer in order to evaluate the ability of the negatively-charged ι-CGN to stabilize ZNPs against flocculation and gravitational separation. Physical stability of 0.01% ZNP (w/v) dispersions with 0% to 0.02% ι-CGN (w/v) was observed during storage at 4°C and during centrifugation. Colloidal properties of the particles during storage, such as hydrodynamic radius, turbidity, and ζ-potential were characterized at pH values above pH 5. At pH 5, ZNPs were present as small aggregates with an average hydrodynamic radius of approximately 500 nm, and at higher pH values these aggregated further so that the average size was greater than 1000 nm. Addition of sufficient ι-CGN to achieve a ZNP:ι-CGN weight ratio less than or equal to 10:1 prevented aggregation in the pH range of 5.25 to 6.75 and limited aggregation at pH 7.0 (average particle radius of 200-400 nm). Enhanced stability was attributed to the adhesion of ι-CGN to the nanoparticle surface, as the ZNPs surface charge became significantly negative with introduction of ι-CGN. These particles remained stable for up to 30 days with significantly lower turbidity and greater resistance to gravitational separation when compared to ZNPs alone. Characterization of ZNPs with an atomic force microscope showed that the particles possessed a nearly spherical geometry with a Young's modulus of ~100 MPa, neither of which was significantly altered after addition of interactive ι-CGN.

2.2 INTRODUCTION

Zein is a protein found in corn that is used to store nitrogen for the seedling. It is a byproduct of starch and ethanol processing, and it accounts for nearly half of the protein content of the corn grain (Patel and Velikov 2014b; Shukla and Cheryan 2001). It is unique in that it is a water insoluble protein that is classified as generally recognized as safe (GRAS) by the Food and Drug Administration (Patel and Velikov 2014b). This protein is hydrophobic and only soluble in up to 70% ethanol or highly alkaline (pH >11) solutions. There are many promising potential applications for zein that would add value to a waste product of corn production. The hydrophobic nature of zein allows it to encapsulate antimicrobial or nutraceutical compounds that are not normally soluble in water such as essential oils. By forming core-shell structures with the ingredient, zein can improve stability (Davidov-Pardo and others 2015b), functionality (Zhang and others 2014), or control the release of the ingredient during digestion (Hu and others 2012a; Tang and others 2015). Zein has already been found to be able to encapsulate nutrients like resveratrol (Davidov-Pardo and others 2015b), tangeretin (Chen and others 2014b), curcumin (Gomez-Estaca and others 2012; Hu and others 2015; Liang and others 2015), Lutein (Hu and others 2012a) and various antimicrobial essential oils and peptides (Chen and Zhong 2015b; Wu and others 2012). Successfully developing a controlled-delivery application for zein would add value to a waste product of corn starch and ethanol processing.

Zein nanoparticles (ZNPs) can be formed by solubilizing zein in 80% aqueous ethanol and then promoting their aggregation into nanoparticles by sudden exposure to large quantities of water (Zhong and Jin 2009). However, the use of ZNPs as a delivery vehicle is limited by its poor stability to aggregation when suspended in water (Zhong and Jin 2009). They are particularly destabilized in non-acidic pH conditions or in solutions of greater ionic strength (Patel and others 2010b). Another major challenge is that lyophilizing these particles will cause them to agglomerate due to their hydrophobic properties (Patel and others 2010b). Fortunately, there is evidence that interactive biopolymers can stabilize ZNP dispersions. For instance, addition of anionic polymers like gum Arabic, pectin, and alginate improved stability of ZNPs to aggregation and sedimentation (Davidov-Pardo and others 2015b; Liang and others 2015; Luo and others 2012; Hu and McClements 2015). In the case of alginate/Tween-80-stabilized-ZNPs, stability was maintained during 45 days of storage at both 4°C and 25°C (Hu and McClements 2015).

Carrageenan is a sulfonated anionic polysaccharide derived from seaweed (Campo and others 2009) with an approximate hydrodynamic radius of 30 nanometers (Croguennoc and others 2000). It has been shown to electrostatically interact with various proteins and form complex coacervates (Dickinson 2003; Galazka and others 1999; Stone and Nickerson 2012). Because the sulfate groups on carrageenan have a pKa of ~2 (Gu and others 2004), it has the potential to stabilize ZNPs by interacting with cationic residues on the ZNP surface and forming a negatively charged outer layer. Carrageenan has a relatively high charge density so it could potentially stabilize protein nanoparticles at a lower usage rate and over a wider pH range when compared to other anionic polysaccharides such as pectin (Dickinson 1998). The objective of this study was then to determine the relative stabilization of ZNPs at different pH values by addition of carrageenan.

2.3 MATERIALS AND METHODS

2.3.1 Materials

Zein was supplied by Sigma-Aldrich (St. Louis, MO). ι-Carrageenan was purchased from FMC Biopolymer (Philadelphia, PA). Dibasic sodium phosphate, sodium hydroxide, and hydrochloric acid were purchased from Fisher Scientific (Waltham, MA). Ethanol was purchased from VWR (Radnor, PA). Ultrapure water (resistivity (σ) $\geq$ 18mΩ-cm) was utilized for the preparation of all aqueous solutions.

2.3.2 Preparation of Zein-Carrageenan Complexes

ZNPs were prepared using the anti-solvent precipitation method as outlined by Zhong (2009). A 2.5% zein solution was first prepared by dissolving 1 g of zein in 40 mL 80% aqueous ethanol. Nanoparticles were formed by drop-wise injection of 20 mL of zein solution into 60 mL of ultrapure water while being homogenized (Ultra Turax T-25 Basic). The ethanol in the dispersion was removed using a rotary evaporator, and the remaining ZNPs dispersion was concentrated to approximately 30 mL. The sample was then centrifuged for 10 min at 2880 x *g*, and the supernatant was stored at 4°C.

ι-carrageenan (ι-CGN) (FMC Biopolymer, Philadelphia, PA) solutions were prepared by adding dry powder to 10 mM sodium phosphate buffer and stirring overnight. After ZNPs were formed, mixtures with ι-CGN were prepared by adding 0.1 % (w/v) ZNP dispersion to the ι-CGN solutions and then vortexed resulting in a final ZNP concentration of 0.01% (w/v). The initial ι-

CGN content of these dispersions was varied between samples to create the following concentrations (w/v) after mixing with ZNP: 0.02%, 0.01%, 0.005%, 0.002%, 0.001%, 0.0005%, and 0.0001%. These concentrations resulted in a ZNP:ι-CGN weight ratios of: 1:2, 1:1, 2:1, 5:1, 10:1, 20:1, 50:1, 100:1, and 1:0. The pH of each component was pre-adjusted to the following pH levels with 1.0M or 0.1M hydrochloric acid or sodium hydroxide solution before mixing: 7.0, 6.75, 6.5, 6.25, 6.0, 5.75, 5.5, 5.25, and 5.0. Samples were stored at 4°C.

2.3.3 Particle Characterization

Particle size was determined using dynamic light scattering (DLS) using an ALV-CGS3 light scattering goniometer (ALV, Langen) with an HeNe laser (wavelength = 632.8 nm) at a 90 degree scattering angle. Hydrodynamic radii of dispersions at 25^{o}C were determined from obtained correlation functions using the CONTIN algorithm within the instrument software (ALV, Langen, Germany). Viscosity of the continuous phase was taken to be 8.90 x 10^{-4} Pa-s. Preliminary experiments verified the lack of concentration-dependent effects on the determined diffusion coefficient at ZNPs concentrations of 0.01% (w/v).

Zeta potential of colloidal materials was determined using particle electrophoresis measurements (Malvern Zetasizer Nano Series Nano ZS; Malvern Instruments, Worcestershire, U.K.) at 25 °C and a 173 degree scattering angle. Samples were analyzed in disposable plastic cuvettes (model DTS 1060C; Malvern Instruments, Worcestshire, U.K.). Electrophoretic mobility of the detected materials was averaged over 10 runs per sample and converted to ζ-potential values using the Henry equation with the Smoluchowski approximation.

Turbidity of biopolymer dispersions was measured in polystyrene cuvettes using a UV-vis spectrophotometer (Beckman Coulter DU 730) set at a wavelength of 450 nm (Hirt and Jones 2014). Turbidity of ZNPs was presented as 100-%T where T is the transmittance of light through the sample. The blank was composed of 10mM sodium phosphate buffer.

2.3.4 Assessing the stability of Zein and ι-CGN complexes

Resistance of protein-polysaccharide complexes to gravitational separation was determined by observing the phase coherence of samples subjected to increasing centrifugation speeds. ZNPs and ι-CGN samples were suspended in 10mM phosphate buffer and were adjusted to pH 5 with 1.0 M hydrochloric acid solution. Samples were centrifuged for 10 min (Eppendorf Model 5415 D) at 1306-5223 x *g*. They were then inspected for the formation of a pellet, and their turbidity was measured using the same method as in section 2.2.

2.3.5 Atomic Force Microscopy (AFM)

Topographical images of nanoparticles were obtained in intermittent-contact mode with an MFP3D atomic force microscope (Asylum Research, Santa Barbara, CA) using aluminum-coated silicon cantilevers with approximate resonance frequency of 150 kHz and force constant of 5 N/m (TAP150AL-G, Ted Pella, Inc., Redding, CA). Samples were prepared by pipetting 12 µL of dilute liquid dispersions containing ZNPs with or without ι-CGN onto freshly cleaved mica discs and dried with filtered air. Images selected for publication were representative of each sample and chosen from at least 20 images.

Elasticity of nanoparticles was determined by analyzing sample deformation during non-oscillatory approach-retract curves on an atomic force microscope (MFP3D, Asylum Research, Santa Barbara, CA) based upon an established protocol (Best and others 2013). Cr/AU reflex coated silicon nitride cantilevers (SINI-30, Ted Pella, Inc., Redding, CA) with a quoted force constant of 0.27 N/m were used for all measurements. Spring constant of each cantilever was calibrated prior to measurement of each sample using the thermal method (Sader and others 1999). Samples were prepared by depositing 12 µL of dilute liquid dispersions containing ZNPs with or without ι-CGN onto freshly cleaved mica discs, drying the discs with filtered air, and further drying the discs in a desiccator for 48 hours. The sample and cantilever were immersed in butanol, a poor solvent, during all measurements in order to minimize adhesive tip-sample forces, as established in prior experiments with food protein structures (Ikeda and Morris 2002). Inverse optical lever sensitivity of the cantilever-detector system was calibrated against the mica substrate initially in air and again in butanol. Particles were located by an initial topographical scan of the sample surface using contact-mode imaging. Indentations were made at the approximate center of particles with a load rate of 75 nN/s, a maximum load of 2.4 nN, and no dwell time. In these settings, force-distance curves of ZNPs samples displayed plastic behavior with a total indentation distance of less than 10% of the nanoparticle height. The Young's modulus was determined from analysis of the unloading curve using the Oliver-Pharr method (Oliver and Pharr 1992). Data for each considered variable was collected from at least 60 force curves performed on 20 or more particles so that multiple measurements were taken for each chosen particle and multiple particles were measured for each sample.

2.3.6 Statistical Analysis

All analyzed samples were prepared in triplicate unless otherwise specified. Significant differences among particle size, ζ-potential, turbidity, and young modulus values ($P < 0.05$) were

determined by one-way analysis of variance with Tukey-Honest Significant Differences (HSD) using JMP statistical software (developed by SAS).

2.4 RESULTS AND DISCUSSION

2.4.1 Stability of Zein Nanoparticles

ZNPs suspended in water at all tested conditions above pH 5 were found to be unstable to aggregation and gradual sedimentation, which agrees with previous studies (Patel and others 2010b). After fresh preparation of ZNPs, the dispersions had a pH of approximately 3.5, and the detected hydrodynamic radius of these particles was approximately 100 nm. Upon adjustment of the ZNP dispersions to pH values above 5, the particle radius increased to about 1000 nm on day 1. After the first day, they were too large to be measured by dynamic light scattering, indicating a continuous aggregation that coincided with an increase in sediment during storage. ZNPs were found to have a positive ζ-potential at low pH, which decreased as the pH increased (Figure 8). The isoelectric point of the protein was found to be about pH 6, which corresponds with prior findings (Shukla and Cheryan 2001). Aggregation and decreased stability between pH 5 and 7 could then be attributed to a low surface charge in proximity to the isoelectric pH of the ZNPs, limiting repulsive interactions between the nanoparticles within aqueous dispersion.

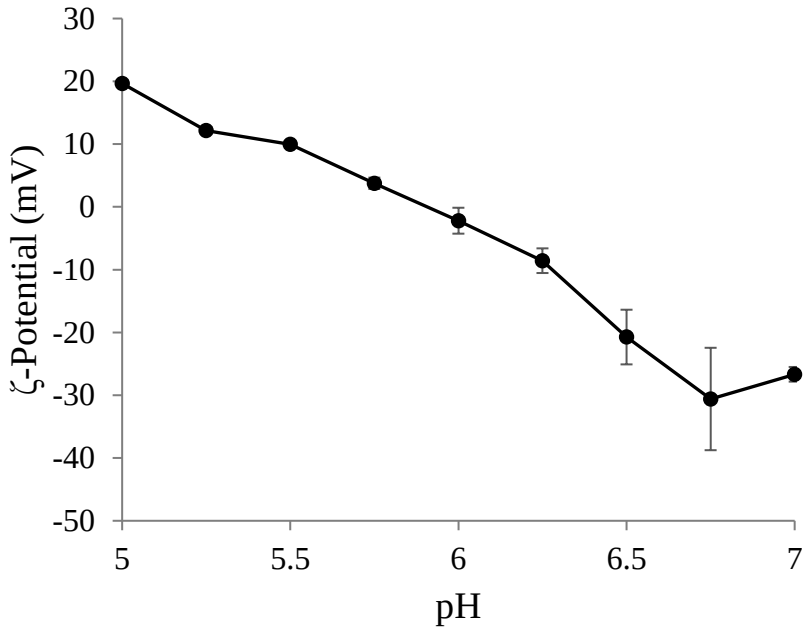

Figure 8. Effect of pH on the ζ-potential of 0.01% ZNP (w/v) in aqueous suspension

2.4.2 Charge Stabilization of ZNPs with ι-CGN

Addition of ι-CGN had an effect on the surface charge of ZNPs in aqueous dispersions at pH 5 (Figure 8). In these conditions, ZNPs alone possessed an average ζ-potential of ~15 mV. Addition of small concentrations of ι-CGN (0.0001% w/v) decreased the observed ζ-potential of ZNPs from positive to nearly zero, which coincided with a visual increase in aggregation and sedimentation. Further addition of ι-CGN inverted the detected surface charge to negative values, reaching an average ζ-potential of approximately -45 mV at an ι-CGN concentration of 0.001% (w/v). Further increases in the concentration of added ι-CGN had no significant effect on the detected surface charge. It should be noted that higher added ι-CGN concentrations of 0.05% induced almost immediate sedimentation, which was contributed to bridging flocculation that has been observed in other polyelectrolyte-stabilized ZNP dispersions (Huang and others 2016).

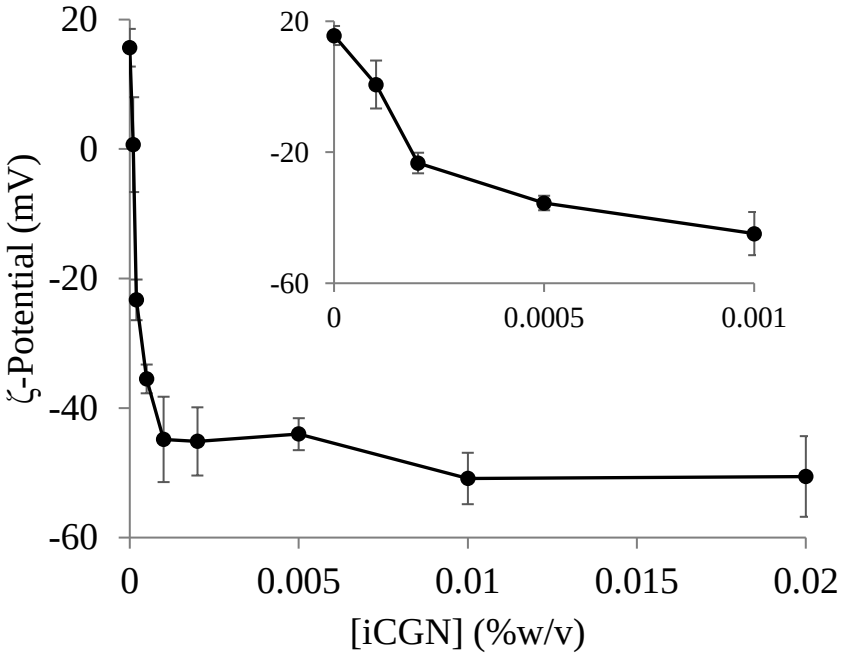

Figure 9. Effect of iCGN addition on detected ζ-potential of 0.01% ZNP (w/v) at pH 5; inset highlights data at low concentration of added iCGN

Hydrodynamic size of ZNPs at pH 5, observed to have an average hydrodynamic radius of about 560 nm, was also significantly affected by the addition of ι-CGN (Figure 9). Addition of 0.0001% ι-CGN (w/v) led to visible aggregation, coinciding with the charge neutralization of ZNPs (Figure 9), and the detected hydrodynamic size was correspondingly beyond the measurable

scale of the light scattering instrument. At 0.0005% of added ι-CGN (w/v), the hydrodynamic size of ZNPs was larger than ZNPs alone, which could be attributed to the relatively low magnitude of negative surface charge and correspondingly modest stabilization of ZNPs at this ι-CGN concentration. Increased ι-CGN concentrations of up to 0.001% (w/v) led to reductions in the observed hydrodynamic radius of ZNPs to about 100 nm. Further increases in ι-CGN concentration had no effect ($p > 0.05$) on the hydrodynamic size of ZNPs. Thus, the lowest concentration of added ι-CGN to achieve the smallest hydrodynamic radius of ZNPs (0.001% w/v) was also the lowest concentration needed to achieve the most negative surface charge. It should be noted that scattering from pure ι-CGN solutions at the tested concentrations was very weak, and scattering in mixtures would have been dominated by ZNP.

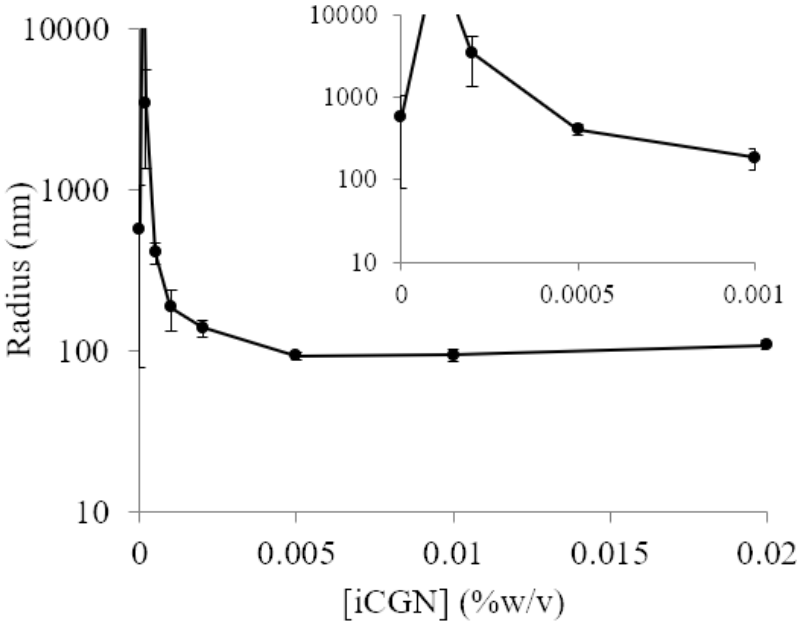

Figure 10. Effect of added iCGN on the hydrodynamic radius of 0.01% ZNP (w/v) at pH 5; inset highlights data at low concentration of added iCGN

ι-CGN is likely stabilizing ZNPs by coating the outer surface of the protein nanoparticles and giving them a negative charge in a concentration dependent manner (Figure 10). A minimum of 0.001% ι-CGN (w/v), reflecting a nanoparticle:ι-CGN weight ratio of 10:1, was needed to adsorb onto all of the binding sites of the zein nanoparticles and provide minimum stability to

aggregation in these conditions. The negatively charged polysaccharide provides electrostatic and steric stabilization by repulsing nearby zein nanoparticles and preventing aggregation.

Many other proteins have been able to interact with carrageenan and form soluble associative complexes, providing stability to the protein component (Dickinson 1998; Stone and Nickerson 2012; Imeson and others 1977). For instance, carrageenan was found to improve the stability of bovine serum albumin to heat and pressure changes. (Dickinson 2003). It has also been shown to improve the stability of casein to changes in calcium ion concentration (Dickinson 1998; Imeson and others 1977). The stabilizing effect of carrageenan has been attributed to it coating the protein surface and diminishing hydrophobically-driven protein aggregation (Dalgleish and Morris 1988; Dickinson 1998).

Other biopolymers have been used to stabilize ZNPs through associative interactions by forming an anionic outer coating (Chen and Zhong 2014; Hu and McClements 2015; Huang and others 2016; Patel and others 2010a). These studies found that pectin, alginate, gum Arabic, and sodium caseinate all were able to decrease the surface charge of ZNPs. In comparison to these studies, the detected ζ-potential of ι-CGN-stabilized-ZNPs (Figure 10) were similar to values reported for gum Arabic/ZNPs complexes and more negative than values for ZNPs with caseinate, pectin, and alginate/pectin. The observed ZNPs particle diameter of 100-200 nm (Figure 10) was also comparable to the findings of polysaccharide-stabilized ZNPs in other studies (Chen and Zhong 2015b; Davidov-Pardo and others 2015a; Hu and others 2015; Huang and others 2016; Patel and others 2010b).

As mentioned, the minimum amount of added ι-CGN to minimize hydrodynamic size of ZNPs at pH 5 corresponded to a ZNP:ι-CGN weight ratio of 10:1. This weight ratio is comparable to or even greater than optimal ratios to stabilize ZNPs with alginate (≤5:1; (Hu and McClements 2015)) or caseinate (≤10:3; (Patel and others 2010b)). A study on the composition of isolated ZNPs stabilized by alginate found that the actual content of alginate adsorbed to the surface corresponded to a ZNP:biopolymer ratio of approximately 6:1 at pH 5 and 10:1 at pH 6 (Chen and Zhong 2015b). While these findings cannot be directly related to the results of this study, it does indicate that charged biopolymers are likely able to saturate the surface of ZNPs in this weight ratio range.

2.4.3 Effect of pH on ZNPs Stability

ZNPs alone was found to be unstable to aggregation when the pH was adjusted to values above 5 (Figure 11). When the pH of the system was at 5, the radius of the nanoparticles was

about 560 nm; however, as the pH was increased to pH 7, the average hydrodynamic radius increased to 1300-2000 nm (Figure 11). The increase in particle size with increasing pH could be attributed to the loss of surface charge of the protein as the pH approached the isoelectric point of ZNPs (Figure 8).

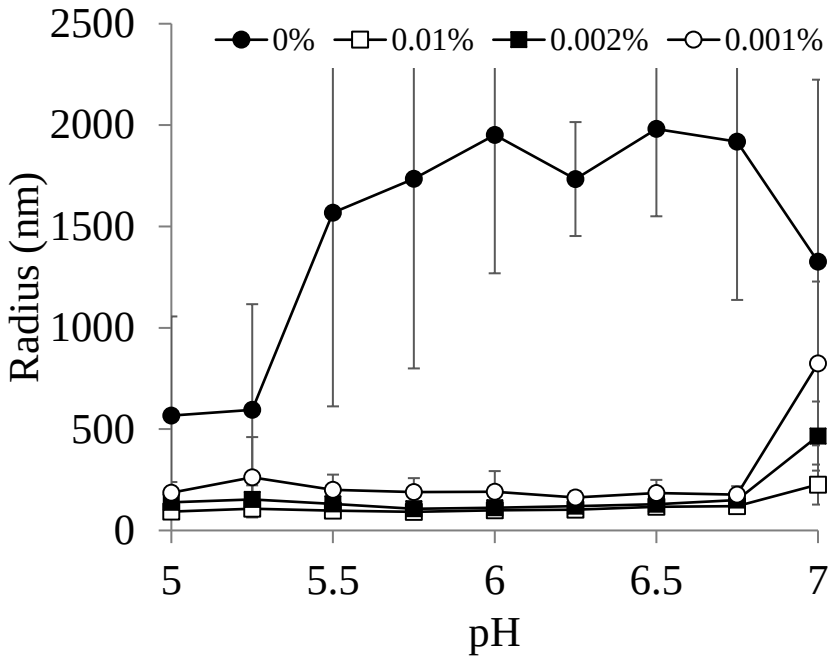

Figure 11. Effect of pH on the hydrodynamic radius of 0.01% ZNP (w/v) alone or with added iCGN at the specified iCGN concentrations (%w/v), measured within 2 hours after preparation

The addition of ι-CGN to the dispersions stabilized ZNPs against aggregation at pH values between 5 and 7, as indicated by the relatively smaller detected hydrodynamic radii values when compared to ZNPs without ι-CGN (Figure 11). When ZNPs was combined with ι-CGN at concentrations of 0.001% (w/v) or greater, the resulting particles were all negatively charged with little change in detected ζ-potential or particle size for the pH levels tested. This indicated a significant interaction between ZNPs and ι-CGN at pH values above the protein's isoelectric point, which has been observed in other electrostatically-driven polysaccharide-protein complexes and attributed to localized charge interactions with cationic residues (Park and others 1992). There was no significant difference ($p<0.05$) in size of ZNPs stabilized by ι-CGN concentrations between 0.001% and 0.02% (w/v) (Figure 11, 0.005% and 0.02% not shown). At these ι-CGN concentrations the hydrodynamic radii of the particles remained at approximately 100 nm over the pH range of 5 – 6.75 (Figure 11), while the ζ-potential remained approximately -40 to -50 mV.

The particle size also remained stable against change for at least 30 days when at least 0.001% ι-CGN (w/v) was added to ZNP dispersions. However, hydrodynamic radii of ZNP-ι-CGN complexes were significantly ($p<0.05$) larger at pH 7 when compared to all other pH levels, increasing to hydrodynamic radii of 200-800 nm.

The addition of ι-CGN also had a concentration-dependent effect on the turbidity of ZNP dispersions (Figure 12). Dispersions of ZNPs alone were more turbid ($p < 0.05$) than samples containing ι-CGN except at pH 7. Below pH 7, turbidity of dispersions stabilized by 0.001% ι-CGN (w/v) was less than ZNPs alone yet was greater than ZNPs stabilized by higher ι-CGN concentrations ($p < 0.05$). This did not agree with radius determination by dynamic light scattering, which did not find any significant difference in particle size among ZNPs with ≥ 0.001% ι-CGN (w/v) (Figure 11). However, greater turbidity of ZNPs with 0.001% ι-CGN concentration could be indicative of a greater proportion of larger particles compared to very small ZNPs, which are relatively de-emphasized in light scattering measurements. Turbidity values of ZNP dispersions combined with higher ι-CGN concentrations of 0.005%, 0.01%, and 0.02% ι-CGN were not significantly different at the tested pH levels. At pH 7, turbidity values of all samples were significantly greater than turbidity of ι-CGN-stabilized ZNPs at other pH levels but were not significantly different from ZNPs alone ($p < 0.05$).

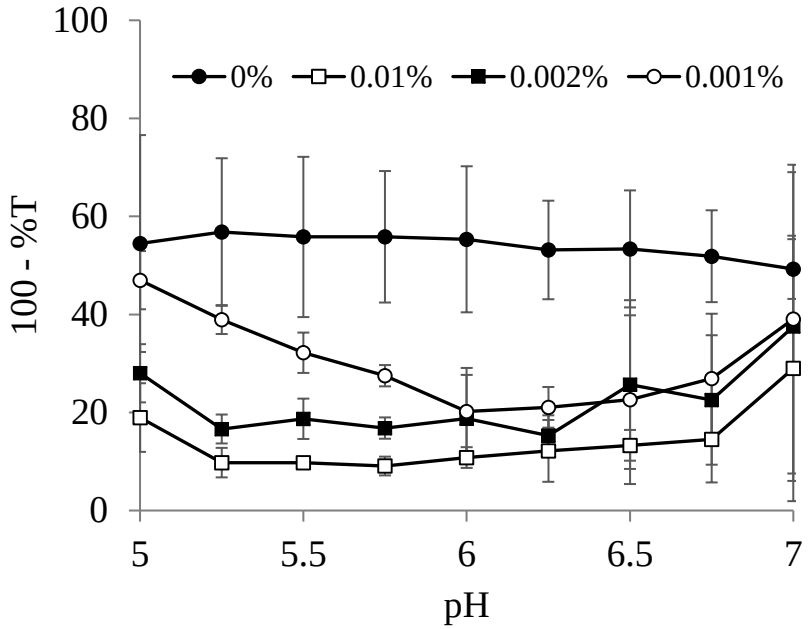

Figure 12. Effect of pH on the turbidity of ZNP suspensions (0.01% w/v) alone or with added iCGN at the specified iCGN concentration (%w/v) measured within 2 hours after preparation

The increase in particle size and turbidity at pH 7 among ZNPs samples with ι-CGN was likely due to weaker binding interactions between ZNPs and ι-CGN, allowing more aggregation between ZNPs in dispersion. Proteins have a net negative charge when pH > pI, determined to be pH > 6 for ZNPs (Figure 8), and the greater density of negative charges on the protein surfaces restricts accessibility of the negatively-charged ι-CGN to bind to remaining cationic binding sites, such as histidine and arginine residues (Shukla and Cheryan 2001). As the pH value was increased, there would then have been an increasing inhibition of interactions between ι-CGN and ZNPs. Although the magnitude of the ζ-potential value of ZNPs alone at pH 7 would imply significant electrostatic repulsions between particles and an increased stability against aggregation, there were obviously other factors driving aggregation between the negatively-charged ZNPs.

In previous studies, other biopolymers have been used to stabilize ZNPs to pH changes with mixed success, where both electrostatic and steric repulsion forces with a peptide-component have been important in stabilizing ZNPs. Gum Arabic, a natural anionic glycopeptide, was able to stabilize oil-encapsulating-ZNPs and maintain the particle diameter at about 100 nm in the pH range of 4-8 (Chen and Zhong 2015b). Caseinate interactions also provided excess negative surface charges to ZNPs alone, and resulting complexes were stable at pH 7.2 and 6.5 (Patel and others 2010b). These studies argued that increased stability over a wide pH range was attained by electrosteric stabilization of the ZNPs, preventing interactions between hydrophobic residues on the ZNPs surfaces. Furthering the argument on the importance of steric contributions, even greater stability was attained when ZNPs was stabilized by Maillard conjugates of dextran and caseinate, maintaining a particle diameter of about 250 nm from pH 3-9 (Davidov-Pardo and others 2015a). In this case, the dextran component of the conjugates imparted enhanced steric stabilization (Davidov-Pardo and others 2015a). Not all proteins are necessarily good stabilizers of ZNPs, as indicated by studies with whey proteins above pH 5 (Chen and others 2014a; Zou and others 2016a).

Polysaccharides without additional peptides have produced mixed results in stabilizing ZNPs to pH changes. Interactions with pectin or alginate, polysaccharides lacking a peptide fraction, were unable to prevent aggregation of ZNPs above pH 5 (Huang and others 2016), which could be attributed to the weak anionic charge of these polysaccharides being unable to significantly interact with ZNPs. An earlier study was able to stabilize ZNPs with alginate over a very wide pH range of 3-8 by also utilizing the surfactant tween 80 at a ZNP:alginate:surfactant

ratio of 40:10:4 (Hu and McClements 2015). Interestingly, both of these studies indicated minimal aggregation among both stabilized and unstabilized ZNPs at pH 7, unlike findings of this study that showed slight destabilization. The reported stability at pH 7 could be attributed to the technique of diluting fresh ZNPs samples in a strong pH 7 buffer, which would quickly shift the pH to 7 rather than the relatively slow alkali titration performed in this study.

In comparison to previous publications, ι-CGN has been found in this study to stabilize ZNPs at the pI of zein and up to pH 6.75 without an additional peptide or surfactant component (Figure 11). This is likely due to the fact that sulfonated polysaccharides such as ι-CGN have been shown to be more effective at binding with proteins when pH > pI, in contrast to carboxylated polysaccharides like pectin (Dickinson 2003; Hansen 1982; Stone and Nickerson 2012). Furthermore, the critical upper pH defining the limit at which anionic polysaccharides are able to significantly interact with protein was found to be higher for carrageenan than pectin (Wagoner and others 2016).

2.4.4 Dispersion Stability to Gravitational Forces

ZNP dispersions were prone to sedimentation during centrifugation and were less prone to sedimentation when stabilized by ι-CGN. Greater centripedal accelerations were required to induce significant sedimentation as the concentration of added ι-CGN was increased, indicating an increase in ZNPs stabilization. An example of the relative destabilization of samples at pH 5 is given in Figure 13, which shows the effect of centrifugation for 10 minutes at either 1306 x *g* or 5223 *x g* on the relative turbidity of bulk dispersion/supernatant. At the lower acceleration of 1306 x *g*, samples with ≤ 0.001% ι-CGN possessed significantly ($p < 0.05$) lower turbidity values and pellet formation was observed, indicating that a significant fraction of ZNPs sedimented from the bulk dispersion. Turbidity values after centrifugation at 1306 x *g* of ZNPs samples with higher ι-CGN concentrations were not significantly different, demonstrating that ≥ 0.002% ι-CGN (w/v) was sufficient to stabilize the particles against gravitational separation. In fact, centrifugation of ZNPs with ≥ 0.002% ι-CGN (w/v) at separation forces up to and including 3999 x *g* did not lead to any notable change in dispersion turbidity or formation of a pellet. A pellet was observed in these samples only after 10 minutes of centrifugation at a separation force of 5223 x *g*, coinciding with decreased turbidity in the supernatant (Figure 13). Very similar results were observed for samples at pH 6 (not shown), indicating excellent stability to sedimentation at pH near the pI of zein. The higher stability to gravitational separation among samples with ≥ 0.002% (w/v) agreed

with other observations of hydrodynamic size and turbidity among these samples during storage over 30 days, which had shown no significant changes. Interestingly, samples with 0.001% ι-CGN (w/v) were not as stable, and it is possible that this was the minimum concentration needed to stabilize ZNPs in static conditions but was insufficient to prevent sedimentation in relatively enhanced separation conditions.

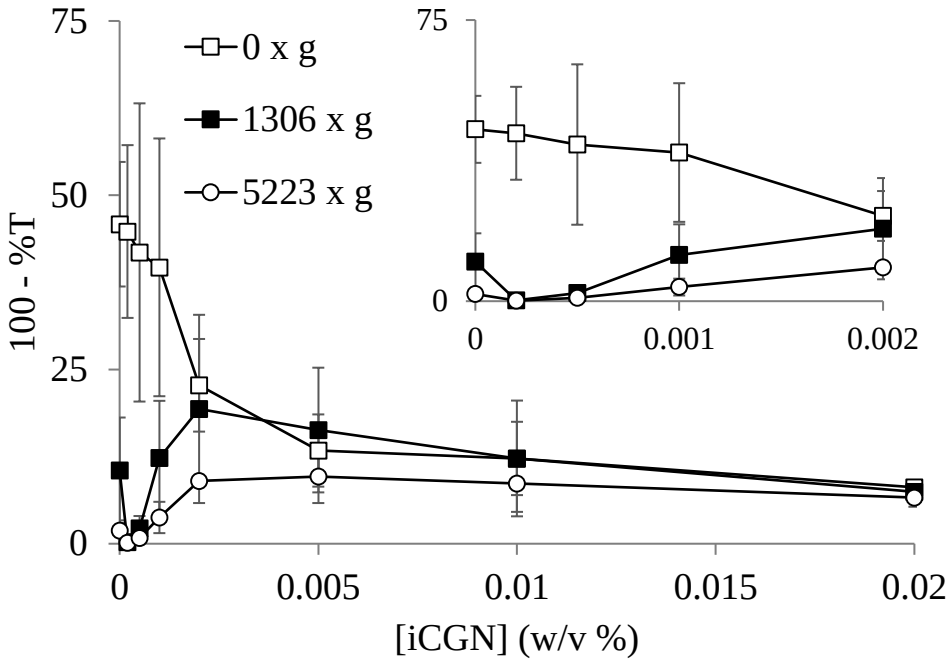

Figure 13. Effect of added iCGN on the turbidity of ZNP suspensions (0.01% w/v) at pH 5 before and after centrifugation at the specified accelerations; inset highlights data at low concentration of added iCGN

2.4.5 Atomic Force Microscopy

AFM was used to determine the morphology of surface-deposited ZNPs with and without ι-CGN, showing spherical particles with typical z-axis height values of ~10-30 nm (indicated by arrows in Figure 14). AFM images also showed what appeared to be agglomerates of individual particles with typical z-axis height values of ~40-80 nm, more than twice the size of smaller observed particles. There were no significant differences to the morphology or the agglomerate structure of ZNPs in samples with added ι-CGN at any of the tested concentrations (Figure 14).

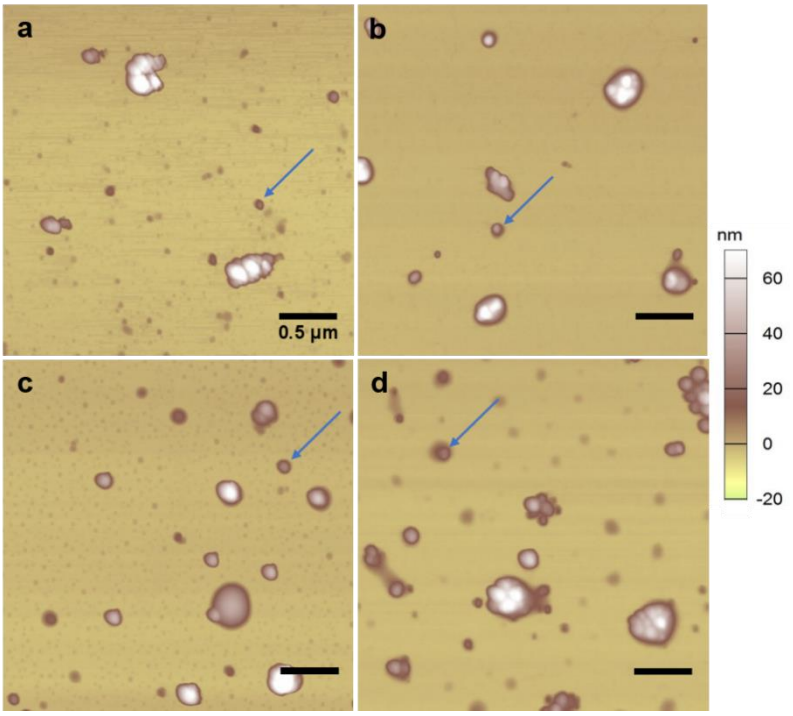

Figure 14. Atomic force microscopy topographical images of ZNP deposited from 0.01% (w/v) ZNP suspensions with (A) no added iCGN, or with iCGN concentrations (%w/v) of (B) 0.002%, (C) 0.01%, or (D) 0.02%. *Scale bars apply to all images; arrows indicate ZNP that did not agglomerate during preparation-related drying*

Prior AFM studies on mica-deposited, desiccated samples have also observed spherical ZNPs particles with comparable dimensions to those found in this study (Chen and others 2013; Li and others 2012a), indicating that these samples were consistent with prior investigations of ZNPs. Shape and dimensions of the particles were also comparable to studies performed with scanning electron microscopy (Gomez-Estaca and others 2012; Zhong and Jin 2009) and transmission electron microscopy imaging (Patel and others 2010b). Since samples were deposited as a dispersion and dried, the appearance of deposited materials in Figure 14 must take into account the highly probable shrinkage of particles as the aqueous solvent was removed, as well as the induced agglomeration of particles as their relative concentration increased during drying. Light scattering measurements of these samples had indicated mean hydrodynamic diameters of about 200-300 nm (Figure 11), which reflected the size of hydrated particles with hydrated/diffuse layers on the periphery of the particles. With shrinkage and drying-induced agglomeration a likely factor in the measured heights among AFM images, comparisons of these values to diffusion-based measurements from light scattering were considered unreliable. However, it was proposed that the

agglomerates of particles found in Figure 14 could be attributed to increased ZNPs interactions during preparatory drying, as (i) light scattering did not indicate significantly larger size populations at the shown ι-CGN concentrations and (ii) the relative agglomerate concentration was observed to be dependent upon the drying rate and ZNPs dilution during sample deposition for AFM.

2.4.6 Elasticity of ZNPs and ι-CGN complexes

Elastic properties of the ZNPss with and without ι-CGN was measured by force spectroscopy. The Young's moduli of select samples as described in Table 1 were determined by the Oliver-Pharr model. Values of Young's moduli were on the order of 50-100 MPa. Furthermore, despite an initial decrease and gradual increase in average values to 140 MPa, there were no significant differences ($p < 0.05$) in determined Young's moduli of ZNPs after addition of different concentrations of ι-CGN. To the authors' knowledge, this is the first report of force spectroscopy successfully characterizing the elastic properties of individual ZNPs.

Table 1. Determined Young's Modulus of ZNP in butanol deposited on a mica surface with or without added iCGN. Letters denote significance groupings

[ICGN] (W/V%)	YOUNG'S MODULUS (MPA)	STD ERROR (MPA)
0%	114.87 [a]	29.51
0.002%	43.03 [a]	21.69
0.01%	71.05 [a]	24.50
0.02%	109.48[a]	23.33

In previous studies, the elasticity of zein-chitosan films measured from nanoindentation have been found to vary between 60-90 MPa whereas zein alone had a Young's modulus of 88 MPa (Escamilla-Garcia and others 2013). Reports of the tensile strength of zein films, a measure of the resistance of macroscopic films to extension before breaking, have varied widely from 6-400 MPa (Shi and others 2009; Xu and others 2012). Determined Young's moduli of ZNPs in this study were then in agreement with these previous reports of macroscopic films, and also indicate that the structural arrangement of zein into nanometer-scale ZNPs had no significant impact on the

observed elasticity. Carrageenan films have also shown similar properties with a tensile strength of 62 MPa (Kanmani and Rhim 2014). Since there was no significant impact of ι-CGN on the determined elasticity of ZNPs, ι-CGN adsorbed on the ZNPs surface likely did not produce any unexpected changes to the structural properties.

2.5 Conclusions

In conclusion, ι-CGN has been shown to be an effective stabilizer for ZNPs by coating the protein with an anionic outer layer. When a sufficient amount of ι-CGN is used, determined here to be at a ZNP:ι-CGN weight ratio of 10 or less, the hydrodynamic radius and dispersion turbidity of the stabilized particles remained consistent for up to 30 days. Addition of ι-CGN had no effect on elasticity of nanoparticles, but it was able to improve the resistance of ZNPs to aggregation from changes in pH and to sedimentation. Further studies are warranted on the stability of ι-CGN-stabilized-ZNPs to high ionic strength media or on their susceptibility to digestion in the gastrointestinal tract. By comparing results in this study with published findings, one could expect that ι-CGN binding to ZNPs should generally be stronger and occur at higher pH when compared to all other polysaccharides possessing carboxylate anions. On the other hand, comparison of these findings to those of caseinate-based or gum Arabic stabilizers has indicated that ι-CGN does not provide as much stability to pH changes as these components, possibly because it lacks the capacity to contribute significant additional interactions, such as hydrophobic association, or produces a thinner sterically-inaccessible layer on the ZNPs surface. Successful stabilization of these ZNPs will provide more conditions for their utility as potential encapsulating agents of bioactive compounds, adding value to these processed-corn byproducts.

2.6 Acknowledgements

The authors would like to thank Profs. Brad Reuhs and Haley Oliver at Purdue University for editorial assistance. Support during preparation of this manuscript was received from the Industry Fellows program, disbursed from the Department of Food Science at Purdue University. There was no scientific contribution or direction from any corporation or industrial interest during the course of this work.

2.7 References

Best, J. P., Cui, J., Müllner, M., & Caruso, F. (2013). Tuning the Mechanical Properties of Nanoporous Hydrogel Particles via Polymer Cross-Linking. *Langmuir, 29*(31), 9824-9831.

Campo, V. L., Kawano, D. F., da Silva, D. B., & Carvalho, I. (2009). Carrageenans: Biological properties, chemical modifications and structural analysis - A review. *Carbohydrate Polymers, 77*(2), 167-180.

Chen, H., & Zhong, Q. (2014). Processes improving the dispersibility of spray-dried zein nanoparticles using sodium caseinate. *Food Hydrocolloids, 35*, 358-366.

Chen, H. Q., & Zhong, Q. X. (2015). A novel method of preparing stable zein nanoparticle dispersions for encapsulation of peppermint oil. *Food Hydrocolloids, 43*, 593-602.

Chen, J., Zheng, J., McClements, D. J., & Xiao, H. (2014). Tangeretin-loaded protein nanoparticles fabricated from zein/β-lactoglobulin: Preparation, characterization, and functional performance. *Food Chemistry, 158*, 466-472.

Chen, J. J., Zheng, J. K., McClements, D. J., & Xiao, H. (2014). Tangeretin-loaded protein nanoparticles fabricated from zein/beta-lactoglobulin: Preparation, characterization, and functional performance. *Food Chemistry, 158*, 466-472.

Chen, Y., Ye, R., & Liu, J. (2013). Understanding of dispersion and aggregation of suspensions of zein nanoparticles in aqueous alcohol solutions after thermal treatment. *Industrial Crops and Products, 50*, 764-770.

Croguennoc, P., Meunier, V., Durand, D., & Nicolai, T. (2000). Characterization of Semidilute κ-Carrageenan Solutions. *Macromolecules, 33*(20), 7471-7474.

Dalgleish, D. G., & Morris, E. R. (1988). Interactions between carrageenans and casein micelles: electrophoretic and hydrodynamic properties of the particles. *Food Hydrocolloids, 2*(4), 311-320.

Davidov-Pardo, G., Joye, I. J., Espinal-Ruiz, M., & McClements, D. J. (2015). Effect of Maillard Conjugates on the Physical Stability of Zein Nanoparticles Prepared by Liquid Antisolvent Coprecipitation. *Journal of Agricultural and Food Chemistry, 63*(38), 8510-8518.

Davidov-Pardo, G., Joye, I. J., & McClements, D. J. (2015). Encapsulation of resveratrol in biopolymer particles produced using liquid antisolvent precipitation. Part 1: Preparation and characterization. *Food Hydrocolloids, 45*, 309-316.

Dickinson, E. (1998). Stability and rheological implications of electrostatic milk protein-polysaccharide interactions. *Trends in Food Science & Technology, 9*(10), 347-354.

Dickinson, E. (2003). Hydrocolloids at interfaces and the influence on the properties of dispersed systems. *Food Hydrocolloids, 17*(1), 25-39.

Escamilla-Garcia, M., Calderon-Dominguez, G., Chanona-Perez, J. J., Farrera-Rebollo, R. R., Andraca-Adame, J. A., Arzate-Vazquez, I., Mendez-Mendez, J. V., & Moreno-Ruiz, L. A. (2013). Physical and structural characterisation of zein and chitosan edible films using nanotechnology tools. *International Journal of Biological Macromolecules, 61*, 196-203.

Galazka, V. B., Smith, D., Ledward, D. A., & Dickinson, E. (1999). Complexes of bovine serum albumin with sulphated polysaccharides: effects of pH, ionic strength and high pressure treatment. *Food Chemistry, 64*(3), 303-310.

Gomez-Estaca, J., Balaguer, M. P., Gavara, R., & Hernandez-Munoz, P. (2012). Formation of zein nanoparticles by electrohydrodynamic atomization: Effect of the main processing variables and suitability for encapsulating the food coloring and active ingredient curcumin. *Food Hydrocolloids, 28*(1), 82-91.

Gu, Y. S., Decker, E. A., & McClements, D. J. (2004). Influence of pH and ι-Carrageenan Concentration on Physicochemical Properties and Stability of β-Lactoglobulin-Stabilized Oil-in-Water Emulsions. *Journal of Agricultural and Food Chemistry, 52*(11), 3626-3632.

Hansen, P. M. T. (1982). Hydrocolloid-protein interactions: relationship to stabilization of fluid milk products. A review. *Progress in Food and Nutrition Science, 6*(1-6), 127-138.

Hirt, S., & Jones, O. G. (2014). Effects of chloride, thiocyanate and sulphate salts on beta-lactoglobulin-pectin associative complexes. *International Journal of Food Science and Technology, 49*(11), 2391-2398.

Hu, D., Lin, C., Liu, L., Li, S., & Zhao, Y. (2012). Preparation, characterization, and in vitro release investigation of lutein/zein nanoparticles via solution enhanced dispersion by supercritical fluids. *Journal of Food Engineering, 109*(3), 545-552.

Hu, K., Huang, X., Gao, Y., Huang, X., Xiao, H., & McClements, D. J. (2015). Core-shell biopolymer nanoparticle delivery systems: Synthesis and characterization of curcumin fortified zein-pectin nanoparticles. *Food Chemistry, 182*, 275-281.

Hu, K., & McClements, D. J. (2015). Fabrication of biopolymer nanoparticles by antisolvent precipitation and electrostatic deposition: Zein-alginate core/shell nanoparticles. *Food Hydrocolloids, 44*, 101-108.

Huang, X. X., Huang, X. L., Gong, Y. S., Xiao, H., McClements, D. J., & Hu, K. (2016). Enhancement of curcumin water dispersibility and antioxidant activity using core-shell protein-polysaccharide nanoparticles. *Food Research International, 87*, 1-9.

Ikeda, S., & Morris, V. J. (2002). Fine-Stranded and Particulate Aggregates of Heat-Denatured Whey Proteins Visualized by Atomic Force Microscopy. *Biomacromolecules, 3*(2), 382-389.

Imeson, A. P., Ledward, D. A., & Mitchell, J. R. (1977). On the nature of the interaction between some anionic polysaccharides and proteins. *Journal of the Science of Food and Agriculture, 28*(8), 661-668.

Kanmani, P., & Rhim, J.-W. (2014). Properties and characterization of bionanocomposite films prepared with various biopolymers and ZnO nanoparticles. *Carbohydrate Polymers, 106*, 190-199.

Li, K. K., Yin, S. W., Yang, X. Q., Tang, C. H., & Wei, Z. H. (2012). Fabrication and Characterization of Novel Antimicrobial Films Derived from Thymol-Loaded Zein-Sodium Caseinate (SC) Nanoparticles. *Journal of Agricultural and Food Chemistry, 60*(46), 11592-11600.

Liang, H., Zhou, B., He, L., An, Y., Lin, L., Li, Y., Liu, S., Chen, Y., & Li, B. (2015). Fabrication of zein/quaternized chitosan nanoparticles for the encapsulation and protection of curcumin. *Rsc Advances, 5*(18), 13891-13900.

Luo, Y. C., Teng, Z., & Wang, Q. (2012). Development of Zein Nanoparticles Coated with Carboxymethyl Chitosn for Encapsulation and Controlled Release of Vitamin D3. *Journal of Agricultural and Food Chemistry, 60*(3), 836-843.

Oliver, W. C., & Pharr, G. M. (1992). An improved technique for determining hardness and elastic modulus using load and displacement sensing indentation experiments. *Journal of Materials Research, 7*(6), 1564-1583.

Park, J. M., Muhoberac, B. B., Dubin, P. L., & Xia, J. L. (1992). Effects of Protein Charge Heterogeneity in Protein-Polyelectrolyte Complexation. *Macromolecules, 25*(1), 290-295.

Patel, A., Hu, Y., Tiwari, J. K., & Velikov, K. P. (2010). Synthesis and characterisation of zein-curcumin colloidal particles. *Soft Matter, 6*(24), 6192-6199.

Patel, A. R., Bouwens, E. C. M., & Velikov, K. P. (2010). Sodium Caseinate Stabilized Zein Colloidal Particles. *Journal of Agricultural and Food Chemistry, 58*(23), 12497-12503.

Patel, A. R., & Velikov, K. P. (2014). Zein as a source of functional colloidal nano- and microstructures. *Current Opinion in Colloid & Interface Science, 19*(5), 450-458.

Sader, J. E., Chon, J. W. M., & Mulvaney, P. (1999). Calibration of rectangular atomic force microscope cantilevers. *Review of Scientific Instruments, 70*(10), 3967-3969.

Shi, K., Kokini, J. L., & Huang, Q. R. (2009). Engineering Zein Films with Controlled Surface Morphology and Hydrophilicity. *Journal of Agricultural and Food Chemistry, 57*(6), 2186-2192.

Shukla, R., & Cheryan, M. (2001). Zein: the industrial protein from corn. *Industrial Crops and Products, 13*(3), 171-192.

Stone, A. K., & Nickerson, M. T. (2012). Formation and functionality of whey protein isolate-(kappa-, iota-, and lambda-type) carrageenan electrostatic complexes. *Food Hydrocolloids, 27*(2), 271-277.

Tang, W.-W., Dong, F., Wong, K.-H., & Wang, Y. (2015). Preparation, Characterization and in vitro Release of Zein-pectin Capsules for Target Delivery. *Current Drug Delivery, 12*(4), 397-405.

Wagoner, T., Vardhanabhuti, B., & Foegeding, E. A. (2016). Designing Whey Protein-Polysaccharide Particles for Colloidal Stability. *Annual Review of Food Science and Technology, Vol 7, 7*, 93-116.

Wu, Y., Luo, Y., & Wang, Q. (2012). Antioxidant and antimicrobial properties of essential oils encapsulated in zein nanoparticles prepared by liquid-liquid dispersion method. *Lwt-Food Science and Technology, 48*(2), 283-290.

Xu, H., Chai, Y. W., & Zhang, G. Y. (2012). Synergistic Effect of Oleic Acid and Glycerol on Zein Film Plasticization. *Journal of Agricultural and Food Chemistry, 60*(40), 10075-10081.

Zhang, Y. Q., Niu, Y. G., Luo, Y. C., Ge, M., Yang, T., Yu, L. L., & Wang, Q. (2014). Fabrication, characterization and antimicrobial activities of thymol-loaded zein nanoparticles stabilized by sodium caseinate-chitosan hydrochloride double layers. *Food Chemistry, 142*, 269-275.

Zhong, Q. X., & Jin, M. F. (2009). Zein nanoparticles produced by liquid-liquid dispersion. *Food Hydrocolloids, 23*(8), 2380-2387.

Zou, L. Q., Zhang, Z. P., Zhang, R. J., Liu, W., Liu, C. M., Xiao, H., & McClements, D. J. (2016). Encapsulation of protein nanoparticles within alginate microparticles: Impact of pH and ionic strength on functional performance. *Journal of Food Engineering, 178*, 81-89.

CHAPTER 3 FATE OF LUTEIN-CONTAINING ZEIN NANOPARTICLES FOLLOWING SIMULATED GASTRIC AND INTESTINAL DIGESTION

Reprinted from Food Hydrocolloids, Volume 87, Author: Chris Cheng, Mario Ferruzzi, Owen Jones, "Fate of Lutein-Containing Zein Nanoparticles Following Simulated Gastric and Intestinal Digestion", p 229-236, Copyright 2018, with permission from Elsevier

3.1 Abstract

Zein nanoparticles (ZNPs) were prepared to encapsulate lutein via solvent-induced nanoprecipitation, and the stability of the zein nanoparticles with encapsulated lutein (ZLNPs) was determined following *in vitro* gastric and intestinal simulation. Stability was assessed by dynamic light scattering, gel electrophoresis, tendency towards sedimentation, and both atomic force and light microscopy. ZNPs possessed a hydrodynamic radius of ~75 nm, which was not altered with incorporation of lutein. Gastric digestion conditions induced significant aggregation and sedimentation of ZLNPs, which were not fully digested by gastric enzymes and were found adhered to lipid droplets in light micrographs. Aggregation was decreased and digestion was promoted during gastric digestion if salt was omitted, indicating that a high ion concentration increased ZLNP aggregation and limited enzymatic digestion. ZLNPs were redispersed in intestinal conditions and completely digested into peptides. In comparison to aqueous lutein dispersions, incorporation within ZNPs increased lutein's digestive stability by ~58% but reduced its micellarization efficiency by ~42%. These findings indicated that ZNPs provided a degree of physical protection to encapsulated carotenoids in gastric conditions yet might partially interfere with certain pathways for carotenoid bioaccessibility.

3.2 INTRODUCTION

Colloidal delivery vehicles provide the means to successfully transport bioactive molecules and improve the efficacy of their delivery to the human body. Necessary properties of colloidal delivery vehicles are stability in the continuous matrix of the product, protection of the active molecule against degradation or loss during storage, and significant release of the active molecules when at the appropriate site (Matalanis and others 2011). Colloidal vehicles prepared from food-grade protein possess the added advantage of providing a natural encapsulating material with

nutritive benefits (Matalanis and others 2011). However, many common protein-based encapsulants are susceptible to rapid digestion/deterioration prior to reaching the desired site in the gastro-intestinal tract unless the protein is modified or coated with secondary non-digestible material (Livney 2010).

Colloidal delivery vehicles assembled from the corn protein, zein, offer unique advantages of low ingredient cost and potentially reduced accessibility to digestive enzymes. As a byproduct of corn biodiesel and starch production, it is an abundant and generally-recognized-as-safe protein source, yet of limited market value (Shukla and Cheryan 2001). As a hydrophobic prolamin, zein is soluble in 70-90% aqueous ethanol mixtures (Patel and Velikov 2014b). Zein nanoparticles (ZNPs) can be formed by dispersing such ethanol mixtures in water under shear, which induces nanoprecipitation (Zhong and Jin 2009). ZNPs have been used to encapsulate a variety of functional compounds, such as resveratrol (Davidov-Pardo and others 2015b), tangeretin (Chen and others 2014b), curcumin (Gomez-Estaca and others 2012; Hu and others 2015; Liang and others 2015), and β-carotene (Chuacharoen and Sabliov 2016b).

ZNPs have great potential to improve the stability and bioaccessibility of other bioactives such as the carotenoid compound lutein. Lutein is a xanthophyll found in leafy green vegetables and corn that is relatively polar because of two extra hydroxyl groups (Reboul and others 2006). It has been associated with reduced cataract formation in the human eye and a reduced risk of coronary heart disease and stroke (Arnal and others 2009; Granado and others 2003). The USDA and HHS recommend an average daily intake of 3.8 mg lutein per day, and 6-14 mg per day has been associated with improved eye health; however, the average daily intake of lutein in the United States is only ~1.7 mg (Alves-Rodrigues and Shao 2004). Furthermore, lutein bioaccessibility in vegetables is moderately low (14-55%) (Serrano and others 2005) and, like many carotenoids, are susceptible to degradation by heat, oxygen, and light (Lin and Chen 2005; Tang and Chen 2000). Previous studies have shown that ZNP can be used to encapsulate lutein (Chuacharoen and Sabliov 2016a; Hu and others 2012b) and can even provide stability against photo-oxidation and storage (Chuacharoen and Sabliov 2016a).

Despite the promise of ZNP as a vehicle for controlled delivery of an important nutrient like lutein, there is little understanding of how digestion processes impact the structure and suspension stability of ZNPs or how this corresponds to relative bioaccessibility of encapsulated carotenoids. It is known that aqueous suspensions of ZNPs remain stable against aggregation in

acidic pH conditions but aggregate quickly at pH values closer to 6 (Cheng and Jones 2017; Shukla and Cheryan 2001), which would be relevant to gastric and intestinal digestion conditions, respectively. Studies have also shown that zein protein has some resistance to pepsin digestion for up to 60 minutes but is susceptible to pancreatic enzymes (Fu and others 2002). Stability of ZNP suspensions in acidic conditions and resistance of zein to pepsin action may allow lutein encapsulated zein nanoparticles (ZLNPs) to improve digestive stability and bioaccessibility of lutein by protecting the carotenoid during gastric digestion and releasing it into the intestine. The objective of this study was then to determine the extent to which *in vitro* digestion conditions impact ZNP structure, suspension stability, and the subsequent relative bioaccessibility of encapsulated lutein.

3.3 MATERIALS AND METHODS

3.3.1 Materials

Zein (98% solids), pancreatin from porcine pancreas (98.5% solids), pepsin from porcine gastric mucosa (19.6% protein, 622 units/mg), lipase (38% protein, 151 units/mg), bile salts, analytical standards of lutein and β-apo-8-carotenal, hydrochloric acid (HCl), glycine, bromophenol blue, tetramethylethylenediamine , fluorescein isothiocyanate, nile red, coomassie blue R-250, bicinchoninic acid (BCA) assay kit reagents, and sodium azide were supplied by Sigma-Aldrich (St. Louis, MO). Xanthan gum was supplied by TIC Gums (Belcamp, MD). Acrylamide/bis acrylamide, sodium dodecyl sulfate, Tris(hydroxymethyl)-aminomethane, glycerol, ammonium persulfate, sodium chloride (NaCl), and sodium bicarbonate were purchased from Fisher Scientific. Solvents used for this study, including dimethyl sulfoxide, ethanol, ethyl acetate, methanol, methyl tert-butyl ether (MTBE), acetone, and acetic acid were purchased from either Sigma-Aldrich or Fisher Scientific. Unless otherwise specified, solutions were prepared with ultrapure water (resistivity (σ) $\geq$ 18 mΩ-cm).

Lutein for encapsulation in nanoparticles was purchased from Roche (Basel, Switzerland) in the form of gelatin-encapsulated beads. Beadlets were hydrated in water (50 mg in 3 mL) and vortexed for 5 minutes. Lutein was extracted in 1:1 MTBE:acetone and dried under Nitrogen.

3.3.2 Preparation of Zein Nanoparticles (ZNP)

The antisolvent precipitation method was used for producing ZNPs as outlined by Zhong (2009). Zein was dissolved in 80% aq. ethanol at a concentration of 25 g/L. Mixtures were then

dispersed drop-wise in water (final ethanol:water volume ratio of 1:3) with simultaneous shear using a benchtop homogenizer (Ultra Turax T-25 Basic). Resulting dispersions were concentrated with a rotary evaporator to approximately 50% or less of the original volume. The sample was then centrifuged for 10 min at 2880 x *g*, and the supernatant containing ZNP was stored at 4°C. The solids content of resulting dispersions was measured gravimetrically by evaporating moisture from aliquots in a vacuum oven at 70°C. Final ZNP content was standardized to 1% (w/v) by dilution with pure water for subsequent use.

3.3.3 Preparation of Zein Nanoparticles with lutein (ZLNP)

ZLNPs were also prepared using the antisolvent precipitation method. Ethanol solutions of lutein (0.5 g/L) were first mixed with the zein solutions dissolved in 80% aq. ethanol at a 1:2 volumetric ratio. Precipitation of the zein/lutein solution into nanoparticles, concentration by rotary evaporation, centrifugation to remove large aggregates, solids content determination of final dispersions, and standardization to 1% (w/v) by dilution were performed using the same procedures outlined in section 2.2.

3.3.4 Particle Characterization

Dynamic light scattering (DLS) was used to determine the hydrodynamic radii of ZNP or ZLNP with an ALV-CGS3 light scattering goniometer (ALV, Langen, Germany) equipped with an HeNe laser (wavelength = 632.8 nm). Measurements were made at 90° scattering angle and a temperature of 25°C. Particle size distributions were obtained with the CONTIN algorithm, supplied by instrument software (ALV, Langen, Germany). Viscosity of the continuous phase, used for calculating hydrodynamic radii from determined diffusion coefficients, was taken to be that of pure water (0.890 mPa-s). Preliminary experiments verified the lack of concentration-dependent effects on the determined diffusion coefficient at ZNP or ZLNP concentrations of 0.01% (w/v).

3.3.5 Quantification of Lutein Content

Lutein was extracted from ZLNP suspensions by adding 1:1 MTBE:acetone and centrifuging (9,300 g, 10 min). The solvent phase containing the carotenoid was then removed and dried under blowing nitrogen. Additional washes were performed until the solvent phase was colorless. Extractions of lutein from aqueous dispersions and accumulations on the surface of ZLNP (not encapsulated) were performed with MTBE in the absence of acetone. All samples were stored at -80^{o}C until further analysis.

Extracted lutein content was quantified by HPLC using the method described by Kean (Kean and others 2008). In brief, a Hewlett-Packard 1090A HPLC system with a 79880A diode array detector with 250-600 nm wavelength was utilized with an YMC carotenoid reverse phase C30 column (2.0 x 250 mm). The injection volume of the sample was 10 uL. The mobile phase was composed of a binary composition of methanol and ethyl acetate with a flow rate of 0.37 mL/min. A sample chromatogram of lutein is provided as supplementary information (Figure S1).

Encapsulation efficiency of ZLNPs (%) was calculated as the lutein content extracted from ZLNPs after their production and isolation in relation to the initial content of lutein incorporated within the zein mixtures. Loading capacity of ZLNPs (%) was calculated as the lutein content extracted from ZLNPs after production and isolation in relation to the zein content of isolated ZLNPs. For the tested system, the average encapsulation efficiency of lutein within ZLNP was 61.39% ± 6.64, while the % loading was 0.91% ± 0.04. For reference, 100 g of kale contains 40 mg of lutein/zeaxanthin (Alves-Rodrigues and Shao 2004). Insignificant lutein contents were found among ZLNP extracts that did not include added acetone (used to disrupt ZLNPs), indicating that the ~39% of lutein not recovered from the ZLNPs were likely accumulated in zein aggregates, which were lost during the preparatory transfer and centrifugation steps. Thus, true encapsulation efficiency within zein (bulk aggregate or ZLNP) was likely much higher, with the encapsulation efficiency of ~61% being a reflection of the conversion efficiency between zein and nanoparticle during antisolvent precipitation.

3.3.6 *In Vitro* Digestion Procedure

In vitro digestion protocol, including a simulated gastric and intestinal phase, was performed on ZLNP suspensions and lutein control as described by Garret and others (1999) with minor modifications. The oral phase was not performed because beverages and liquids have short exposure times to oral conditions (Minekus and others 2014). Samples taken before or after each phase were stored at -80^{o}C until further preparation or analysis.

Gastric simulation was performed by combining 10 mL of ZLNP or control suspensions with 1g canola oil and 20 mL 0.9 % NaCl solution. The pH was adjusted to 3.5 with 1.0 N HCl solution. 2 mL of 10 mg/mL pepsin solution suspended in 0.1N HCl was then added to the sample. The pH was adjusted to 2.5 and they were then incubated for 1 hr at 37°C in a shaking water bath at 90 RPM.

After gastric digestion, intestinal simulation was performed by submerging ZLNP or control samples in ice and adjusting the pH to 5.0 with 1 N sodium bicarbonate. A 2 mL solution of 0.1 N sodium bicarbonate containing 40 mg pancreatin and 20 mg lipase, as well as a 3 mL solution of 0.1 N sodium bicarbonate containing 90 mg bile extract, was then added to samples. The pH was adjusted to 6.5 and the samples were incubated for 2 hrs at 37°C in a shaking water bath at 90 RPM. Molar lutein content in the total digesta following intestinal simulation, $[L]_I$, was quantified after extraction (section 2.5). Comparison to the total lutein content determined from pre-digested ZLNP samples, $[L]_T$, was used to calculate the Digestive Stability (DS) of the lutein with eqn. 1:

$$DS = [L]_I/[L]_T \quad [1]$$

To isolate the aqueous micellar fraction believed to contain lutein, aliquots of the digesta following intestinal simulation were centrifuged at 10,000 x g for 1 h. Supernatants were then passed through 0.45 μm syringe filters before extraction and quantification of the molar lutein content, $[L]_M$. Bioaccessibility was assessed by the Micellarization Efficiency (ME), given by eqn. 2:

$$ME = [L]_M/[L]_I \quad [2]$$

Lutein solutions (1 mg/mL) were prepared in pure ethanol as a control. These solutions were diluted in water at a 1:10 volumetric ratio, and ethanol was removed by rotary evaporation directly prior to beginning the *in vitro* digestion stages. Complete transfer of lutein content into the initial digestion media was verified by extraction and quantification (section 2.5), and the lutein content was subsequently determined after simulated digestion.

To identify the pH-stability of ZNP suspensions relevant to the *in vitro* gastric digestion process, suspensions were prepared with or without oil and salt but without any added enzymes. Suspensions were acidified to reflect the gastric conditions, as described above. Large, visible aggregates formed in some of the suspensions, and aliquots were taken from the middle of sample suspensions after allowing the large aggregates to sediment during storage. Quantity of protein-based material that remained dispersed and did not sediment was determined from these aliquots by protein content determination with the BCA assay.

3.3.7 Confocal Laser Scanning Microscopy

Confocal laser microscopy was used to characterize the microstructure of digested ZNPs (Nikon's A1Rsi, Nikon, Melville, NY). A 10x eyepiece and a 60x oil-immersion objective lens

was used. Nile Red (0.1%) dissolved in acetone and fluorescein isothiocyanate (0.1%) dissolved in dimethyl sulfoxide were used to stain the lipids and proteins, respectively, of digested samples.

3.3.8 SDS-PAGE

Sodium dodecyl sulfate polyacrylamide gel electrophoresis (SDS-PAGE) was performed to analyze digested protein samples. Samples were prepared by adding sodium dodecyl sulfate reducing buffer with tris(hydroxymethyl)aminomethane, stained with bromophenol blue tracking dye, and boiled for 5 minutes at 95°C. Sample aliquots (10 μL) were then loaded onto a polyacrylamide gel composed of a 5% stacking gel and a 15% resolving gel. After separation, gels were stained with Coomassie Blue R-250. Molecular weights of protein bands were determined using known molecular weight standards (Precision Plus Protein All Blue Standards, Bio-Rad Laboratories, Hercules, CA). Gels were imaged with a GelDoc XR system using transwhite illumination (BioRad).

3.3.9 Atomic Force Microscopy (AFM)

Topographical images of nanoparticles were obtained in intermittent-contact mode with an MFP3D atomic force microscope (Asylum Research, Santa Barbara, CA). Aluminum-coated silicon cantilevers with approximate resonance frequency of 150 kHz and force constant of 5 N/m (TAP150AL-G, Ted Pella, Inc., Redding, CA) were used. The typical scan rate of 0.7-0.8 Hz was used. Samples were prepared by pipetting 12 μL of dilute sample onto freshly cleaved mica discs and dried with filtered air. Images selected for publication were representative of each sample and chosen from at least 20 images.

3.3.10 Statistical Analysis

All analyzed samples were prepared in triplicate unless otherwise specified. Digestive stability and micellarization efficiency was determined with paired t-test ($P < 0.05$). Multivariate analysis ($P < 0.05$) were determined by one-way analysis of variance with Tukey-Honest Significant Differences (HSD). Both methods were calculated using JMP statistical software (developed by SAS).

3.4 RESULTS AND DISCUSSION

3.4.1 Characterization of Lutein Encapsulated Zein Nanoparticles (ZLNPs)

DLS and AFM were used to characterize the size and morphology of ZLNPs (Figure 15). DLS measurements showed that ZLNPs had an average radius of 72.1 ± 25.3 nm, while ZNPs

without lutein had an average radius of 71.9 ± 25.3 nm, which was consistent with previous literature (Chen and Zhong 2015b; Huang and others 2016; Patel and others 2010b). AFM images taken of the surface-deposited and dried ZLNPs and ZNPs showed spherical particles with approximate edge-to-edge diameters of 100-200 nm (Figure 15), consistent with AFM images of similar ZNPs from previous studies (Chen and others 2013; Cheng and Jones 2017). Diameter values from AFM images were then highly consistent with the radii values observed from DLS measurements, which would indicate an average diameter of ~145 nm.

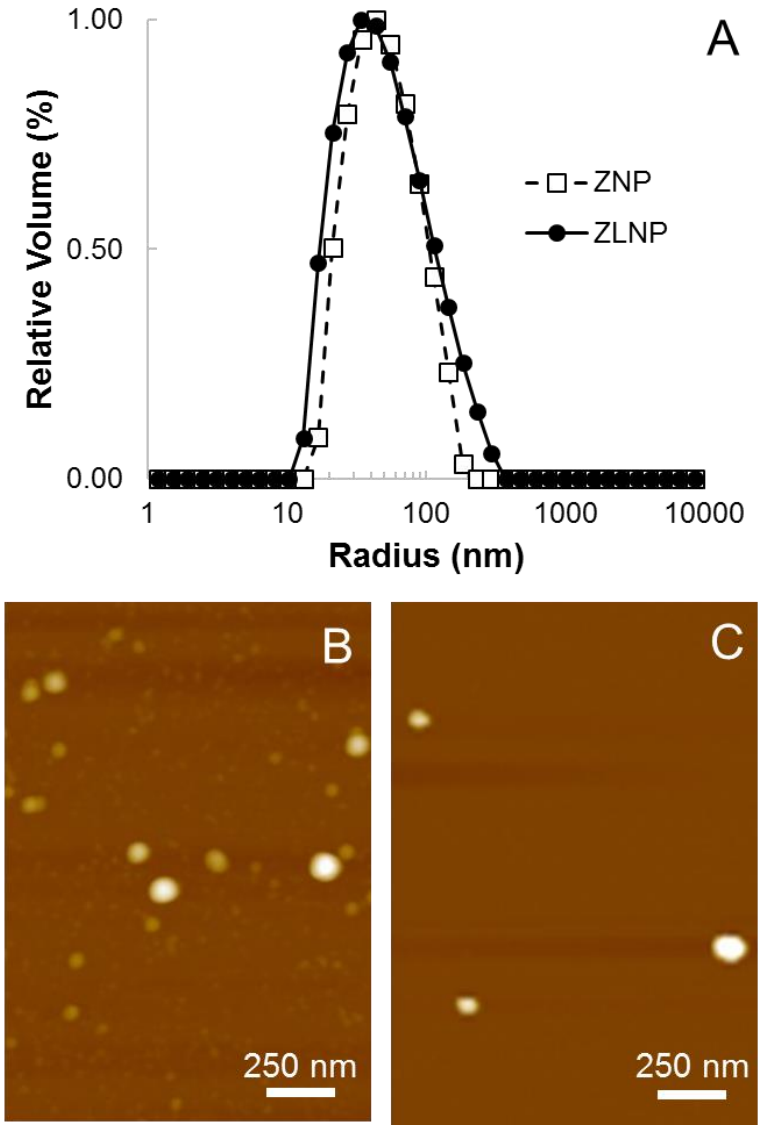

Figure 15. Particle size of nanoprecipitated zein suspension determined by dynamic light scattering of ZNP or ZLNP suspensions (A) and AFM topographical height of ZNPs (B) or ZLNPs (C).

Particles and clusters of particles were also observed among confocal micrographs of ZLNPs (Figure 16). Clustering of the particles in the micrographs was not observed by initial light scattering measurements and was attributed to the tendency of particles to aggregate during storage. This is consistent with prior observations of ZNP, which aggregated significantly in aqueous suspensions unless stabilized by acidic conditions or interactive additives such as surfactants or charged polysaccharides (Chen and Zhong 2015b; Cheng and Jones 2017; Davidov-Pardo and others 2015a; Patel and others 2010b).

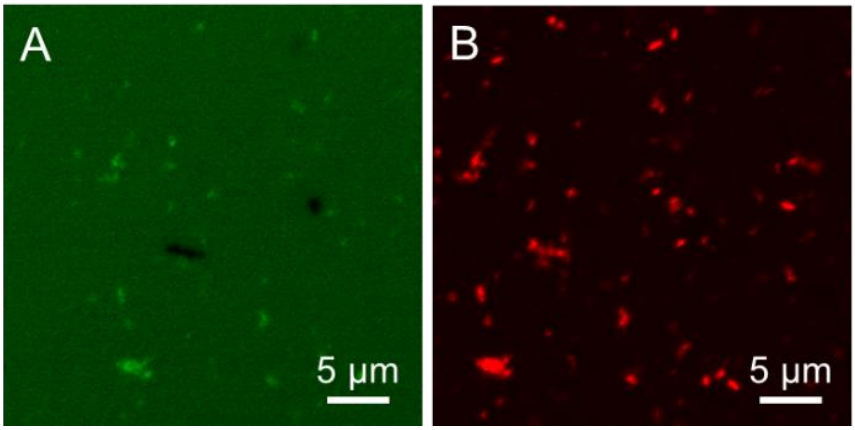

Figure 16. Confocal microscopy images of ZLNP with fluorescence labelling by (A) Fluorescein Isothiocyanate and (B) Nile Red

3.4.2 Impact of simulated digestion conditions on lutein

To determine whether lutein was protected against deterioration or loss during digestive conditions, the total content of lutein was characterized after simulated gastric and small intestinal digestive conditions and reported as Digestive Stability (DS) (Figure 17). It was found that DS of lutein within ZLNPs was significantly greater (77.7%) than the control of lutein without zein (49.1%), indicating that ZNPs were successfully protecting the encapsulated lutein from degradation caused by exposure to digestive conditions. Previous studies among several spinach samples have demonstrated high variability in lutein digestive stability with as little as 25% being observed in some samples (Serrano and others 2005). Negligible content of lutein was observed in the aqueous phase of ZLNP suspensions before or after gastric digestion, which could be ascribed to the poor aqueous solubility of lutein and its likely association with either undigested particles or digested products.

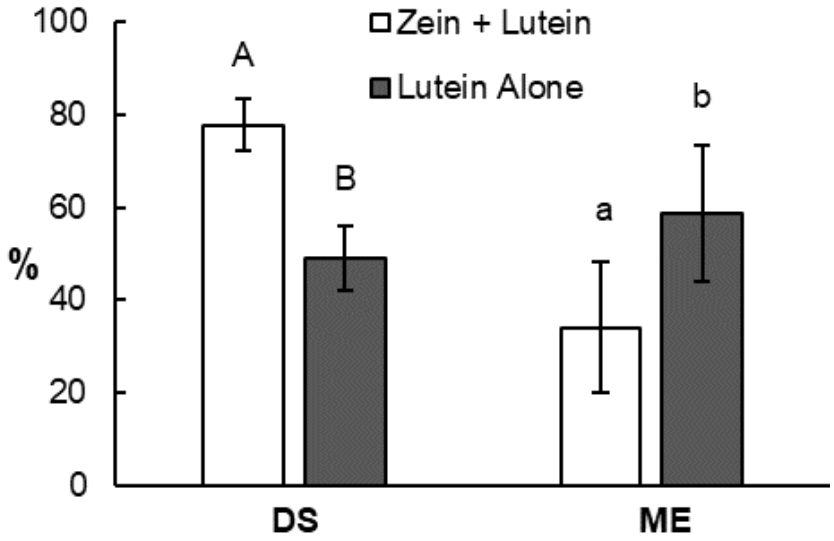

Figure 17. Digestive stability (DS) and micellarization efficiency (ME) of lutein entrapped in ZLNPs ("Zein + Lutein") or from zein-free aqueous dispersions ("Lutein Alone").

To be absorbed in the intestine, passed to the bloodstream, and made bioavailable, lutein is believed to be incorporated into micelles within the intestinal lumen and transported through the intestine by a combination of active and passive transport mechanisms (Yonekura and Nagao 2007). The first step (micellarization) is considered a critical step in this process and can be estimated effectively using *in vitro* digestion models (Reboul and others 2006), which were utilized on suspensions of ZLNPs. Micellarization efficiency (ME) of lutein from ZLNP was found to be significantly less than the control (Figure 17), implying that ZLNP in some way inhibited release of intact lutein to surfactant micelles. Values were comparable with findings for the release of curcumin from ZNPs following intestinal digestion conditions (Zou and others 2016b; Zou and others 2016c). These studies further implied that lipid is a superior vehicle when compared to ZNPs for transferring hydrophobic molecules to micelles (Zou and others 2016b; Zou and others 2016c). However, the content of micellarized lutein from ZLNP was still significant, and if all micellarized lutein were subsequently absorbed into enterocytes the relative bioaccessibility of lutein would be comparable to many vegetables (~40-60% (Reboul and others 2006)). Further, at this determined load of 0.91% and bioaccessibility of 49.1%, digesting 0.5 g of ZLNP would yield

about 2.23 mg of accessible lutein, which is comparable to the lutein content in 100g of raw broccoli (Alves-Rodrigues and Shao 2004).

ZNPs have been shown to improve the bioaccessibility of other hydrophobic bioactive compounds if the zein was modified or if lipid carriers were incorporated in the ZNPs. For instance, curcumin bioaccessibility from loaded ZNPs increased from 35.2% in the absence of added lipid to 91.2% after lipid nanoparticles were incorporated with the ZNP (Zou and others 2016b), suggesting that the digested lipid nanoparticles acted as a carrier to transport curcumin to the mixed micelle phase (Zou and others 2016b). Another study found that micellarized resveratrol was increased from ~60% to ~70% when encapsulated in ZNPs formed from dextran-conjugated zein in the presence of lecithin (Davidov 2015). The role of lipid in defining ultimate bioaccessibility is logical, given that increasing the dispersion of relatively hydrophobic carotenoids will improve their transfer through the predominately aqueous lumen (Yonekura and Nagao 2007) and that delivery of carotenoids into mixed micelles is linked to the content of free fatty acids and monoglycerides formed during digestion of lipids (Mutsokoti and others 2017). Previous studies have also indicated that triacylglyercols and their digested products during in vitro processes will provide a small yet significant increase in bioaccessibility of lutein and other carotenoids (Chitchumroonchokchai and others 2004; Nagao and others 2013). The presence of surface-active compounds such as lecithin could potentially improve the micellarization of lutein.

3.4.3 Physical stability of nanoparticles in simulated digestion conditions

As a means of resolving the chief objective and identifying the influence of digestion on ZNP structure, the general morphology of structures within digested suspensions of ZLNPs was characterized by AFM (Figure 18). Samples utilized for these images were prepared from digestion media that did not contain saline because the sodium chloride would cause visual artifacts due to crystallization on the mica substrates. Resulting AFM images of deposited samples showed a variety of apparent 2-dimensional amorphous assemblies, particulates varying in size between 10 and 700 nm in diameter, and aggregates of particulates. Due to the complexity of the system, it was not possible to distinguish which structures were composed of zein and which structures were digestive media components (e.g., bile salts, enzymes), which may have assembled during the preparatory drying process. Given the resemblance to particulate structures and clusters of particulates among ZNP and ZLNP suspensions (Figure 15), it could be speculated that at least some of the particulate aggregates observed in Figure 18 were ZLNPs that remained after the

digestive process or even zein-based peptides that re-assembled after their digestion in the digestive media. Further information was then required to understand whether ZNPs were completely degraded or if there was a fraction that escaped digestion.

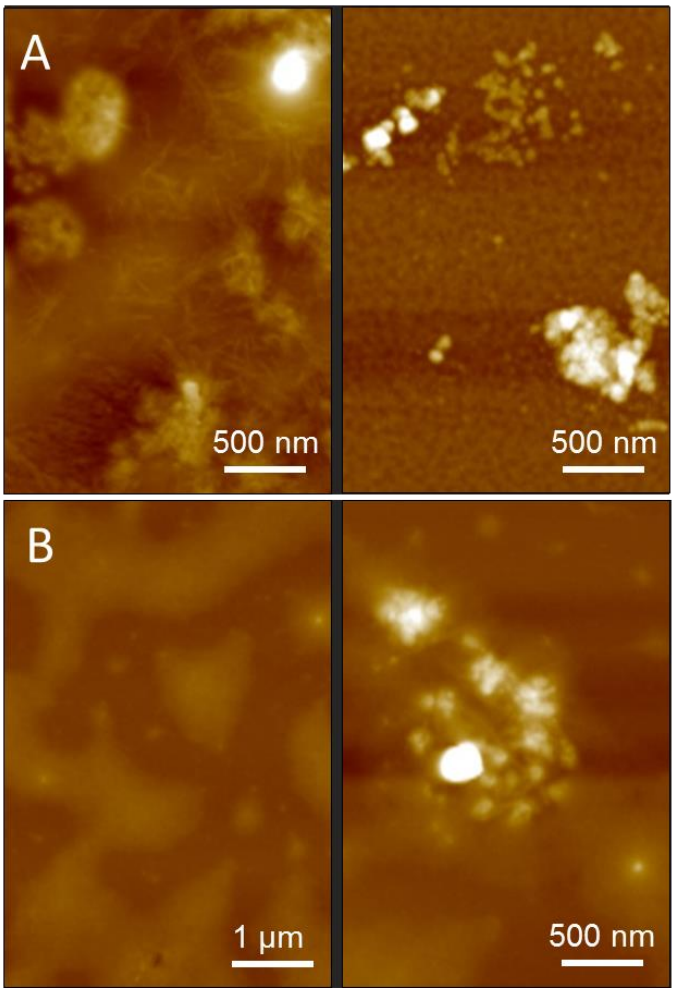

Figure 18. AFM topographical images of (A) gastric digested ZLNPs, showing amorphous assemblies and large clusters of particulate aggregates, and (B) intestinal digested ZLNPs, showing irregular deposition of films and occasional, diffuse clusters of aggregated ZLNPs

Samples were characterized by confocal microscopy to visualize structures in liquid and avoid potential artifacts due to drying (Figure 19). In all digestion conditions, micrographs of control samples containing only oil and lutein showed only spherical lipid droplets (Figure 19, bottom row). Micrographs of samples subjected to gastric phase digestion showed large aggregates of protein and spherical lipid droplets that appeared to be partially associated with protein (Figure 19, top left and inset). Large protein aggregates could be attributed to aggregates of ZLNPs, while

the presence of protein associated with lipid droplets indicated that ZLNP or fragments of digested zein were surface active and adsorbed to the droplet surfaces. Such protein-lipid associations were not observed among samples subsequently subjected to intestinal digestion conditions (Figure 19, top middle), indicating that the protein-lipid complexes may have disassociated into separate protein aggregates and lipid droplets. Few small protein-based aggregates could be observed in samples after intestinal digestion conditions. However, the scarcity of large protein aggregates not associated with lipid in the confocal images was attributed to the sedimentation of such large, dense structures following the preparatory centrifugation of samples, which had been used to improve light transmission for microscopy. Prior studies found micrometer-scale aggregates following gastric and intestinal digestion of zein nanoparticles (Zou and others 2016b; Zou and others 2016c). However, it was also plausible that some of the ZLNP had been digested into peptides too small to be visualized by the light microscope objective.

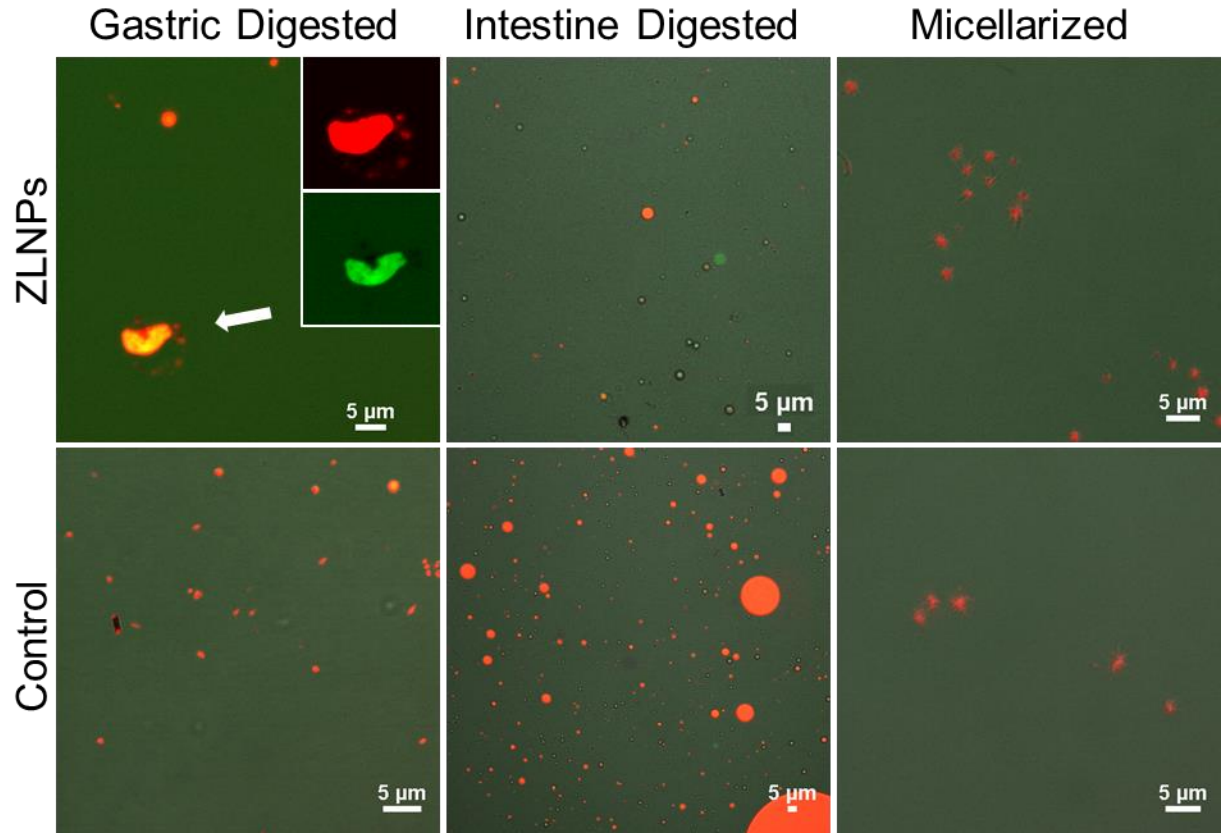

Figure 19. Confocal Microscopy images of digested samples of ZLNPs or control (lutein dispersions without zein); inset images (top left) show individual fluoresence signatures from lipids with Nile Red (Red) and proteins with FITC (Green)

ZNPs were more or less prone to aggregation and sedimentation during different phases of the simulated digestion process, which may have impacted the relative digestion of the ZNPs or the release of the lutein. Typical *in vitro* gastro-intestinal simulations, such as the conditions used in this study, include physiologically-relevant saline to contribute an added ionic strength of ~150 mM (Garrett and others 1999). After exposing ZNP suspensions to such saline conditions, aggregation and sedimentation was observed in a very short time frame (Figure 20c); subsequent subjection to gastric conditions (acidic pH, pepsin) appeared to reduce the quantity of sediment but increased the quantity of material adhered to the sample vessel. If saline was omitted from ZNP suspensions before or after simulated gastric digestion (i.e., low pH and addition of pepsin), there was no evidence of significant aggregation or sedimentation (Figure 20 a,b). Although dilute ZNP suspensions in the absence of salt are stable against significant aggregation at pH values below their isoelectric pH (~6.2), ZNPs have been shown to aggregate extensively with as little as 75 mM sodium chloride at pH 4, which is less than half of the added salt concentration used in this study (Patel and others 2010b).

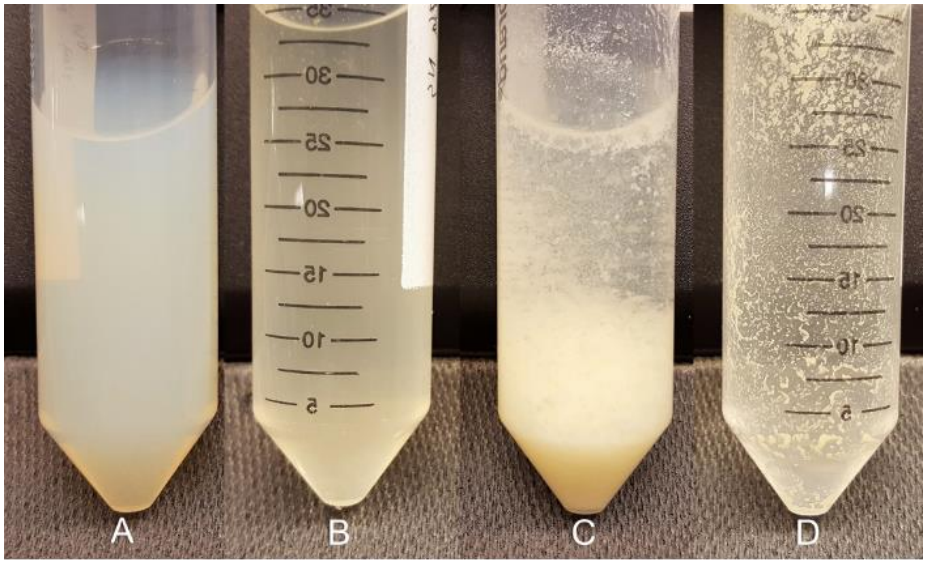

Figure 20. Photographs of ZNP suspensions demonstrating the impact of gastric digestion conditions and saline content on suspension stability: before digestion with no added ions (A), after pepsin digestion with no added ions (B), before digestion with saline (C), after digestion with saline (D)

To identify whether saline induced total or only partial precipitation of ZNP from the suspensions, protein contents were determined among the dispersed fractions of suspensions with

or without added oil and salt after allowing large aggregates to sediment. Among samples subjected to gastric conditions with no added salt or oil, dispersed fractions contained approximately 56.03% ± 0.01 of the total added protein content. This decreased to only 47.22% ± 0.04 of the total added protein when salt and oil were included in the samples. This finding indicated that approximately half of ZNPs (as intact ZNPs or partially digested components) were still suspended after gastric conditions and that salt and oil caused a slight yet significant decrease in dispersed, non-aggregated ZNP that could resist sedimentation during the typical time associated with gastric digestion. This small decrease in suspended protein content was surprising given the evident aggregates visually observed (Figure 20c), and it was speculated that added ions increased not only the amount of non-dispersed protein but also the tendency for particles to assemble into larger aggregates viewable by the naked eye (as opposed to smaller aggregates without added salt). Combined with the evidence of particles and particle aggregates in micrographs, these results supported the notion that the metastable suspension of ZNPs in gastric simulation conditions existed as individual nanoparticles or in clusters of varying size, which shifted more towards the latter when ionic strength increased.

Visually observable aggregates or sediments were not observed in suspensions subsequently subjected to intestinal simulation conditions, regardless of saline inclusion (identical to gastric simulation), demonstrating that aggregates could be re-dispersed and re-suspended with changing conditions (not shown). Increased pH of the intestinal simulation conditions would have only further decreased physical stability of ZNP suspensions, which have been shown to aggregate and sediment near pH 6 (Cheng and Jones 2017; Patel and Velikov 2014b). If it were assumed that aggregates observed at low pH with saline (Figure 20d) were composed of ZNP, redispersion in the intestinal conditions would have to be attributed to the proteolytic action of added enzymes and/or detergent action of bile salts.

3.4.4 Effect of enzymatic digestion on nanoparticle structure

Approximate molecular weights of peptides existing in ZNP suspensions were characterized before digestion or after gastric and intestinal simulation conditions in order to identify the impact of the digestion stages. After treatment with SDS, all samples were solubilized into the sample buffer and appeared to enter the gel during electrophoresis. SDS-PAGE analysis of ZNP (Figure 21, lane A) showed distinctive bands at 22 kDa and 24 kDa, which matches results for intact zein from previous studies (Shukla and Cheryan 2001). Those distinctive bands were

also observed among ZNPs after gastric digestion if saline was included (Figure 21, lane C). After intestinal digestion (with or without saline), no traces of the typical zein bands were observed (Figure 21, lane E); instead, numerous bands between 15 and 50 kDa were attributed to residual pancreatin and lipase from the digestion media, as indicated by the comparison to those controls (Figure 21, lanes G/H). Lack of significant bands from zein indicated that the protein within ZNPs was significantly digested by the simulated intestinal conditions.

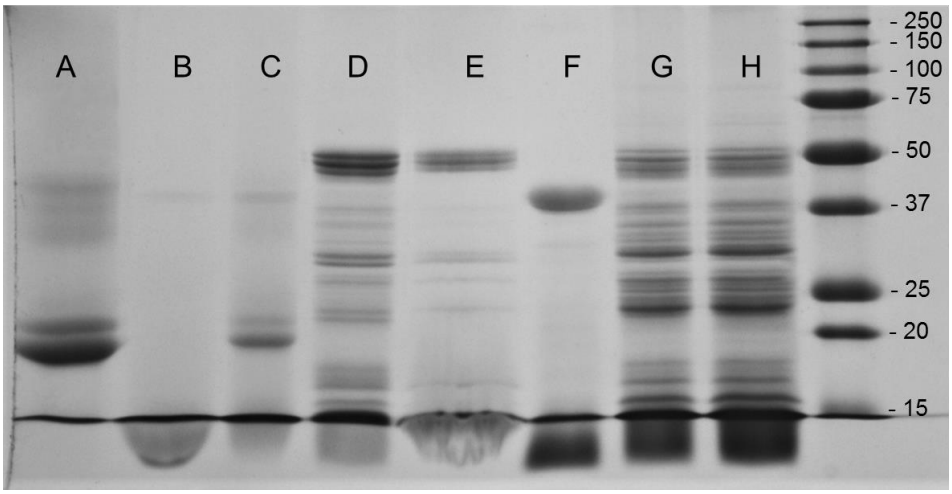

Figure 21. SDS-PAGE analysis of undigested ZNPs (A), pepsin-digested ZNPs with no saline (B), pepsin-digested ZNPs with saline (C), intestinal-digested ZNPs with no saline (D), intestinal-digested ZNPs with saline (E), pepsin (F), pancreatin (G), and lipase (H).

Aggregation and adhesion of ZNPs to the sample vessels, influenced by the addition of salt to the aqueous suspensions (Figure 20), also appeared to influence digestion of ZNP in simulated gastric conditions. If salt was omitted from samples during digestion, bands of 22 and 24 kDa, associated with intact zein, were not observed in the gels (Figure 21, lane B). This indicated that the presence of salt led to a greater breakdown of the zein proteins by the pepsin and/or acid conditions within ZNPs. It was speculated that the reduced dispersion of ZNPs with incorporation of salt, as indicated by the appearance of aggregation and adhesion to the vessel walls (Figure 20), might have protected the ZNPs from enzymatic action. Pepsin is a water-soluble enzyme and its activity is limited if peptide substrates are not well dispersed in the media (Sweeney and Walker 1993). This limitation in digestion only appeared to be effective in the simulated gastric conditions, as protein aggregates were redispersed into the liquid phase with no evident adhesion to vessel

walls after subjecting the suspensions to simulated intestinal conditions. Furthermore, the presence of salt and oil made no evident difference in observed bands for samples subjected to intestinal conditions (Figure 21, lanes D/E).

Pepsin has a broad specificity, but it prefers cleaving the peptide bonds of aromatic amino acids. It will also cleave the carboxyl side of leucine and glutamic acid but ignores alanine, valine, and glycine (Sweeney and Walker 1993). If a molecule of zein is cleaved at those sites, it is theoretically broken down into 55 different individual peptides and amino acids with molecular weights ranging from 131 Da to 1500 Da.

There is no prior evidence to indicate that zein is resistant to enzymatic digestion in intestinal conditions, and the thorough digestion of the ZNPs and ZLNPs in this study demonstrated that structuring of zein into desolvated nanoparticles provided no further restriction on digestion in intestinal conditions. A prior study had shown that unstructured zein dispersions were digested within 5 min of intestinal conditions (Fu and others 2002). However, limited digestion of unstructured zein in gastric conditions has been observed even after 120 min if 0.03 M sodium chloride was included (Fu and others 2002). Other studies have shown that structuring of the zein may be important during gastric conditions, as zein nanoparticles formed in the presence of tween 20 and polyvinyl pyrrolidone, which aided their dispersion in the aqueous phase, were completely digested within 60 minutes (Hurtado-López and Sudax 2006) while digestibility among films of zein was reduced by ~25% (Matthews and others 2011). This further supported the theory that increased dispersion of zein in the aqueous phase enhances digestion by increasing its exposed surface area.

Although the SDS-PAGE results described thorough digestion of ZNPs in intestinal conditions, micellarization efficiency of lutein originally incorporated within ZLNPs was significantly less than in simple aqueous dispersions (Figure 17). Digestion of ZNPs to smaller peptides would imply dismantling of the particulate structure to release peptides and exposed lutein. However, the reduced lutein micellarization efficiency indicated that the digested ZNP components had at least some restrictive impact on the capacity of lutein to be transferred to surfactant micelles. It is possible that the lutein was favorably associating with hydrophobic digested peptides, decreasing their availability for micellarization. Further, the peptides from ZNP could have restricted the action of lipase or bile salts by specific interactions with lipase, bile salts,

or even the lipid phases, decreasing the number of surface active substances that contribute to carotenoid micellarization (Mutsokoti and others 2017).

3.5 Conclusions

Encapsulation of lutein into ZNPs improved its digestive stability but reduced micellarization efficiency. The ion concentration relevant to physiological conditions caused ZNP to aggregate into relatively enzyme-inaccessible clusters during the simulated gastric conditions, so a significant fraction of ZNPs was not digested. All ZNP, including such aggregated clusters, were completely digested into shorter peptides in the simulated intestinal conditions, likely because the added bile salts, pancreatin, and lipase assisted the redispersion of ZNPs into the aqueous phase. Lutein was potentially protected within the ZNPs during the gastric phase because of the limited ZNP digestion, explaining the increased digestive stability. However, complete digestion of ZNP during the intestinal phase meant that the original capsule structure was lost; decreased micellarization efficiency of lutein could then be attributed to favorable association between digested ZNP peptides and lutein, bile salts, or lipid components. The potential interactivity between zein-based peptides and these components needs to be investigated in future studies. Without improvement in the micellarization efficiency and associated bioaccessibility of carotenoids entrapped in ZNPs, the utility of ZNPs as vehicles for bioactive, hydrophobic compounds to be delivered for intestinal absorption may be limited.

3.6 Acknowledgements

The authors would like to thank Prof. Bruce Hamaker at Purdue University for experimental advice and Giovanna Junqueira Cardoso for assistance in the laboratory during the course of the project. Support during preparation of this manuscript was received from the Industry Fellows program, disbursed from the Department of Food Science at Purdue University, and HATCH Act formula funds supplied by the U.S. National Institute of Food and Agriculture. There was no scientific contribution or direction from any corporation or industrial interest during the course of this work.

3.7 References

Alves-Rodrigues, A., & Shao, A. (2004). The science behind lutein. *Toxicology Letters, 150*(1), 57-83.

Arnal, E., Miranda, M., Almansa, I., Muriach, M., Barcia, J. M., Romero, F. J., Diaz-Llopis, M., & Bosch-Morell, F. (2009). Lutein prevents cataract development and progression in diabetic rats. *Graefes Archive for Clinical and Experimental Ophthalmology, 247*(1), 115-120.

Chen, H. Q., & Zhong, Q. X. (2015). A novel method of preparing stable zein nanoparticle dispersions for encapsulation of peppermint oil. *Food Hydrocolloids, 43*, 593-602.

Chen, J. J., Zheng, J. K., McClements, D. J., & Xiao, H. (2014). Tangeretin-loaded protein nanoparticles fabricated from zein/beta-lactoglobulin: Preparation, characterization, and functional performance. *Food Chemistry, 158*, 466-472.

Chen, Y., Ye, R., & Liu, J. (2013). Understanding of dispersion and aggregation of suspensions of zein nanoparticles in aqueous alcohol solutions after thermal treatment. *Industrial Crops and Products, 50*, 764-770.

Cheng, C. J., & Jones, O. G. (2017). Stabilizing zein nanoparticle dispersions with ι-carrageenan. *69*, 28-35.

Chitchumroonchokchai, C., Schwartz, S. J., & Failla, M. L. (2004). Assessment of Lutein Bioavailability from Meals and a Supplement Using Simulated Digestion and Caco-2 Human Intestinal Cells. *The Journal of Nutrition, 134*(9), 2280-2286.

Chuacharoen, T., & Sabliov, C. M. (2016a). The potential of zein nanoparticles to protect entrapped beta-carotene in the presence of milk under simulated gastrointestinal (GI) conditions. *Lwt-Food Science and Technology, 72*, 302-309.

Chuacharoen, T., & Sabliov, C. M. (2016b). Stability and controlled release of lutein loaded in zein nanoparticles with and without lecithin and pluronic F127 surfactants. *Colloids and Surfaces a-Physicochemical and Engineering Aspects, 503*, 11-18.

Davidov-Pardo, G., Joye, I. J., Espinal-Ruiz, M., & McClements, D. J. (2015). Effect of Maillard Conjugates on the Physical Stability of Zein Nanoparticles Prepared by Liquid Antisolvent Coprecipitation. *Journal of Agricultural and Food Chemistry, 63*(38), 8510-8518.

Davidov-Pardo, G., Joye, I. J., & McClements, D. J. (2015). Encapsulation of resveratrol in biopolymer particles produced using liquid antisolvent precipitation. Part 1: Preparation and characterization. *Food Hydrocolloids, 45*, 309-316.

Fu, T. T., Abbott, U. R., & Hatzos, C. (2002). Digestibility of food allergens and nonallergenic proteins in simulated gastric fluid and simulated intestinal fluid - A comparative study. *Journal of Agricultural and Food Chemistry, 50*(24), 7154-7160.

Garrett, D. A., Failla, M. L., & Sarama, R. J. (1999). Development of an in vitro digestion method to assess carotenoid bioavailability from meals. *Journal of Agricultural and Food Chemistry, 47*(10), 4301-4309.

Gomez-Estaca, J., Balaguer, M. P., Gavara, R., & Hernandez-Munoz, P. (2012). Formation of zein nanoparticles by electrohydrodynamic atomization: Effect of the main processing variables and suitability for encapsulating the food coloring and active ingredient curcumin. *Food Hydrocolloids, 28*(1), 82-91.

Granado, F., Olmedilla, B., & Blanco, I. (2003). Nutritional and clinical relevance of lutein in human health. *British Journal of Nutrition, 90*(3), 487-502.

Hu, D., Lin, C., Liu, L., Li, S., & Zhao, Y. (2012). Preparation, characterization, and in vitro release investigation of lutein/zein nanoparticles via solution enhanced dispersion by supercritical fluids. *109*(3), 545-552.

Hu, K., Huang, X., Gao, Y., Huang, X., Xiao, H., & McClements, D. J. (2015). Core-shell biopolymer nanoparticle delivery systems: Synthesis and characterization of curcumin fortified zein-pectin nanoparticles. *Food Chemistry, 182*, 275-281.

Huang, X. X., Huang, X. L., Gong, Y. S., Xiao, H., McClements, D. J., & Hu, K. (2016). Enhancement of curcumin water dispersibility and antioxidant activity using core-shell protein-polysaccharide nanoparticles. *Food Research International, 87*, 1-9.

Hurtado-López, P., & Sudax, M. (2006). Zein microspheres as drug/antigen carriers: A study of their degradation and erosion, in the presence and absence of enzymes. *Journal of Microencapsulation, 23*(3), 303-314.

Kean, E. G., Hamaker, B. R., & Ferruzzi, M. G. (2008). Carotenoid Bioaccessibility from Whole Grain and Degermed Maize Meal Products. *Journal of Agricultural and Food Chemistry, 56*(21), 9918-9926.

Liang, H., Zhou, B., He, L., An, Y., Lin, L., Li, Y., Liu, S., Chen, Y., & Li, B. (2015). Fabrication of zein/quaternized chitosan nanoparticles for the encapsulation and protection of curcumin. *Rsc Advances, 5*(18), 13891-13900.

Lin, C. H., & Chen, B. H. (2005). Stability of carotenoids in tomato juice during storage. *Food Chemistry, 90*(4), 837-846.

Livney, Y. D. (2010). Milk proteins as vehicles for bioactives. *Current Opinion in Colloid & Interface Science, 15*(1), 73-83.

Matalanis, A., Jones, O. G., & McClements, D. J. (2011). Structured biopolymer-based delivery systems for encapsulation, protection, and release of lipophilic compounds. *Food Hydrocolloids, 25*(8), 1865-1880.

Matthews, L., Kunkel, J., Action, A., Ogale, & Dawson, P. (2011). Bioavailability of Soy Protein and Corn Zein Films. In (Vol. 2, pp. 1105-1113): Food and Nutrition Sciences.

Minekus, M., Alminger, M., Alvito, P., Ballance, S., Bohn, T., Bourlieu, C., Carriere, F., Boutrou, R., Corredig, M., Dupont, D., Dufour, C., Egger, L., Golding, M., Karakaya, S., Kirkhus, B., Le Feunteun, S., Lesmes, U., Macierzanka, A., Mackie, A., Marze, S., McClements, D. J., Menard, O., Recio, I., Santos, C. N., Singh, R. P., Vegarud, G. E., Wickham, M. S. J., Weitschies, W., & Brodkorb, A. (2014). A standardised static in vitro digestion method suitable for food - an international consensus. *Food & Function, 5*(6), 1113-1124.

Mutsokoti, L., Panozzo, A., Pallares, A. P., Jaiswal, S., Van Loey, A., Grauwet, T., & Hendrickx, M. (2017). Carotenoid bioaccessibility and the relation to lipid digestion: A kinetic study. *Food Chemistry, 232*, 124-134.

Nagao, A., Kotake-Nara, E., & Hase, M. (2013). Effects of Fats and Oils on the Bioaccessibility of Carotenoids and Vitamin E in Vegetables. *Bioscience, Biotechnology, and Biochemistry, 77*(5), 1055-1060.

Patel, A. R., Bouwens, E. C. M., & Velikov, K. P. (2010). Sodium Caseinate Stabilized Zein Colloidal Particles. *Journal of Agricultural and Food Chemistry, 58*(23), 12497-12503.

Patel, A. R., & Velikov, K. P. (2014). Zein as a source of functional colloidal nano- and microstructures. *Current Opinion in Colloid & Interface Science, 19*(5), 450-458.

Reboul, E., Richelle, M., Perrot, E., Desmoulins-Malezet, C., Pirisi, V., & Borel, P. (2006). Bioaccessibility of carotenoids and vitamin E from their main dietary sources. *Journal of Agricultural and Food Chemistry, 54*(23), 8749-8755.

Serrano, J., Goni, I., & Saura-Calixto, F. (2005). Determination of ss-carotene and lutein available from green leafy vegetables by an in vitro digestion and colonic fermentation method. *Journal of Agricultural and Food Chemistry, 53*(8), 2936-2940.

Shukla, R., & Cheryan, M. (2001). Zein: the industrial protein from corn. *Industrial Crops and Products, 13*(3), 171-192.

Sweeney, P. J., & Walker, J. M. (1993). *Enzymes of Molecular Biology*: Humana Press

Tang, Y. C., & Chen, B. H. (2000). Pigment change of freeze-dried carotenoid powder during storage. *Food Chemistry, 69*(1), 11-17.

Yonekura, L., & Nagao, A. (2007). Intestinal absorption of dietary carotenoids. *Molecular Nutrition & Food Research, 51*(1), 107-115.

Zhong, Q. X., & Jin, M. F. (2009). Zein nanoparticles produced by liquid-liquid dispersion. *Food Hydrocolloids, 23*(8), 2380-2387.

Zou, L. Q., Zheng, B. J., Zhang, R. J., Zhang, Z. P., Liu, W., Liu, C. M., Xiao, H., & McClements, D. J. (2016a). Enhancing the bioaccessibility of hydrophobic bioactive agents using mixed colloidal dispersions: Curcumin-loaded zein nanoparticles plus digestible lipid nanoparticles. *Food Research International, 81*, 74-82.

Zou, L. Q., Zheng, B. J., Zhang, R. J., Zhang, Z. P., Liu, W., Liu, C. M., Xiao, H., & McClements, D. J. (2016b). Food-grade nanoparticles for encapsulation, protection and delivery of curcumin: comparison of lipid, protein, and phospholipid nanoparticles under simulated gastrointestinal conditions. *Rsc Advances, 6*(4), 3126-3136.

CHAPTER 4 EFFECT OF DRYING TEMPERATURE AND PARTICLE DISPERSIBILITY ON COMPOSITE FILMS OF METHYLCEULLULOSE AND ZEIN NANOPARTICLES

4.1 ABSTRACT

Composite films composed of methylcellulose (MC) and zein nanoparticles (ZNPs) were prepared as a potential biodegradable alternative for synthetic packaging. The effects of ZNP aggregation on mechanical and moisture barrier properties as affected by drying temperature, pH, and stabilizers were tested. The phase separation of composite films was determined to be detrimental to both its mechanical and moisture barrier properties. The drying temperature, pH, and composition of the solvent casting solution all affected the distribution of ZNPs dispersed in MC films. Drying films at 23°C or setting the pH to 6.5 resulted in ZNP aggregation and weaker, brittle films that were poor moisture barriers. The presence of CGN was able to provide stability to ZNPs at both pH 4 and 6.5, thus improving its mechanical and moisture barrier properties.

4.2 INTRODUCTION

The widespread use of unsustainable petroleum-based packaging has a serious negative environmental impact. From 1950 to 2015, approximately 6300 million metric tons of plastic waste has been generated. Of that amount, only 9% was recycled and 79% of plastic waste was disposed in landfills or polluted the environment (Geyer and others 2017). The physical and chemical stability of these materials causes pollution in natural ecosystems for long periods of time where it can be ingested by wildlife causing detrimental effects (Hammer and others 2012; Geyer and others 2017). A large fraction of plastic use is for packaging. As of 2015 in Europe, nearly 40% of plastic is used for packaging (Kaiser and others 2018).

Methylcellulose (MC), a modified cellulose, is a potential biodegradable alternative material to replace petroleum based packaging (Rhim and others 2013). However, when compared to synthetic plastics, MC is not yet a viable replacement because of its weaker mechanical strength and moisture barrier properties (Rhim and others 2013; Siracusa and others 2008). Specifically, MC films are rigid and brittle with a young's modulus on the order of 1 GPa, a tensile strength of ~30-60 MPa, and an elongation at break of 5-10% (de Moura and others 2009; Jiménez and others 2010). In comparison, polyethylene terephthalate, the material used for soft drink bottles, is able

to provide greater strength (tensile strength = 48 MPa) with more flexibility (elongation at break of 410%). Incorporating protein nanoparticles into MC films to form nanocomposites is a promising method for improving both mechanical strength and moisture barrier properties (Rhim and others 2013; Arora and Padua 2010; Akbari and others 2007).

Beyond its use as a film-forming agent, methylcellulose is a commonly used emulsifier and stabilizer in food applications (BeMiller and Huber 2008). Its solubility in 23°C water makes it an ideal candidate for not only food and beverage applications but also for film preparation by drying aqueous suspensions (1995). However, this hygroscopic nature of MC reduces the moisture barrier properties of prepared MC films, typically displaying high water vapor permeability (Moller and others 2004; de Moura and others 2009; Jiménez and others 2010). Various additives have been used to improve the functionality of MC films including lipids like stearic acid (Sebti and others 2002; Kamper and Fennema 1984; Jiménez and others 2010), other carbohydrates (Sebti 2007; de Moura and others 2009), and proteins such as zein (Gilbert 2017). Biopolymer nanoparticles in particular such as chitosan/tripolyphosphate particles, zein nanoparticles, and microcrystalline cellulose particles have successfully improved both the mechanical and water barrier properties of cellulose derived films (de Moura and others 2009; Bilbao-Sáinz and others 2010).

Zein can be a good material to use in nanocomposite materials. This protein is major nitrogen storage protein that accounts for nearly half of the protein content of the corn grain (Patel and Velikov 2014a; Shukla and Cheryan 2001). As a byproduct of starch and ethanol processing, it is generally recognized as safe (GRAS) and soluble in up to 70% ethanol (Patel and Velikov 2014a). When this protein is formed into a nanoparticle, there are many promising applications such as improving the bioaccessibility and storage stability of many nutraceutical compounds (Chen and Zhong 2015a; Hu and others 2015; Zou and others 2016b; Li and others 2012a; Chuacharoen and Sabliov 2016a).

Zein nanoparticles (ZNPs) have been found to augment the water barrier properties and tensile strength of MC and whey protein isolate films, but such improvements were limited at higher concentrations of ZNP usage (Oymaci and Altinkaya 2016; Gilbert and others 2018). It is commonly thought that an even distribution of nanoparticles in synthetic nanocomposite films provides improved functional properties (Rhim and Ng 2007). However, no studies have determined the effect of nanoparticle distribution in biopolymer derived composite films. It is

possible that previous clustering and uneven distribution of ZNPs at high concentrations negatively impacted the functional properties of MC films, and this clustering could be attributed to ZNP aggregation in the casting solution before significant evaporation of solvent arrested the particle motion. One factor contributing to aggregation among particle dispersions is the drying temperaturee. Methyl cellulose also undergoes a solubility transition above 40^{o}C (Donhowe 1977), and so the local viscosity and tendency for phase segregation leading towards instabilities could be significantly influenced by the temperatures during drying. Apart from drying temperature, studies have found that ι-carrageenan (CGN) has been able to improve ZNP stability in aqueous dispersions at various pH levels (Cheng and Jones 2017). This sulfonated polysaccharide can potentially improve ZNP distribution in MC films and thus improve the mechanical and water barrier properties of the composite film. The objective of this work is then to investigate the effects of drying temperature and stabilizing additives on the distribution of ZNP within MC composite films and their resultant mechanical and water barrier properties.

4.3 MATERIALS AND METHODS

4.3.1 Materials

Zein and tween-20 was supplied from Sigma-Aldrich (St. Louis, MO). The MC was donated by Dow Chemical's (Methocel A15 Food Grade Modified Cellulose). ι-carrageenan (CGN) was supplied by FMC biopolymer (Philadelphia, PA). HCl was purchased from Sigma-Aldrich. NaOH was purchased from Fisher Scientific (Waltham, MA). Ethanol was purchased from VWR (Radnor, PA). Ultrapure water (resistivity (σ) $\geq$ 18 mΩ-cm) was utilized for the preparation of all aqueous dispersions.

4.3.2 Sample Preparation

ZNP were prepared using the antisolvent precipitation method as outlined by Zhong and Jin.(2009) Zein was first dissolved in 80% aqueous ethanol to make a final concentration of 2.5% (w/v). The solution was then injected into pure water at a 1:3 zein:water ratio while simultaneously being dispersed using a bench-top homogenizer (Ultra Turax T-25 Basic). A rotary evaporator was then used to remove the ethanol and concentrate the ZNP dispersion. Water was then added to adjust the ZNP concentration to 1.0% (w/v) which was confirmed gravimetrically with a vacuum oven. Large aggregates were removed from the sample by centrifugation for 10 min at 2880 x g, and the supernatant was stored at 4°C. ZNP complexed with CGN (ZC) were also prepared with the antisolvent precipitation method as outlined above. However, twenty mL of the dissolved zein

solution was injected into a 100 mL solution containing 50 mg CGN with 5 uL Tween 20 to stabilize the ZNP/CGN complexes. Dynamic light scattering (DLS) was used to verify the particle size of ZNP using the same method as outlined by Cheng et al (Cheng and Jones 2017) using an ALV-CGS3 light scattering goniometer (ALV, Langen).

Films were prepared using the protocol outlined by Gilbert et al with the following modifications (Gilbert and others 2018). ZNP suspensions were first diluted to 0.5% (w/v) with water. The pH of freshly made ZNP dispersions were 3.5 due to the processing and extraction of the commercial zein. It was then adjusted to 4 or 6.5 using 0.1N HCl or 0.1N NaOH respectively (Sigma; St. Louis, MO). Powdered MC was then added to achieve a final MC concentration of 3% (w/w). MC solutions were also prepared at 3% (w/w) without zein nanoparticles as a control, and all mixtures were stirred with a stir bar overnight. Once the MC was hydrated, 25g of the solvent casting dispersion was poured in individual square petri plates and degassed for 2 hours (Ted Pella; Product # 14008). The plates were either dried in a 48°C oven at 30% RH for 24 hours or in a fume hood with a face velocity of 85 fpm on a rotating plate with an approximate speed of 2 RPM at 23°C and for 24 hours. Films with CGN were prepared in the same way as ZNP films that were dried at low temperature. Upon drying, the films were cut to the proper dimensions for analysis as described by Gilbert et al and placed in store-bought plastic bags at room temperature and 30% RH until analysis (Gilbert and others 2018).

4.3.3 Tensile Test

Tensile testing was done using the same method as reported by Gilbert et al (Gilbert and others 2018). Films cut into 30mm x 120mm rectangles and analyzed on an MTS Criterion Model 43 utilizing a 500 N load cell. The films were gripped using a 38mm x 58mm rubber grip face set, and the extension speed was 1.5mm/s. The Young's modulus was calculated by determining the initial slope of the resulting stress/strain plot. The tensile strength was determined by measuring the maximum load when the film broke, and the elongation percentage was calculated by dividing the final stretched length of the film by the initial length.

4.3.4 Water Contact Angle

Film hydrophilicity was tested by recording the contact angle of a sessile drop of water on the surface using a droplet shape analyzer (KRÜSS DSA30; Hamburg, Germany) using the same

method adapted from (Gilbert and others 2018). The average water contact angle was taken from at least 5 droplets/film at room temperature.

4.3.5 Water Vapor Permeability (WVP)

WVP of the films were determined using a modified approach of the ASTM E96 method (McHugh and others 1993). The protocol is outlined by Gilbert et al (Gilbert and others 2018). Films were cut into circles with a diameter of 2.5 cm. Circular cups having an inner diameter of 1.27 cm and a height of 1.75 cm were filled with 1ml of saturated $MgCl_2$ solution to produce an internal relative humidity of 33%. The films were then fixed to the top of the prepared cups using fixative and were allowed to dry for up to 2 hours. Samples were placed in an SPSx-1μ Dynamic Vapor Sorption Analyzer (Projekt Messtechnik, Ulm, Germany) equipped with a 23-sample holder containing 18 mm aluminum pans. Samples were held in the SPS for a total of 36 hours, and the external RH was set to 50%, 70%, or 90% at 12-hour intervals for each RH level. The sample was weighed every 15 minutes throughout the experiment. At least four samples were analyzed for each film. The water vapor transmission rate (WVTR) in units of $mg\ hr^{-1}$ was recorded by measuring the rate of mass gain of the cup due to water transmission into the cell. WVP was calculated using the following equation in units of $mg\ mm\ m^{-2}\ hr^{-1}\ kPa^{-1}$

$$WVP = \frac{WVTR}{\Delta P} L_{film} \quad [1]$$

where ΔP is the difference in the partial pressure on either side of the film and L_{film} is the film thickness.

4.3.6 Atomic Force Microscopy (AFM)

The surface topography of the tops of the films was imaged with AFM (Asylum MFP3D, Asylum Research, Santa Barbara, CA). Films were scanned in intermittent-contact mode at a scan rate of 0.8 Hz using silicon cantilevers with a reflective aluminum coating (TAP150AL-G, Ted Pella, Inc., Redding, CA), a resonance frequency of 150 kHz, and a nominal spring constant of 5 N/m. Film samples were fixed to a glass slide with double-sided tape.

4.3.7 Cryo Scanning Electron Microscopy (SEM)

Cross-sectional analysis of the prepared films was performed using a Nanova SEM with a Gatan Alto 2500 cryo system. The films were cryo-fractured by first placing the sample into a cryo-specimen holder and immersing it into slush nitrogen for cryo-fixing. It was then transferred to the cryo-unit to be fractured. The film was then sputter coated with platinum for 120 s. The sample was then transferred to the imaging chamber where it was imaged at 5 kV.

4.3.8 Statistical Analysis

Displayed data presents the average and standard deviation from measurements of replicate samples ($n \geq 3$). Significant differences in tensile strength, WVP, and water contact angle, ($p < 0.05$) were determined by one-way analysis of variance with Tukey-Honest Significant Differences (HSD) using JMP statistical software (SAS).

4.4 Results and Discussion

4.4.1 Zein Nanoparticle (ZNP) Characterization

Zein nanoparticles (ZNP) with and without CGN were characterized with DLS and AFM. It was found that the particle size of ZNPs alone had a diameter of approximately 100 nm (Figure 22). When combined with ι-carrageenan (CGN), ZNPs were found to have a mean diameter of 500 nm with DLS; however, edge-to-edge diameters of deposited ZNPs with CGN were approximately 100-200 nm when measured by AFM. The morphology of ZNPs with and without CGN match previous findings showing spherical structures (Cheng and Jones 2017). DLS results in previous studies showed that ZNP complexed with CGN had a radius of about 100 nm, however the protein and polysaccharide were complexed in more dilute conditions. The size discrepancy of ZNPs between DLS and AFM could be due to the ZNPs with CGN forming loosely associated clusters or the CGN was only loosely bound with ZNP and broke apart upon dilution for AFM imaging. A population of ZNPs with CGN imaged on AFM appeared to form loose clusters (Figure 22 inset).

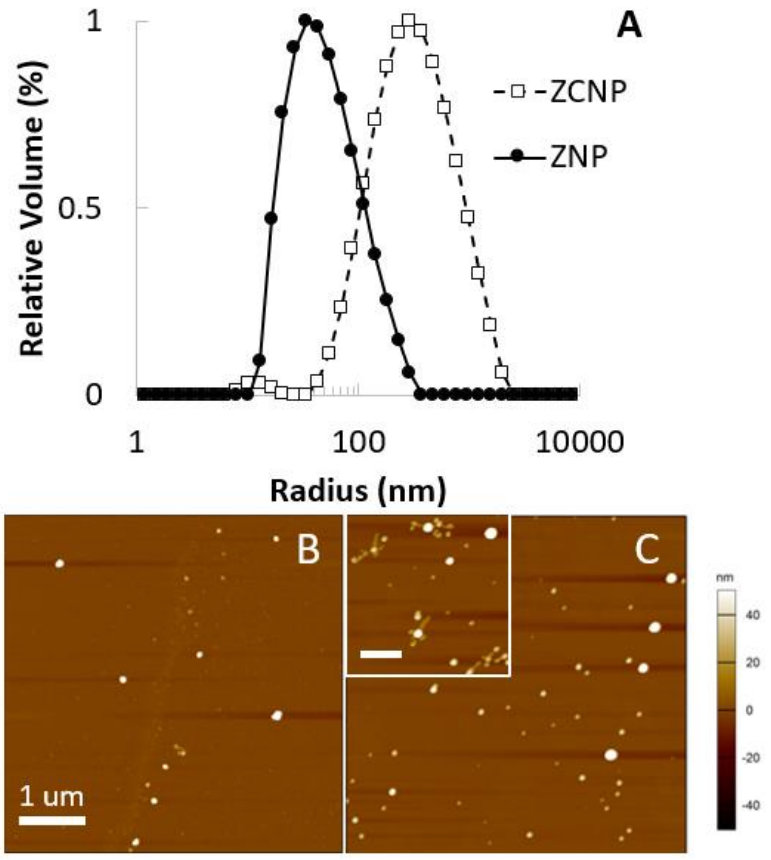

Figure 22. Particle Size of ZNP with and without CGN (A) determined by dynamic light scattering, (B) AFM topographical images of ZNP, (C) ZNP with CGN. Inset scale bar = 500 nm

4.4.2 Film Microstructure

The effect of drying temperature and casting solvent composition on the microstructure of MC/ZNP composite films were tested. The drying temperature and the pH had no effect on the appearance of MC films, but differences were apparent in films with ZNP. All films were dried at 23°C or 48°C. In general, drying composite films at room temperature resulted in opaque and brittle films. The pH of the films were also adjusted to either at pH 4 or pH 6.5 during the casting process. Composite films set to pH 6.5 caused irreversible aggregation of ZNPs. The solvent casting solution of some films were also altered with the addition of CGN and tween to improve the pH stability of ZNP in MC films.

The drying temperature significantly changed the composite film's appearance. When cast and dried into a film at 23°C, large opaque zones of zein on the film were still apparent, especially at pH 6.5 (Figure 23). Films were also noticeably more brittle and wrinkled. Drying films at 48°C

produced more translucent films, but aggregates were still observable at pH 6.5. Films with CGN were only dried at 23°C, because the addition of the surfactant would cause the films to shrink and tear when dried at 48°C.

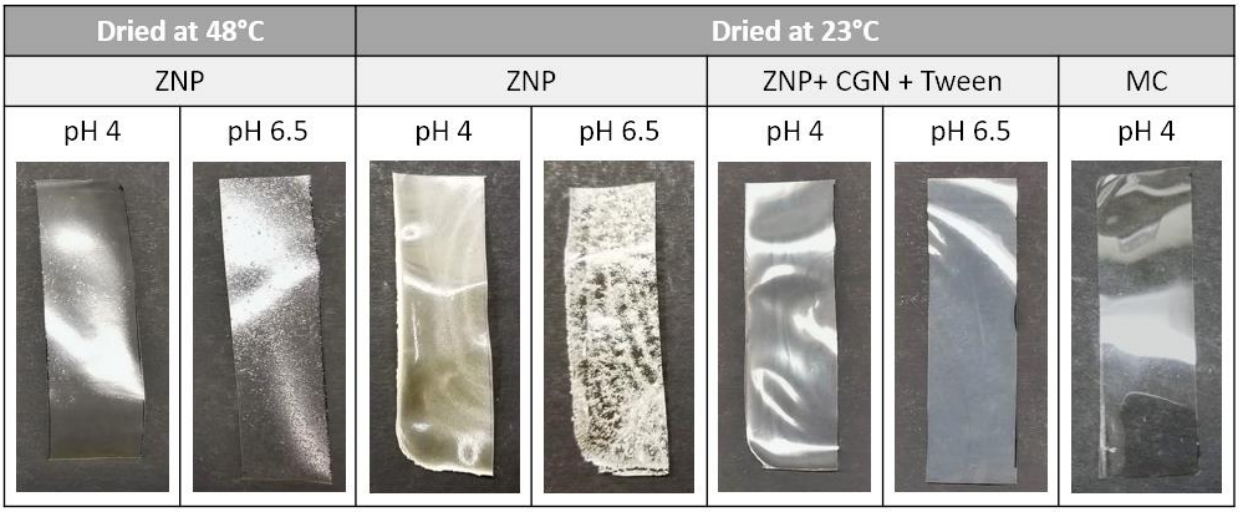

Figure 23. Zein/MC composite films prepared at various drying and pH conditions

The pH of the casting solution changed the appearance of the final dried composite film. With an isoelectric point of about 6.2 (Patel and others 2010b), the ZNPs dispersed in the casting solution predictably precipitated out when the pH was adjusted to 6.5. At pH 4, ZNP remained well dispersed, but solubilization of MC into the dispersion triggered enough ZNP aggregation to cause them to settle to the bottom of the petri dish during the drying process. Films containing CGN appeared more translucent and homogenous.

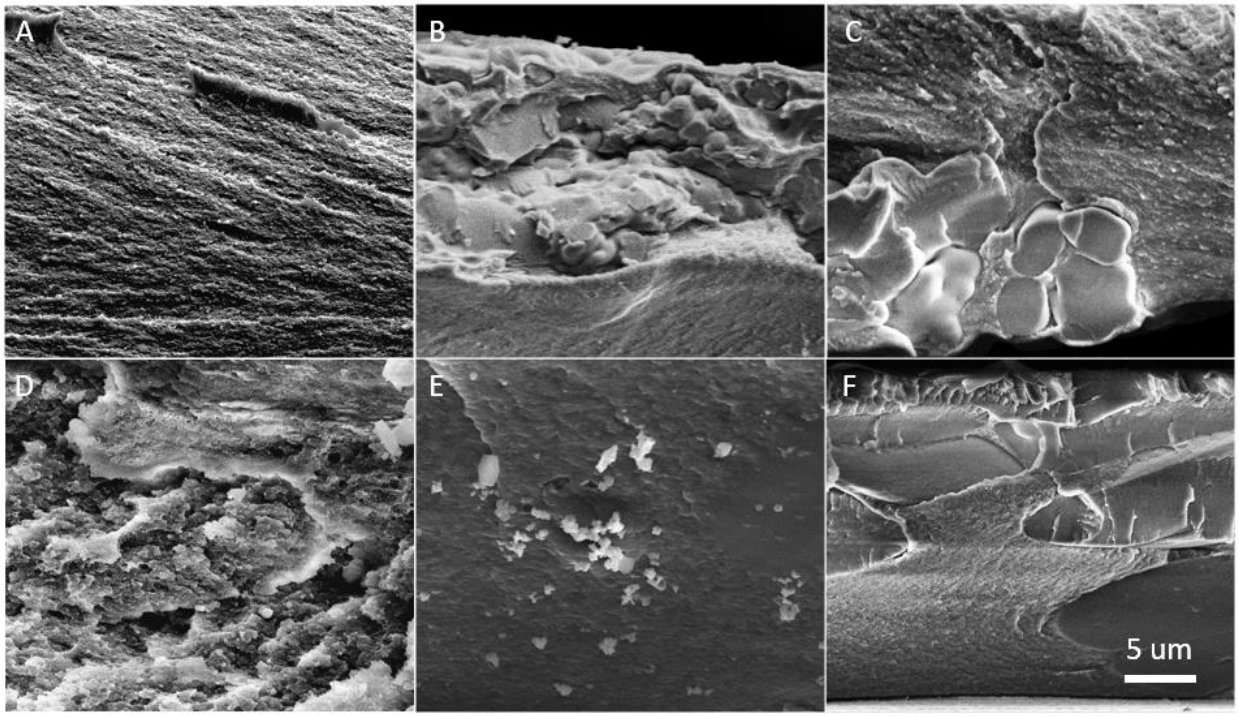

Figure 24. Cryo-SEM Images of Cross Sections of ZNP/MC composite films, (A) MC Alone 23°C pH 6.5, (B) ZNP 23°C pH 4, (C) ZNP 23°C pH 6.5, (D) ZC tween 23°C pH 6.5, (E) ZNP 48°C pH 4, (F) ZNP 48°C pH 6.5

Cryo-SEM images of cross sections of the composite films were performed to determine ZNP distribution throughout the film (Figure 24). The cross section of the MC film without ZNP appeared uniform with no distinct phases. Films with ZNP dried at room temperature without CGN, regardless of pH, appeared to have two separate phases with large >5 μm spherical clusters at the edges of the film (Figure 24,b,c). After addition of CGN, large ZNP were also visible in films, but they did not appear to form a separate phase on a side the film (Appendix 1) indicating that they did not settle out of dispersion during the drying process. When MC/ZNP composite films were dried at 48°C and the pH was set to 4, ZNPs appeared to be well dispersed with minimal aggregation matching what was found in previous studies (Gilbert and others 2018). When the pH of the film was set to 6.5, phase separation appeared to occur (Figure 24,f). The zones appeared flatter and more elongated when compared to the spherical aggregates in the films dried at room temperature. In previous studies on both synthetic and natural biopolymer based composite films, higher drying temperatures appeared to have an effect on nanoparticle dispersion (Perez-Gago and Krochta 2000; Chandran and Basu 2011).

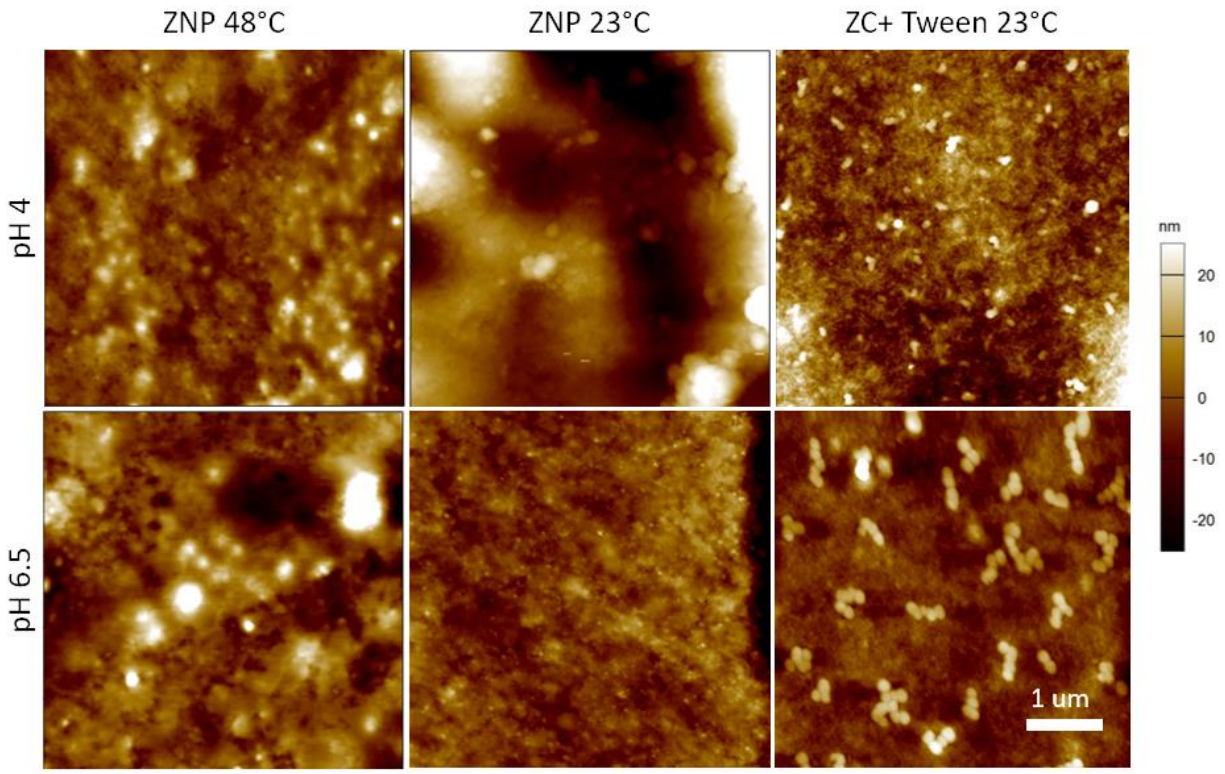

Figure 25. AFM Topographical Images of Zein/MC composite Films with and without CGN

Topographical imaging of the top of the film surface (the side facing the air during drying) done with AFM gave insight into the dispersion of ZNP on the surface of MC films (Figure 25). ZNP/MC films dried at 48°C had observable nanoparticles on the surface with a diameter ranging from ~100-500 nm. The film dried at pH 4 appeared to have smaller particles than the one set at pH 6.5. When dried at 23°C, the film surface had large visible aggregates which were too large to be captured in their entirety within a single AFM scan window. The height differences of these aggregates were also too large to be accurately captured by the instrument as well. ZNP/MC films containing CGN showed well dispersed nanoparticles at pH 4. However, when the pH was raised to 6.5, the nanoparticles appeared to form small clusters on the surface (Figure 25), which are not visible from the cross section of the film as imaged by cryo-SEM (Figure 24).

The stability of ZNPs had a major impact on the visual appearance and distribution of ZNPs in MC films. Previous work has already shown that CGN can improve the pH stability of ZNPs (Cheng and Jones 2017). Tween was used to minimize ZNP aggregation during complexation with CGN, because in previous studies, surfactants have been found to improve the stability of ZNP encapsulating lutein (Chuacharoen and Sabliov 2016a). As expected, addition of CGN and tween stabilized the ZNP and made them resistant to aggregation when the pH was raised near the

protein's isoelectric point. The resulting films had no visible aggregates or zones, and the film remained relatively translucent indicating a better ZNP distribution (Figure 23). The transparency of a colloidal dispersions is generally dictated by its particle size and its ability to scatter light (Finsy 1994). The clarity of films or hydrogels is generally dictated by the uniformity of the polymer (Haraguchi 2007). In nanocomposite films, greater degree of exfoliation of nanoparticles, an even distribution through the continuous phase, resulted in greater optical transmission (Petersson and Oksman 2006). The increased opacity of films dried at room temperature indicates poor dispersion of ZNPs and larger particle size.

There are many factors that affect a film's properties during the drying process such as temperature, airflow, differences in relative humidity, and the composition of the solvent casting solution. In nanocomposite films, the affinity of the nanoparticle to polymer of the continuous phase was a significant factor for nanoparticle aggregation during the drying process (Kim and others 2016). It was found that when the nanoparticle has poor affinity for the continuous phase, a greater degree of aggregation as observed, which was attributed to greater amounts of depletion forces. Zein is a hydrophobic protein that is poorly soluble in water while MC is highly hydrophilic. There is likely low affinity between these two polymers which would cause aggregation during the drying process. However, at 48°C, the secondary structure of zein does change, which may expose more hydrophilic zones on the polypeptide. This may improve its affinity for MC and improve its dispersibility (Cabra and others 2006).

4.4.3 Mechanical Properties of ZNP/MC Composite Films

The drying temperature of MC films alone had no significant effect on their tensile strength and elongation (Figure 26). The addition of ZNP into MC films did significantly increase the young's modulus of the films by about 25% (Appendix 2), which match previous findings (Gilbert and others 2018). However, there was no difference in tensile strength and elongation. Both the pH of the casting solution and the drying temperature had a significant effect on the mechanical properties of ZNP/MC composite films. ZNP/MC composite films dried at room temperature had a significantly lower ultimate tensile strength that was ~20-30 MPa lower than films dried at 48°C (Figure 26). They were also about 0.04 mm/mm lower in elongation until break.

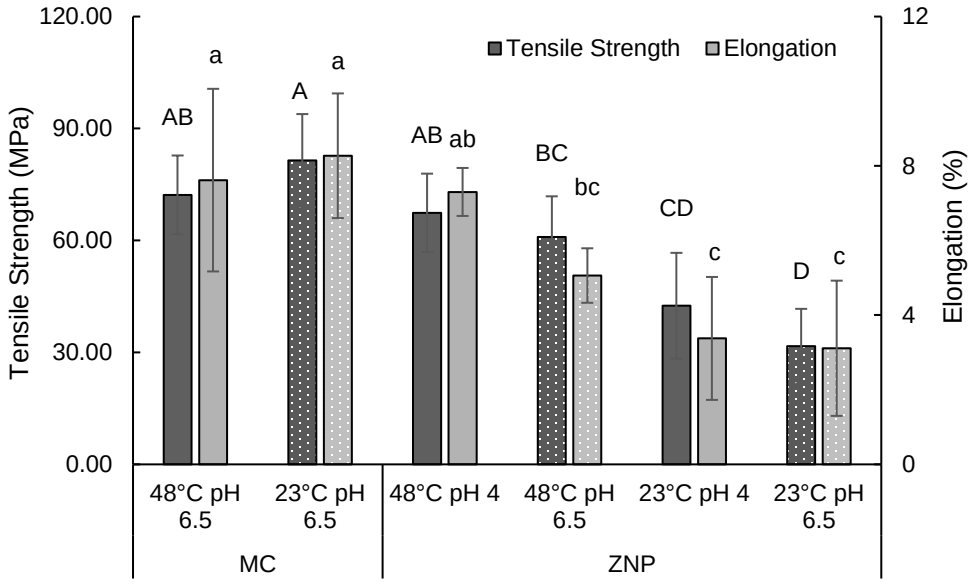

Figure 26. The Effect of Drying Temperature on Mechanical Properties of Zein/MC Composite Films

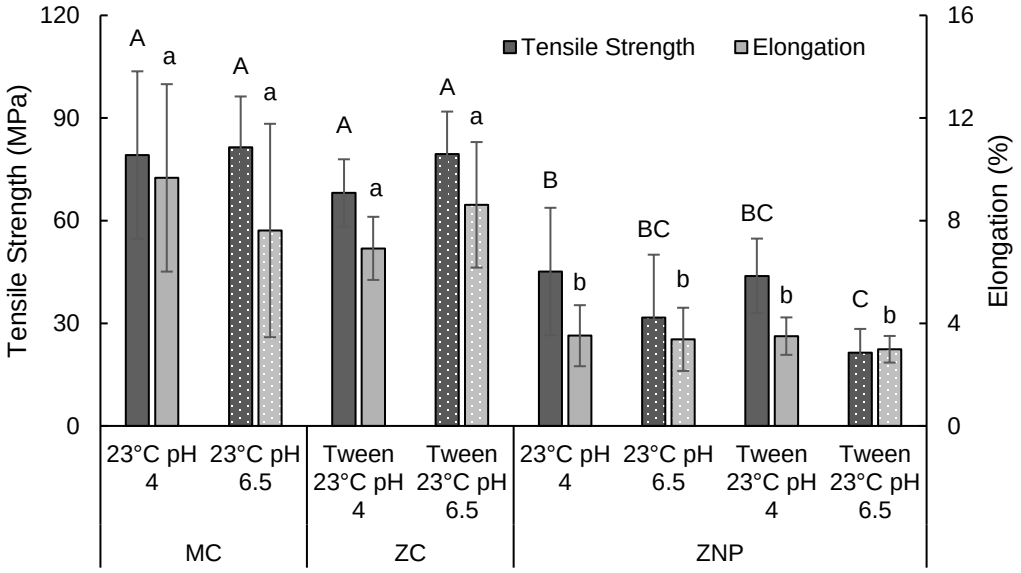

Figure 27. The Effect of CGN on Mechanical Properties of Zein/MC Composite Films

The pH of the casting solutions of MC films without ZNP had no significant effect on mechanical properties. When composite films were dried at room temperature, the addition of ZNP to MC films significantly decreased the elongation and the tensile strength of the composite film at both pH 4 and pH 6.5 regardless of the presence of tween. The addition of CGN was able to restore both the elongation and tensile strength of ZNP composite films to match those of MC

films at both tested pH values. However, only films with CGN at pH 6.5 had a higher young's modulus than the ZNP film with tween at pH 6.5 (Appendix 2). Overall, there were no differences in films at different pH levels, and it appears that the drying temperature was the major factor that affected mechanical properties for composite films.

In regards to previous studies, the effect of drying temperature has a different effect on mechanical properties of biopolymer films depending on the choice of molecule used. High temperature drying was determined to increase the tensile strength of whey protein isolate films while decreasing the elongation (Alcantara and others 1998). However, oven drying chitosan films at 80°C decreased its elongation and tensile strength compared to films dried at ambient temperatures which was attributed to over-drying of the films (Srinivasa and others 2004).

It is commonly thought that well dispersed nanoparticles in nanocomposite films results in better mechanical and water barrier properties. For nanocomposites containing clay nanoparticles, the dispersion of the nanoparticle through the continuous phase can result in changes in the film's mechanical and water barrier properties. Exfoliated nanocomposites where the nanoparticle is well dispersed in the continuous phase are believed to lead to the greatest improvements in functionality (Rhim and Ng 2007). However, unexpectedly, in this study destabilizing ZNPs by raising the pH appeared to not have a significant impact on mechanical properties whereas drying temperature was the significant factor.

When looking at films without ZNPs, heating during the drying process had no effect on the mechanical strength. Previous work has found that MC film casting solutions dried at higher temperatures exhibited more crystalline structure, but there was also no significant difference in mechanical strength for films dried at different temperatures (Donhowe 1977). Any differences in tensile strength and elongation were probably due to changes in ZNP and their dispersibility. MC is a carbohydrate that exhibits thermo-gelling properties. Upon heating to 41°C, a thermo-reversible gel forms (Li and others 2001). The increased viscosity of the heated MC could allow for greater stability of ZNPs by slowing their movement in the continuous phase and preventing them from settling to the bottom of the casting plate as predicted by the Stokes-Einstein equation.

It is expected that zein heated to 48°C will not be completely denatured. In previous studies heating zein to 50°C showed minor changes in the protein's secondary structure (Cabra and others 2006). However, previous work indicates higher temperatures were needed to completely denature zein. One study heated zein to 70°C for 15 min and determined the primary structure of zein was

altered (Selling and others 2007). Another study learned that when the zein/ethanol solution was heated up to 95°C for 15 minutes then formed into ZNPs through the antisolvent precipitation method, the alpha helix and beta sheet content of the protein increased with a decrease in random coils. Zein only began to denature with a greater formation of random coils when the heating time increased to 30 min (Sun and others 2016). It is possible that any changes in secondary structure of zein improved its affinity for the MC in the continuous phase thus reducing its aggregation state and improving mechanical properties.

Nanoparticles are thought to improve mechanical strength of composite films when any exterior stress on the film transfers efficiently from the matrix to the nanoparticle (Fu and others 2008). There are two theories on how particles reinforce the surrounding matrix: coupling and particle jamming. For coupling, the nanoparticles are thought to fill gaps between the polymer matrix and reduce mobility. In particle jamming, the particles are thought to interact with each other to form a reinforcing structure (Hassanabadi and Rodrigue 2014). The particle size, interfacial adhesion of the particle and matrix, and loading of the particle are all factors that affect mechanical properties of composite films (Fu and others 2008).

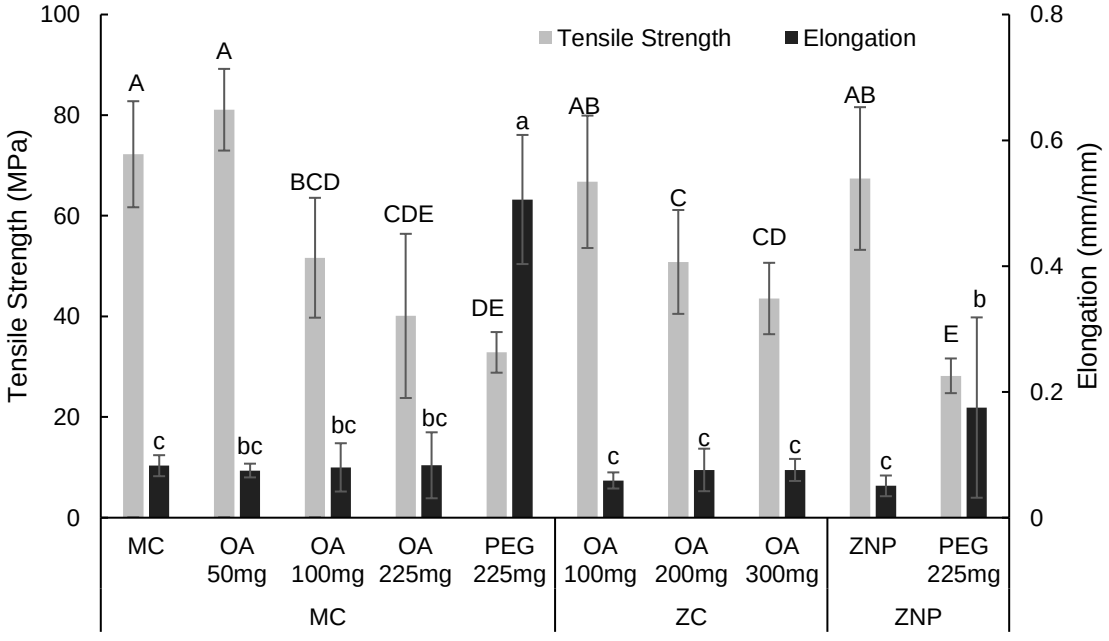

Figure 28. Effect of Polyethylene Glycol (PEG) and Oleic Acid (OA) on ZNP/MC Film Mechanical Properties

In previous studies, addition of ZNP into MC films did significantly increase the tensile strength at the cost of elongation, so plasticizers were tested on to see if they would improve elasticity (Gilbert and others 2018). Addition of PEG significantly increased the elongation of films with and without ZNP. It consequently also decreased the tensile strength of these films, as well (Figure 28). Plasticizers associate with polymers in a film, which would prevent tight binding between chains and allow for greater molecular mobility (Vieira and others 2011). When OA was incorporated into MC films with ZNP, CGN was needed to stabilize ZNP and prevent aggregation during the drying process. OA did not significantly affect the elongation of MC films regardless of the presence of ZNP. Higher concentrations (100-200 mg) of OA did significantly decrease the tensile strength of MC films as well as MC/ZNP films with CGN (Figure 28). Since the tensile strength and elongation were not significantly different from MC control films with OA, it was concluded that the surface-active properties of OA failed to change the contribution of ZNP to the MC matrix, as well.

PEG is known to be an effective plasticizer of MC films. It has been found that addition of 30% PEG 400 into a MC increased elongation from ~1% to ~7% while decreasing tensile strength from ~22 MPa to ~10 MPa (Debeaufort and Voilley 1997). Oleic acid did effectively plasticize hydroxypropyl-methylcellulose by increasing elongation from 7% to 14% and decreasing tensile strength from 255 to 168 MPa (Jiménez and others 2010). Similarly, both OA and PEG have also been shown to be effective plasticizers for zein films (Xu and others 2012; Lawton 2002). The ineffectiveness of OA is likely due to its uneven distribution throughout the film, which could be resolved by the use of intermediate HLB surfactants in the films. Hydrophobic oleic acid also has a low affinity for MC which is water soluble, thus the casting solution underwent phase separation. Conversely, PEG is water soluble which ensured even distribution throughout the film and effective plasticization.

4.4.4 Water Vapor Permeability (WVP) of ZNP/MC Composite Films

The pH and drying conditions of the solvent casting solutions have significant effects on the WVP of dried films. There were no significant differences in WVP of MC films without ZNP when the pH and drying temperature were altered (Figure 29). Films containing ZNP dried at 48°C had significantly lower WVP than those dried at 23°C. When films were dried at 23°C, pH 6.5 films were more permeable than those cast at pH 4. Both setting the pH to 6.5 and drying at 23°C appeared to aggregate ZNPs (Figure 29) which results in large channels of pure MC formed

that easily allows moisture to directly pass through. It is possible that only the combination of those aggregation conditions creates a large enough phase separation that significant differences in WVP exist. Whey protein isolate films dried at higher rates had significantly lower WVP than those dried at room temperature (Alcantara and others 1998). This was attributed to the change in film morphology.

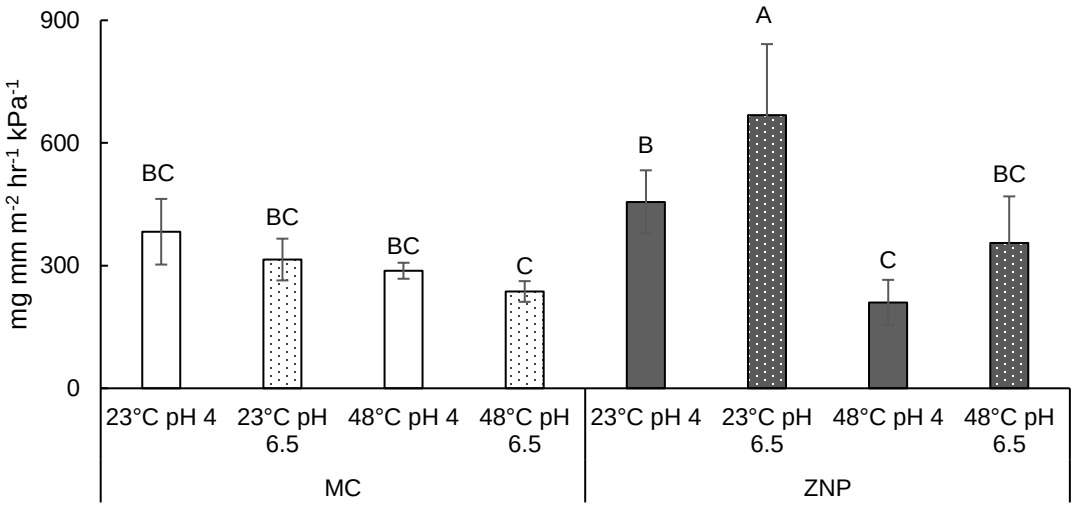

Figure 29. The Effect of Drying Temperature on WVP (mg mm m^{-2} hr^{-1} kPa^{-1}) of Zein/MC Composite Films at 70% RH

When testing the effect of CGN, all films were dried at room temperature to prevent cracking of the film during the drying process. Tween and pH of the film had no effect on the WVP of MC films without ZNP. Films containing only ZNP and tween at pH 6.5 had a significantly higher WVP at all three RH levels (Figure 30). Addition of CGN or setting the pH to 4 decreased the WVP of the films to match those of MC alone indicating CGN is able to improve the pH stability of ZNP and thus its WVP.

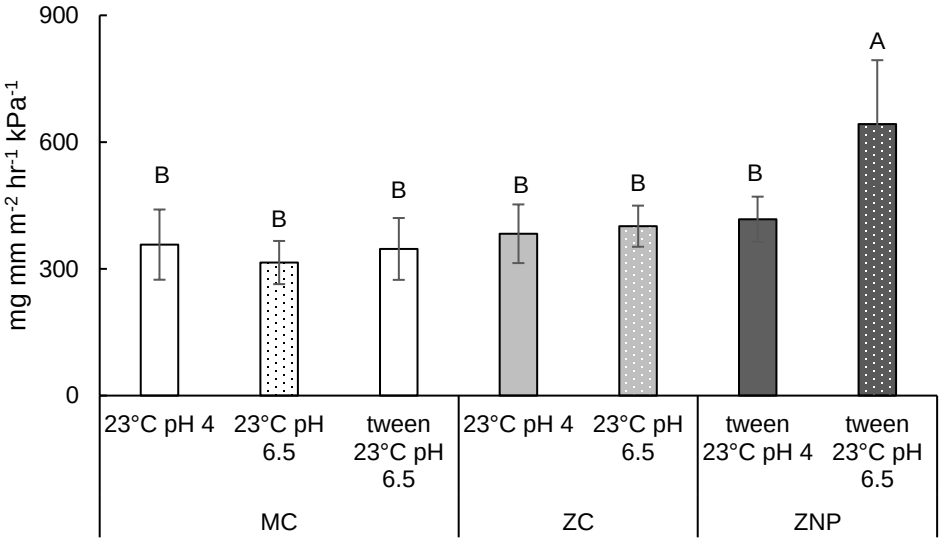

Figure 30. The Effect of CGN and pH on WVP (mg mm m-2 hr-1 kPa-1) of Zein/MC Composite Films at 70% RH

In addition to the ability of water to diffuse through a film, the WVP is also affected by the sorption of moisture on the surface of the film (Harnkarnsujarit 2017). The contact angle of a sessile drop of water on the films was measured to determine the surface hydrophilicity of ZNP/MC composite films. MC films free of ZNP had contact angles <60°, whereas addition of ZNP increased the contact angle to ~80°. It was found that the pH of the casting solution and the drying temperature had no significant impact on the films containing only MC and ZNPs. These results matched previous contact angle results of modified cellulose films containing ZNP (Gilbert and others 2018). The presence of Tween alone or with CGN significantly decreased the contact angle. CGN is a hydrophilic carbohydrate, and Tween 20 is a hydrophilic surfactant. It would be expected that incorporation of these compounds into films would result in lower contact angle.

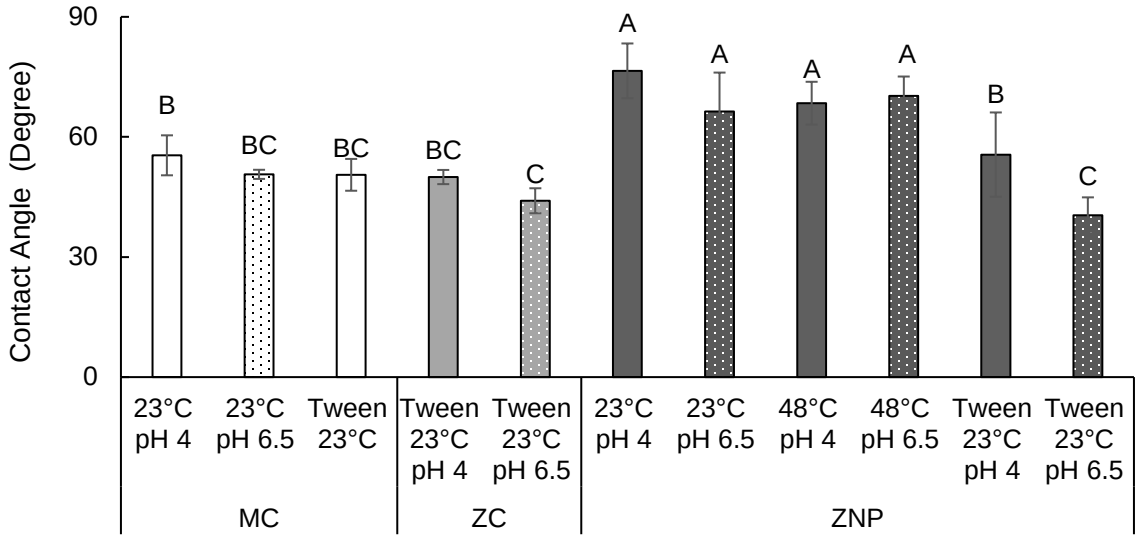

Figure 31. Contact Angle of ZNP/MC Composite Films

The surface hydrophilicity of ZNP/MC composite films does not appear to correlate well with their WVP. The chemical composition of the films dictated its hydrophilicity. Samples containing tween or CGN had lower contact angle, whereas presence of ZNP increased it. However, the presence of tween and CGN did not have a significant impact on WVP (Figure 31). Instead, it was the drying temperature and the pH of the films that were significant factors (Figure 31).

The dispersion of nanoparticles is known to be a critical factor affecting the WVP of a film. The improved barrier properties of nanocomposite films are attributed to the increased length of the tortuous path that water vapor or gas must take to traverse through the film (Honarvar and others 2016). The aggregation of ZNP caused by increasing pH or the settling of the nanoparticles at room temperature likely created large channels of MC which would allow water vapor to have a shorter direct path through the film. However, when the ZNP remained stable by increasing temperature, decreasing the pH < Pi of Zein, or adding CGN resulted in a lower WVP. The importance of particle stability can also be seen in previous work. When montmorillonite nanoparticles were incorporated into polycaprolactone films, it was found that the dispersion of the nanoparticles in addition to its concentration were both important factors influencing the WVP of the composite film (Gorrasi and others 2003). In another study, the WVP of whey protein isolate films containing lipid particles composed of beeswax, candelilla wax, and anhydrous

milkfat fraction, also decreased when the films were dried at higher temperatures. This was attributed to the increased polymer adhesion and lipid particle distribution induced by the higher temperatures (Perez-Gago and Krochta 2000).

4.5 Conclusions

In conclusion, the phase separation of composite films is detrimental to both its mechanical and moisture barrier properties. The drying temperature, pH, and composition of the solvent casting solution all affected the distribution of ZNPs dispersed in MC films. High temperature drying and low pH both improved ZNP distribution. This resulted in stronger and more elastic films as well as lower moisture permeability. The presence of CGN was also able to provide stabilize ZNPs at both pH 4 and 6.5, thus improving its mechanical and moisture barrier properties.

4.6 References

1995. Comparison of compatibilizer effectiveness for PET/HDPE blends. Polymer 36(23):4453 - 62.

1999. Physical properties of polyol-plasticized edible blends made of methyl cellulose and soluble starch. Carbohydrate Polymers 38(1):47 - 58.

Abdollahi M, Rezaei M, Farzi G. 2012. A novel active bionanocomposite film incorporating rosemary essential oil and nanoclay into chitosan. Journal of Food Engineering 111(2):343-50.

Aguirre-Alvarez G, Pimentel-Gonzalez DJ, Campos-Montiel RG, Foster T, Hill SE. 2011. The effect of drying temperature on mechanical properties of pig skin gelatin films. Cyta-Journal of Food 9(3):243-9.

Akbari Z, Ghomashchi T, Moghadam S. 2007. Improvement in Food Packaging Industry with Biobased Nanocomposites. International Journal of Food Engineering 3(4).

Alcantara CR, Rumsey TR, Krochta AM. 1998. Drying rate effect on the properties of whey protein films. Journal of Food Process Engineering 21(5):387-405.

Alves-Rodrigues A, Shao A. 2004. The science behind lutein. Toxicology Letters 150(1):57-83.

Anderson TJ, Lamsal BP. 2011. Zein Extraction from Corn, Corn Products, and Coproducts and Modifications for Various Applications: A Review. Cereal Chemistry 88(2):159-73.

Argos P, Pedersen K, Marks MD, Larkins BA. 1982. A STRUCTURAL MODEL FOR MAIZE ZEIN PROTEINS. Journal of Biological Chemistry 257(17):9984-90.

Arnal E, Miranda M, Almansa I, Muriach M, Barcia JM, Romero FJ, Diaz-Llopis M, Bosch-Morell F. 2009. Lutein prevents cataract development and progression in diabetic rats. Graefes Archive for Clinical and Experimental Ophthalmology 247(1):115-20.

Arora A, Padua GW. 2010. Review: Nanocomposites in Food Packaging. Journal of Food Science 75(1):R43-R9.

BeMiller JN, Huber KC. 2008. Chapter 3: Carbohydrates, Fourth ed. Boca Raton, FL: CRC Press.

Best JP, Cui J, Müllner M, Caruso F. 2013. Tuning the Mechanical Properties of Nanoporous Hydrogel Particles via Polymer Cross-Linking. Langmuir 29(31):9824-31.

Bilbao-Sáinz C, Avena-Bustillos RJ, Wood DF, Williams TG, McHugh TH. 2010. Composite Edible Films Based on Hydroxypropyl Methylcellulose Reinforced with Microcrystalline Cellulose Nanoparticles. Journal of Agricultural and Food Chemistry 58(6):3753-60.

Borel P, Grolier P, Armand M, Partier A, Lafont H, Lairon D, AzaisBraesco V. 1996. Carotenoids in biological emulsions: Solubility, surface-to-core distribution, and release from lipid droplets. Journal of Lipid Research 37(2):250-61.

Cabra V, Arreguin R, Vazquez-Duhalt R, Farres A. 2006. Effect of temperature and pH on the secondary structure and processes of oligomerization of 19 kDa alpha-zein. Biochimica Et Biophysica Acta-Proteins and Proteomics 1764(6):1110-8.

Campo VL, Kawano DF, da Silva DB, Carvalho I. 2009. Carrageenans: Biological properties, chemical modifications and structural analysis - A review. Carbohydrate Polymers 77(2):167-80.

Carter M, Shieh J. 2015. Chapter 5 - Microscopy.117 - 44.

Chandran S, Basu JK. 2011. Effect of nanoparticle dispersion on glass transition in thin films of polymer nanocomposites. European Physical Journal E 34(9).

Chen H, Zhong Q. 2014. Processes improving the dispersibility of spray-dried zein nanoparticles using sodium caseinate. Food Hydrocolloids 35:358-66.

Chen H, Zhong Q. 2015a. A novel method of preparing stable zein nanoparticle dispersions for encapsulation of peppermint oil. Food Hydrocolloids 43:593-602.
Chen HQ, Zhong QX. 2015b. A novel method of preparing stable zein nanoparticle dispersions for encapsulation of peppermint oil. Food Hydrocolloids 43:593-602.
Chen J, Zheng J, McClements DJ, Xiao H. 2014a. Tangeretin-loaded protein nanoparticles fabricated from zein/β-lactoglobulin: Preparation, characterization, and functional performance. Food Chemistry 158:466-72.
Chen JJ, Zheng JK, McClements DJ, Xiao H. 2014b. Tangeretin-loaded protein nanoparticles fabricated from zein/beta-lactoglobulin: Preparation, characterization, and functional performance. Food Chemistry 158:466-72.
CHEN MC, YEH GHC, CHIANG BH. 1996. Antimicrobial and physicochemical properties of methylcellulose and chitosan films containing a preservative. Journal of Food Processing and Preservation 20(5):379-90.
Chen Y, Ye R, Liu J. 2013. Understanding of dispersion and aggregation of suspensions of zein nanoparticles in aqueous alcohol solutions after thermal treatment. Industrial Crops and Products 50:764-70.
Cheng CJ, Jones OG. 2017. Stabilizing zein nanoparticle dispersions with ι-carrageenan. 69:28-35.
Chiou BS, Avena-Bustillos RJ, Bechtel PJ, Imam SH, Glenn GM, Orts WJ. 2009. Effects of drying temperature on barrier and mechanical properties of cold-water fish gelatin films. Journal of Food Engineering 95(2):327-31.
Chitchumroonchokchai C, Schwartz SJ, Failla ML. 2004. Assessment of Lutein Bioavailability from Meals and a Supplement Using Simulated Digestion and Caco-2 Human Intestinal Cells. The Journal of Nutrition 134(9):2280-6.
Chuacharoen T, Sabliov CM. 2016a. Stability and controlled release of lutein loaded in zein nanoparticles with and without lecithin and pluronic F127 surfactants. Colloids and Surfaces a-Physicochemical and Engineering Aspects 503:11-8.
Chuacharoen T, Sabliov CM. 2016b. The potential of zein nanoparticles to protect entrapped beta-carotene in the presence of milk under simulated gastrointestinal (GI) conditions. Lwt-Food Science and Technology 72:302-9.
Clogston JD, Patri AK. 2011. Zeta Potential Measurement. In: McNeil SE, editor. Characterization of Nanoparticles Intended for Drug Delivery. Totowa, NJ: Humana Press. p. 63-70.
Corradini E, Curti PS, Meniqueti AB, Martins AF, Rubira AF, Muniz EC. 2014. Recent Advances in Food-Packing, Pharmaceutical and Biomedical Applications of Zein and Zein-Based Materials. International Journal of Molecular Sciences 15(12):22438-70.
Croguennoc P, Meunier V, Durand D, Nicolai T. 2000. Characterization of Semidilute κ-Carrageenan Solutions. Macromolecules 33(20):7471-4.
Dalgleish DG, Morris ER. 1988. Interactions between carrageenans and casein micelles: electrophoretic and hydrodynamic properties of the particles. Food Hydrocolloids 2(4):311-20.
Davidov-Pardo G, Joye IJ, Espinal-Ruiz M, McClements DJ. 2015a. Effect of Maillard Conjugates on the Physical Stability of Zein Nanoparticles Prepared by Liquid Antisolvent Coprecipitation. Journal of Agricultural and Food Chemistry 63(38):8510-8.

Davidov-Pardo G, Joye IJ, McClements DJ. 2015b. Encapsulation of resveratrol in biopolymer particles produced using liquid antisolvent precipitation. Part 1: Preparation and characterization. Food Hydrocolloids 45:309-16.

Davidov-Pardo G, Perez-Ciordia S, Marin-Arroyo MR, McClements DJ. 2015c. Improving Resveratrol Bioaccessibility Using Biopolymer Nanoparticles and Complexes: Impact of Protein-Carbohydrate Maillard Conjugation. Journal of Agricultural and Food Chemistry 63(15):3915-23.

de Almeida CB, Corradini E, Forato LA, Fujihara R, Lopes JF. 2018. Microstructure and thermal and functional properties of biodegradable films produced using zein. Polimeros-Ciencia E Tecnologia 28(1):30-7.

de Moura MR, Aouada FA, Avena-Bustillos RJ, McHugh TH, Krochta JM, Mattoso LHC. 2009. Improved barrier and mechanical properties of novel hydroxypropyl methylcellulose edible films with chitosan/tripolyphosphate nanoparticles. Journal of Food Engineering 92(4):448-53.

Debeaufort F, Voilley A. 1997. Methylcellulose-based edible films and coatings: 2. Mechanical and thermal properties as a function of plasticizer content. Journal of Agricultural and food chemistry 45(3):685-9.

Delorme V, Dhouib R, Canaan S, Fotiadu F, Carriere F, Cavalier JF. 2011. Effects of Surfactants on Lipase Structure, Activity, and Inhibition. Pharmaceutical Research 28(8):1831-42.

Dickinson E. 1998. Stability and rheological implications of electrostatic milk protein-polysaccharide interactions. Trends in Food Science & Technology 9(10):347-54.

Dickinson E. 2003. Hydrocolloids at interfaces and the influence on the properties of dispersed systems. Food Hydrocolloids 17(1):25-39.

Donhowe IG, Fennema O. 1993. The effects of plasticizers on crystallinity, permeability, and mechanical properties of methylcellulose films. Journal of Food Processing and Preservation 17(4):247-57.

Donhowe IGaFO. THE EFFECTS of SOLUTION COMPOSITION and DRYING TEMPERATURE ON CRYSTALLINITY, PERMEABILITY and MECHANICAL PROPERTIES of METHYLCELLULOSE FILMS. Journal of Food Processing and Preservation 17(4):231-46.

Donhowe IGaFO. 1977. THE EFFECTS of SOLUTION COMPOSITION and DRYING TEMPERATURE ON CRYSTALLINITY, PERMEABILITY and MECHANICAL PROPERTIES of METHYLCELLULOSE FILMS. Journal of Food Processing and Preservation 17(4):231-46.

Duodu KG, Taylor JRN, Belton PS, Hamaker BR. 2003. Factors affecting sorghum protein digestibility. Journal of Cereal Science 38(2):117-31.

Escamilla-Garcia M, Calderon-Dominguez G, Chanona-Perez JJ, Farrera-Rebollo RR, Andraca-Adame JA, Arzate-Vazquez I, Mendez-Mendez JV, Moreno-Ruiz LA. 2013. Physical and structural characterisation of zein and chitosan edible films using nanotechnology tools. International Journal of Biological Macromolecules 61:196-203.

Espin JC, Garcia-Conesa MT, Tomas-Barberan FA. 2007. Nutraceuticals: Facts and fiction. Phytochemistry 68(22-24):2986-3008.

Fernandez-Garcia E, Carvajal-Lerida I, Perez-Galvez A. 2009. In vitro bioaccessibility assessment as a prediction tool of nutritional efficiency. Nutrition Research 29(11):751-60.

Finsy R. 1994. Particle sizing by quasi-elastic light scattering. Advances in Colloid and Interface Science 52:79 - 143.

Fu SY, Feng XQ, Lauke B, Mai YW. 2008. Effects of particle size, particle/matrix interface adhesion and particle loading on mechanical properties of particulate-polymer composites. Composites Part B-Engineering 39(6):933-61.

Fu TT, Abbott UR, Hatzos C. 2002. Digestibility of food allergens and nonallergenic proteins in simulated gastric fluid and simulated intestinal fluid - A comparative study. Journal of Agricultural and Food Chemistry 50(24):7154-60.

Galazka VB, Smith D, Ledward DA, Dickinson E. 1999. Complexes of bovine serum albumin with sulphated polysaccharides: effects of pH, ionic strength and high pressure treatment. Food Chemistry 64(3):303-10.

Garcia R, Proksch R. 2013. Nanomechanical mapping of soft matter by bimodal force microscopy. European Polymer Journal 49(8):1897-906.

Garrett DA, Failla ML, Sarama RJ. 1999. Development of an in vitro digestion method to assess carotenoid bioavailability from meals. Journal of Agricultural and Food Chemistry 47(10):4301-9.

Geyer R, Jambeck JR, Law KL. 2017. Production, use, and fate of all plastics ever made. Science Advances 3(7).

Gilbert J, Charnley M, Cheng C, Reynolds NP, Jones OG. 2017. Quantifying Young's moduli of protein fibrils and particles with bimodal force spectroscopy. Biointerphases 12(4).

Gilbert J, Cheng CJ, Jones OG. 2018. Vapor Barrier Properties and Mechanical Behaviors of Composite Hydroxypropyl Methylcelluose/Zein Nanoparticle Films. Food Biophysics 13(1):25-36.

Goldburg WI. 1999. Dynamic light scattering. American Journal of Physics 67(12):1152-60.

Gomez-Estaca J, Balaguer MP, Gavara R, Hernandez-Munoz P. 2012. Formation of zein nanoparticles by electrohydrodynamic atomization: Effect of the main processing variables and suitability for encapsulating the food coloring and active ingredient curcumin. Food Hydrocolloids 28(1):82-91.

Gorrasi G, Tortora M, Vittoria V, Pollet E, Lepoittevin B, Alexandre M, Dubois P. 2003. Vapor barrier properties of polycaprolactone montmorillonite nanocomposites: effect of clay dispersion. Polymer 44(8):2271-9.

Granado F, Olmedilla B, Blanco I. 2003. Nutritional and clinical relevance of lutein in human health. British Journal of Nutrition 90(3):487-502.

Grewal R, Sweesy W, Jur JS, Willoughby J. 2012. Moisture Vapor Barrier Properties of Biopolymers for Packaging Materials. Functional Materials from Renewable Sources: American Chemical Society. p. 271-96.

Gu YS, Decker EA, McClements DJ. 2004. Influence of pH and ι-Carrageenan Concentration on Physicochemical Properties and Stability of β-Lactoglobulin-Stabilized Oil-in-Water Emulsions. Journal of Agricultural and Food Chemistry 52(11):3626-32.

Guerrier B, Bouchard C, Allain C, Benard CJAJ. 1998. Drying kinetics of polymer films. 44(4):791-8.

Hammer J, Kraak MHS, Parsons JR. 2012. Plastics in the Marine Environment: The Dark Side of a Modern Gift. Reviews of Environmental Contamination and Toxicology, Vol 220 220:1-44.

Hansen PMT. 1982. Hydrocolloid-protein interactions: relationship to stabilization of fluid milk products. A review. Progress in Food and Nutrition Science 6(1-6):127-38.

Haraguchi K. 2007. Nanocomposite hydrogels. Current Opinion in Solid State & Materials Science 11(3-4):47-54.
Harnkarnsujarit N. 2017. Glass-Transition and Non-equilibrium States of Edible Films and Barriers. Non-Equilibrium States and Glass Transitions in Foods: Processing Effects and Product-Specific Implications:349-77.
Hassanabadi HM, Rodrigue D. 2014. Effect of Particle Size and Shape on the Reinforcing Efficiency of Nanoparticles in Polymer Nanocomposites. Macromolecular Materials and Engineering 299(10):1220-31.
He XJ, Hwang HM. 2016. Nanotechnology in food science: Functionality, applicability, and safety assessment. Journal of Food and Drug Analysis 24(4):671-81.
Hirt S, Jones OG. 2014. Effects of chloride, thiocyanate and sulphate salts on beta-lactoglobulin-pectin associative complexes. International Journal of Food Science and Technology 49(11):2391-8.
Hof KHV, West CE, Weststrate JA, Hautvast J. 2000. Dietary factors that affect the bioavailability of carotenoids. Journal of Nutrition 130(3):503-6.
Honarvar Z, Hadian Z, Mashayekh M. 2016. Nanocomposites in food packaging applications and their risk assessment for health. Electronic Physician 8(6):2531-8.
Hu D, Lin C, Liu L, Li S, Zhao Y. 2012a. Preparation, characterization, and in vitro release investigation of lutein/zein nanoparticles via solution enhanced dispersion by supercritical fluids. Journal of Food Engineering 109(3):545-52.
Hu D, Lin C, Liu L, Li S, Zhao Y. 2012b. Preparation, characterization, and in vitro release investigation of lutein/zein nanoparticles via solution enhanced dispersion by supercritical fluids. 109(3):545-52.
Hu K, Huang X, Gao Y, Huang X, Xiao H, McClements DJ. 2015. Core-shell biopolymer nanoparticle delivery systems: Synthesis and characterization of curcumin fortified zein-pectin nanoparticles. Food Chemistry 182:275-81.
Hu K, McClements DJ. 2015. Fabrication of biopolymer nanoparticles by antisolvent precipitation and electrostatic deposition: Zein-alginate core/shell nanoparticles. Food Hydrocolloids 44:101-8.
Huang XX, Huang XL, Gong YS, Xiao H, McClements DJ, Hu K. 2016. Enhancement of curcumin water dispersibility and antioxidant activity using core-shell protein-polysaccharide nanoparticles. Food Research International 87:1-9.
Hurtado-López P, Sudax M. 2006. Zein microspheres as drug/antigen carriers: A study of their degradation and erosion, in the presence and absence of enzymes. Journal of Microencapsulation 23(3):303-14.
Ikeda S, Morris VJ. 2002. Fine-Stranded and Particulate Aggregates of Heat-Denatured Whey Proteins Visualized by Atomic Force Microscopy. Biomacromolecules 3(2):382-9.
Imeson AP, Ledward DA, Mitchell JR. 1977. On the nature of the interaction between some anionic polysaccharides and proteins. Journal of the Science of Food and Agriculture 28(8):661-8.
Jalal F, Nesheim MC, Agus Z, Sanjur D, Habicht JP. 1998. Serum retinol concentrations in children are affected by food sources of beta-carotene, fat intake, and anthelmintic drug treatment. American Journal of Clinical Nutrition 68(3):623-9.
Jimenez A, Fabra MJ, Talens P, Chiralt A. 2010. Effect of lipid self-association on the microstructure and physical properties of hydroxypropyl-methylcellulose edible films containing fatty acids. Carbohydrate Polymers 82(3):585-93.

Jiménez A, Fabra MJ, Talens P, Chiralt A. 2010. Effect of lipid self-association on the microstructure and physical properties of hydroxypropyl-methylcellulose edible films containing fatty acids. Carbohydrate Polymers 82(3):585-93.
Kaiser K, Schmid M, Schlummer M. 2018. Recycling of Polymer-Based Multilayer Packaging: A Review. Recycling 3(1):1.
Kamper SL, Fennema O. 1984. Water vapor permeability of an edible, fatty acid, bilayer film. Journal of Food Science 49:1482-5.
Kanmani P, Rhim J-W. 2014. Properties and characterization of bionanocomposite films prepared with various biopolymers and ZnO nanoparticles. Carbohydrate Polymers 106:190-9.
Kean EG, Hamaker BR, Ferruzzi MG. 2008. Carotenoid Bioaccessibility from Whole Grain and Degermed Maize Meal Products. Journal of Agricultural and Food Chemistry 56(21):9918-26.
Keith MO, Bell JM. 1988. DIGESTIBILITY OF NITROGEN AND AMINO-ACIDS IN SELECTED PROTEIN-SOURCES FED TO MICE. Journal of Nutrition 118(5):561-8.
Kim S, Hyun K, Struth B, Ahn KH, Clasen C. 2016. Structural Development of Nanoparticle Dispersion during Drying in Polymer Nanocomposite Films. Macromolecules 49(23):9068-79.
Kulkarni V, Shaw C. 2016. Chapter 10 - Microscopy Techniques.183 - 92.
Lawton JW. 2002. Zein: A history of processing and use. Cereal Chemistry 79(1):1-18.
Lee SH, Hamaker BR. 2006. Cys155 of 27 kDa maize gamma-zein is a key amino acid to improve its in vitro digestibility. Febs Letters 580(25):5803-6.
Li KK, Yin SW, Yang XQ, Tang CH, Wei ZH. 2012a. Fabrication and Characterization of Novel Antimicrobial Films Derived from Thymol-Loaded Zein-Sodium Caseinate (SC) Nanoparticles. Journal of Agricultural and Food Chemistry 60(46):11592-600.
Li L, Thangamathesvaran PM, Yue CY, Tam KC, Hu X, Lam YC. 2001. Gel network structure of methylcellulose in water. Langmuir 17(26):8062-8.
Li YQ, Li J, Xia QY, Zhang B, Wang Q, Huang QR. 2012b. Understanding the Dissolution of alpha-Zein in Aqueous Ethanol and Acetic Acid Solutions. Journal of Physical Chemistry B 116(39):12057-64.
Liang H, Zhou B, He L, An Y, Lin L, Li Y, Liu S, Chen Y, Li B. 2015. Fabrication of zein/quaternized chitosan nanoparticles for the encapsulation and protection of curcumin. Rsc Advances 5(18):13891-900.
Liang Y, Hilal N, Langston P, Starov V. 2007. Interaction forces between colloidal particles in liquid: Theory and experiment. Advances in Colloid and Interface Science 134-35:151-66.
Lin CH, Chen BH. 2005. Stability of carotenoids in tomato juice during storage. Food Chemistry 90(4):837-46.
Livney YD. 2010. Milk proteins as vehicles for bioactives. Current Opinion in Colloid & Interface Science 15(1):73-83.
Luo YC, Teng Z, Wang Q. 2012. Development of Zein Nanoparticles Coated with Carboxymethyl Chitosn for Encapsulation and Controlled Release of Vitamin D3. Journal of Agricultural and Food Chemistry 60(3):836-43.
Madeka H, Kokini JL. 1996. Effect of glass transition and cross-linking on rheological properties of zein: Development of a preliminary state diagram. Cereal Chemistry 73(4):433-8.

Maftoonazad N, Ramaswamy HS, Marcotte M. 2008. Shelf- life extension of peaches through sodium alginate and methyl cellulose edible coatings. International journal of food science & technology 43(6):951-7.

Maiani G, Caston MJP, Catasta G, Toti E, Cambrodon IG, Bysted A, Granado-Lorencio F, Olmedilla-Alonso B, Knuthsen P, Valoti M, Bohm V, Mayer-Miebach E, Behsnilian D, Schlemmer U. 2009. Carotenoids: Actual knowledge on food sources, intakes, stability and bioavailability and their protective role in humans. Molecular Nutrition & Food Research 53:S194-S218.

Mariana Altenhofen da Silva and Andréa Cristiane Krause Bierhalz and Theo Guenter K. Influence of Drying Conditions on Physical Properties of Alginate Films. Drying Technology 30(1):72-9.

Matalanis A, Jones OG, McClements DJ. 2011. Structured biopolymer-based delivery systems for encapsulation, protection, and release of lipophilic compounds. Food Hydrocolloids 25(8):1865-80.

Matthews L, Kunkel J, Action A, Ogale, Dawson P. 2011. Bioavailability of Soy Protein and Corn Zein Films. Food and Nutrition Sciences. p. 1105-13.

McClements DJ, Decker EA, Park Y, Weiss J. 2009. Structural Design Principles for Delivery of Bioactive Components in Nutraceuticals and Functional Foods. Critical Reviews in Food Science and Nutrition 49(6):577-606.

McHugh TH, Avena-Bustillos R, Krochta JM. 1993. Hydrophilic edible films: Modified procedure for water vapor permeability and explanation of thickness effects. Journal of Food Science 58(4):899-903.

Minekus M, Alminger M, Alvito P, Ballance S, Bohn T, Bourlieu C, Carriere F, Boutrou R, Corredig M, Dupont D, Dufour C, Egger L, Golding M, Karakaya S, Kirkhus B, Le Feunteun S, Lesmes U, Macierzanka A, Mackie A, Marze S, McClements DJ, Menard O, Recio I, Santos CN, Singh RP, Vegarud GE, Wickham MSJ, Weitschies W, Brodkorb A. 2014. A standardised static in vitro digestion method suitable for food - an international consensus. Food & Function 5(6):1113-24.

Moller H, Grelier S, Pardon P, Coma V. 2004. Antimicrobial and physicochemical properties of chitosan-HPMC based films. Journal of Agriculture and Food Chemistry 52:6585-91.

Mutsokoti L, Panozzo A, Pallares AP, Jaiswal S, Van Loey A, Grauwet T, Hendrickx M. 2017. Carotenoid bioaccessibility and the relation to lipid digestion: A kinetic study. Food Chemistry 232:124-34.

Nagao A, Kotake-Nara E, Hase M. 2013. Effects of Fats and Oils on the Bioaccessibility of Carotenoids and Vitamin E in Vegetables. Bioscience, Biotechnology, and Biochemistry 77(5):1055-60.

Navarro-Tarazaga ML, Sothornvit R, Perez-Gago MB. 2008. Effect of Plasticizer Type and Amount on Hydroxypropyl Methylcellulose-Beeswax Edible Film Properties and Postharvest Quality of Coated Plums (Cv. Angeleno). Journal of Agricultural and Food Chemistry 56(20):9502-9.

Facts About Age-Related Macular Degeneration. National Eye Institute; 2015 [Accessed 2017 November 2] Available from: https://nei.nih.gov/health/maculardegen.

Oliver WC, Pharr GM. 1992. An improved technique for determining hardness and elastic modulus using load and displacement sensing indentation experiments. Journal of Materials Research 7(6):1564-83.

Othman SH. 2014. Bio-nanocomposite Materials for Food Packaging Applications: Types of Biopolymer and Nano-sized Filler. 2nd International Conference on Agricultural and Food Engineering (Cafe 2014) - New Trends Forward 2:296-303.
Oymaci P, Altinkaya SA. 2016. Improvement of barrier and mechanical properties of whey protein isolate based food packaging films by incorporation of zein nanoparticles as a novel bionanocomposite. Food Hydrocolloids 54:1-9.
Park C-E, Park D-J, Kim B-K. 2015. Effects of a chitosan coating on properties of retinol-encapsulated zein nanoparticles. Food Science and Biotechnology 24(5):1725-33.
Park JM, Muhoberac BB, Dubin PL, Xia JL. 1992. Effects of Protein Charge Heterogeneity in Protein-Polyelectrolyte Complexation. Macromolecules 25(1):290-5.
Park JW, Testin RF, Park HJ, Vergano PJ, Weller CL. 1994. FATTY-ACID CONCENTRATION-EFFECT ON TENSILE-STRENGTH, ELONGATION, AND WATER-VAPOR PERMEABILITY OF LAMINATED EDIBLE FILMS. Journal of Food Science 59(4):916-9.
Patel A, Hu Y, Tiwari JK, Velikov KP. 2010a. Synthesis and characterisation of zein-curcumin colloidal particles. Soft Matter 6(24):6192-9.
Patel AR, Bouwens ECM, Velikov KP. 2010b. Sodium Caseinate Stabilized Zein Colloidal Particles. Journal of Agricultural and Food Chemistry 58(23):12497-503.
Patel AR, Velikov KP. 2014a. Zein as a source of functional colloidal nano- and microstructures. Current Opinion in Colloid & Interface Science 19(5):450-8.
Patel AR, Velikov KP. 2014b. Zein as a source of functional colloidal nano- and microstructures. Current Opinion in Colloid & Interface Science 19(5):450-8.
Paulis JW. 1981. DISULFIDE STRUCTURES OF ZEIN PROTEINS FROM CORN ENDOSPERM. Cereal Chemistry 58(6):542-6.
Pepi Hurtado-López and Sudax M. Zein microspheres as drug/antigen carriers: A study of their degradation and erosion, in the presence and absence of enzymes. Journal of Microencapsulation 23(3):303-14.
Peressini D, Bravin B, Lapasin R, Rizzotti C, Sensidoni A. 2003. Starch–methylcellulose based edible films: rheological properties of film-forming dispersions. Journal of Food Engineering 59(1):25-32.
Perez-Gago MB, Krochta JM. 2000. Drying temperature effect on water vapor permeability and mechanical properties of whey protein-lipid emulsion films. Journal of Agricultural and Food Chemistry 48(7):2687-92.
Persico P, Ambrogi V, Carfagna C, Cerruti P, Ferrocino I, Mauriello G. 2009. Nanocomposite polymer films containing carvacrol for antimicrobial active packaging. Polymer Engineering & Science 49(7):1447-55.
Petersson L, Oksman K. 2006. Biopolymer based nanocomposites: Comparing layered silicates and microcrystalline cellulose as nanoreinforcement. Composites Science and Technology 66(13):2187-96.
Reboul E, Richelle M, Perrot E, Desmoulins-Malezet C, Pirisi V, Borel P. 2006. Bioaccessibility of carotenoids and vitamin E from their main dietary sources. Journal of Agricultural and Food Chemistry 54(23):8749-55.
Reiners R, Pressick J, Morris L, inventors; Unilever Bestfoods North America Inc, assignee. 1972. Method of Treating Gluten. United States patent.
Rhim JW, Ng PKW. 2007. Natural biopolymer-based nanocomposite films for packaging applications. Critical Reviews in Food Science and Nutrition 47(4):411-33.

Rhim JW, Park HM, Ha CS. 2013. Bio-nanocomposites for food packaging applications. Progress in Polymer Science 38(10-11):1629-52.

Rich GT, Faulks RM, Wickham MSJ, Fillery-Travis A. 2003. Solubilization of carotenoids from carrot juice and spinach in lipid phases: II. Modeling the duodenal environment. Lipids 38(9):947-56.

Rimdusit S, Jingjid S, Damrongsakkul S, Tiptipakorn S, Takeichi T. 2008. Biodegradability and property characterizations of Methyl Cellulose: Effect of nanocompositing and chemical crosslinking. Carbohydrate Polymers 72(3):444-55.

Rugar D, Hansma P. 1990. Atomic force microscopy. Physics today 43(10):23-30.

Sader JE, Chon JWM, Mulvaney P. 1999. Calibration of rectangular atomic force microscope cantilevers. Review of Scientific Instruments 70(10):3967-9.

Salvia-Trujillo L, Qian C, Martin-Belloso O, McClements DJ. 2013. Influence of particle size on lipid digestion and beta-carotene bioaccessibility in emulsions and nanoemulsions. Food Chemistry 141(2):1472-80.

Salvia-Trujillo L, Verkempinck SHE, Sun L, Van Loey AM, Grauwet T, Hendrickx ME. 2017. Lipid digestion, micelle formation and carotenoid bioaccessibility kinetics: Influence of emulsion droplet size. Food Chemistry 229:653-62.

Sebti I, Chollet, E., Degraeve, P., Noel, C., Pyrol, E. 2007. Water sensitivity, antimicrobial, and physicochemical analysis of edible films based on HPMC and/or chitosan. Journal of Agriculture and Food Chemistry 55(3):693-9.

Sebti I, Ham-Pichavant F, Coma V. 2002. Edible bioactive fatty acid-cellulosic derivative composites used in food packaging applications. Journal of Agriculture and Food Chemistry 50:4290-4.

Sekhon BS. 2010. Food nanotechnology – an overview. Nanotechnology, Science and Applications 3:1-15.

Selling GW, Biswas A, Patel A, Walls DJ, Dunlap C, Wei Y. 2007. Impact of solvent on electrospinning of zein and analysis of resulting fibers. Macromolecular Chemistry and Physics 208(9):1002-10.

Serrano J, Goni I, Saura-Calixto F. 2005. Determination of ss-carotene and lutein available from green leafy vegetables by an in vitro digestion and colonic fermentation method. Journal of Agricultural and Food Chemistry 53(8):2936-40.

Shahidi F, Han XQ. 1993. ENCAPSULATION OF FOOD INGREDIENTS. Critical Reviews in Food Science and Nutrition 33(6):501-47.

Shi K, Kokini JL, Huang QR. 2009. Engineering Zein Films with Controlled Surface Morphology and Hydrophilicity. Journal of Agricultural and Food Chemistry 57(6):2186-92.

Shukla R, Cheryan M. 2001. Zein: the industrial protein from corn. Industrial Crops and Products 13(3):171-92.

Siracusa V, Rocculi P, Romani S, Dalla Rosa M. 2008. Biodegradable polymers for food packaging: a review. Trends in Food Science & Technology 19(12):634-43.

Slade L, Levine H. 1991. BEYOND WATER ACTIVITY - RECENT ADVANCES BASED ON AN ALTERNATIVE APPROACH TO THE ASSESSMENT OF FOOD QUALITY AND SAFETY. Critical Reviews in Food Science and Nutrition 30(2-3):115-360.

Sozer N, Kokini JL. 2009. Nanotechnology and its applications in the food sector. Trends in Biotechnology 27(2):82-9.

Srinivasa P, Ramesh M, Kumar K, Tharanathan R. 2004. Properties of chitosan films prepared under different drying conditions. Journal of Food Engineering 63(1):79 - 85.

Stahl W, Sies H. 1992. UPTAKE OF LYCOPENE AND ITS GEOMETRICAL-ISOMERS IS GREATER FROM HEAT-PROCESSED THAN FROM UNPROCESSED TOMATO JUICE IN HUMANS. Journal of Nutrition 122(11):2161-6.

Stone AK, Nickerson MT. 2012. Formation and functionality of whey protein isolate-(kappa-, iota-, and lambda-type) carrageenan electrostatic complexes. Food Hydrocolloids 27(2):271-7.

Sun CX, Dai L, He XY, Liu FG, Yuan F, Gao YX. 2016. Effect of heat treatment on physical, structural, thermal and morphological characteristics of zein in ethanol-water solution. Food Hydrocolloids 58:11-9.

Sweeney PJ, Walker JM. 1993. Enzymes of Molecular Biology: Humana Press

Tang W-W, Dong F, Wong K-H, Wang Y. 2015. Preparation, Characterization and in vitro Release of Zein-pectin Capsules for Target Delivery. Current Drug Delivery 12(4):397-405.

Tang YC, Chen BH. 2000. Pigment change of freeze-dried carotenoid powder during storage. Food Chemistry 69(1):11-7.

Tiss A, Carriere F, Verger R. 2001. Effects of gum Arabic on lipase interfacial binding and activity. Analytical Biochemistry 294(1):36-43.

Torres FG, Troncoso OP, Torres C, Diaz DA, Amaya E. 2011. Biodegradability and mechanical properties of starch films from Andean crops. International Journal of Biological Macromolecules 48(4):603-6.

Tunç S, Duman O. 2011. Preparation of active antimicrobial methyl cellulose/carvacrol/montmorillonite nanocomposite films and investigation of carvacrol release. LWT-Food Science and Technology 44(2):465-72.

Tyssandier V, Lyan B, Borel P. 2001. Main factors governing the transfer of carotenoids from emulsion lipid droplets to micelles. Biochimica Et Biophysica Acta-Molecular and Cell Biology of Lipids 1533(3):285-92.

Vieira MGA, da Silva MA, dos Santos LO, Beppu MM. 2011. Natural-based plasticizers and biopolymer films: A review. European Polymer Journal 47(3):254-63.

Vishnevetsky M, Ovadis M, Vainstein A. 1999. Carotenoid sequestration in plants: the role of carotenoid-associated proteins. Trends in Plant Science 4(6):232-5.

Wagoner T, Vardhanabhuti B, Foegeding EA. 2016. Designing Whey Protein-Polysaccharide Particles for Colloidal Stability. Annual Review of Food Science and Technology, Vol 7 7:93-116.

Wang YH, Yuan Y, Yang XQ, Wang JM, Guo J, Lin Y. 2016. Comparison of the colloidal stability, bioaccessibility and antioxidant activity of corn protein hydrolysate and sodium caseinate stabilized curcumin nanoparticles. Journal of Food Science and Technology-Mysore 53(7):2923-32.

Wu Y, Luo Y, Wang Q. 2012. Antioxidant and antimicrobial properties of essential oils encapsulated in zein nanoparticles prepared by liquid-liquid dispersion method. Lwt-Food Science and Technology 48(2):283-90.

Xu H, Chai YW, Zhang GY. 2012. Synergistic Effect of Oleic Acid and Glycerol on Zein Film Plasticization. Journal of Agricultural and Food Chemistry 60(40):10075-81.

Yi J, Li Y, Zhong F, Yokoyama W. 2014. The physicochemical stability and in vitro bioaccessibility of beta-carotene in oil-in-water sodium caseinate emulsions. Food Hydrocolloids 35:19-27.

Yonekura L, Nagao A. 2007. Intestinal absorption of dietary carotenoids. Molecular Nutrition & Food Research 51(1):107-15.

Zhang YQ, Niu YG, Luo YC, Ge M, Yang T, Yu LL, Wang Q. 2014. Fabrication, characterization and antimicrobial activities of thymol-loaded zein nanoparticles stabilized by sodium caseinate-chitosan hydrochloride double layers. Food Chemistry 142:269-75.

Zhang ZH, Han Z, Zeng XA, Xiong XY, Liu YJ. 2015. Enhancing mechanical properties of chitosan films via modification with vanillin. International Journal of Biological Macromolecules 81:638-43.

Zhong QX, Jin MF. 2009. Zein nanoparticles produced by liquid-liquid dispersion. Food Hydrocolloids 23(8):2380-7.

Zou LQ, Zhang ZP, Zhang RJ, Liu W, Liu CM, Xiao H, McClements DJ. 2016a. Encapsulation of protein nanoparticles within alginate microparticles: Impact of pH and ionic strength on functional performance. Journal of Food Engineering 178:81-9.

Zou LQ, Zheng BJ, Zhang RJ, Zhang ZP, Liu W, Liu CM, Xiao H, McClements DJ. 2016b. Enhancing the bioaccessibility of hydrophobic bioactive agents using mixed colloidal dispersions: Curcumin-loaded zein nanoparticles plus digestible lipid nanoparticles. Food Research International 81:74-82.

Zou LQ, Zheng BJ, Zhang RJ, Zhang ZP, Liu W, Liu CM, Xiao H, McClements DJ. 2016c. Food-grade nanoparticles for encapsulation, protection and delivery of curcumin: comparison of lipid, protein, and phospholipid nanoparticles under simulated gastrointestinal conditions. Rsc Advances 6(4):3126-36.

Zou Y, Zhong JJ, Pan RT, Wan ZL, Guo J, Wang JM, Yin SW, Yang XQ. 2017. Zein/tannic acid complex nanoparticles-stabilised emulsion as a novel delivery system for controlled release of curcumin. International Journal of Food Science and Technology 52(5):1221-8.

4.7 Appendix 1

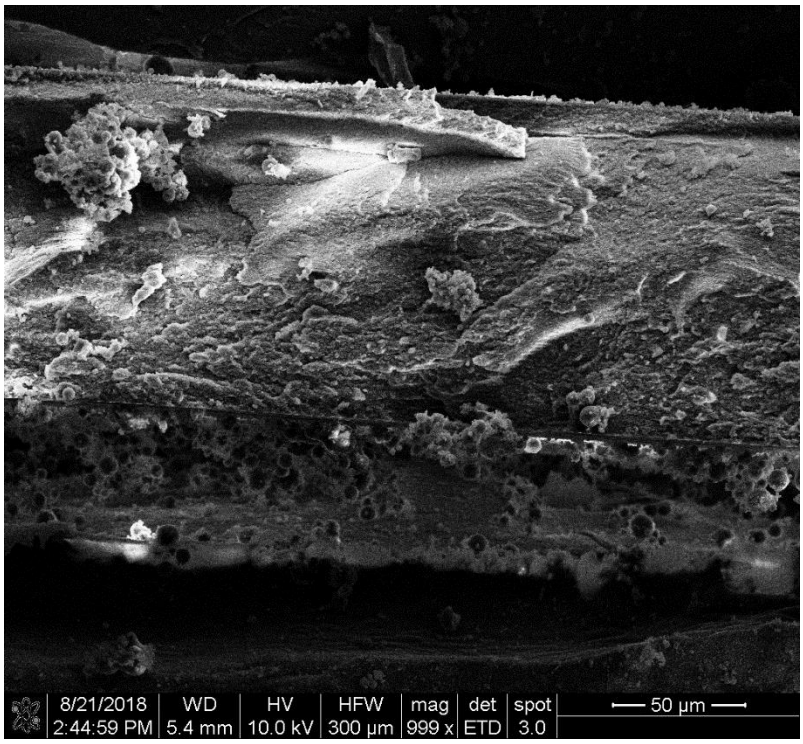

Cryo SEM Cross Section of ZNP/MC Composite Film with CGN and Tween

4.8 Appendix 2

The Effect of Carrageenan on Mechanical Properties of Zein/MC Composite Films

	Tensile Strength (MPa)	Elongation (mm/mm)	Young's Modulus (MPa)
MC 23°C pH 4	79.20 ± 24.46 ^{A}	0.097 ± 0.037 ^{A}	1,792.61 ± 355.10 ^{AB}
MC 23°C pH 6.5	81.45 ± 14.86 ^{A}	0.076 ± 0.042 ^{A}	1,872.11 ± 417.79 ^{A}
ZC Tween 23°C pH 4	68.11 ± 9.83 ^{A}	0.069 ± 0.012 ^{A}	1,446.44 ± 92.72 ^{BC}
ZC Tween 23°C pH 6.5	79.46 ± 12.42 ^{A}	0.086 ± 0.024 ^{A}	1,576.01 ± 373.18 ^{AB}
ZNP 23°C pH 4	45.14 ± 18.62 ^{B}	0.035 ± 0.012 ^{B}	1,386.97 ± 429.16 ^{BC}
ZNP 23°C pH 6.5	31.68 ± 18.38 ^{BC}	0.034 ± 0.012 ^{B}	1,046.37 ± 271.17 ^{CD}
ZNP Tween 23°C pH 4	43.86 ± 10.90 ^{BC}	0.035 ± 0.007 ^{B}	1,308.11 ± 261.61 ^{C}
ZNP Tween 23°C pH 6.5	21.41 ± 6.94 ^{C}	0.030 ± 0.005 ^{B}	757.97 ± 233.32 ^{D}

The Effect of Drying Temperature on Mechanical Properties of Zein/MC Composite Films

	Tensile Strength (MPa)	Elongation (mm/mm)	Young's Modulus (MPa)
MC 48°C pH 6.5	72.23 ± 10.54 ^{A}	0.083 ± 0.017 ^{A}	1,487.21 ± 328.26 ^{B}
ZNP 23°C pH 4	42.50 ± 14.18 ^{B}	0.031 ± 0.018 ^{C}	1,426.07 ± 261.61 ^{B}
ZNP 23°C pH 6.5	31.68 ± 10.00 ^{B}	0.034 ± 0.016 ^{BC}	1,046.37 ± 212.10 ^{B}
ZNP 48°C pH 4	67.41 ± 10.50 ^{A}	0.051 ± 0.007 ^{B}	2,047.62 ± 278.73 ^{A}
ZNP 48°C pH 6.5	60.93 ± 10.90 ^{A}	0.073 ± 0.006 ^{A}	1,410.48 ± 546.36 ^{B}

4.9 Appendix 3

The Effect of Drying Temperature on WVP (mg mm m^{-2} hr^{-1} $kPa^{-}1$) of Zein/MC Composite Films

	50% RH	70% RH	90% RH
MC 23°C pH 4	128.78 ± 27.22 ^{BC}	382.86 ± 80.28 ^{BC}	1,099.72 ± 291.13 ^{C}
MC 48°C pH 4	92.47 ± 7.69 ^{BC}	287.47 ± 19.56 ^{BC}	1,036.48 ± 244.18 ^{B}
MC 23°C pH 6.5	104.03 ± 15.54 ^{BC}	314.89 ± 51.08 ^{BC}	1,010.08 ± 84.74 ^{B}
MC 48°C pH 6.5	77.08 ± 7.40 ^{C}	236.77 ± 25.34 ^{C}	843.80 ± 93.40 ^{BC}
ZNP 23°C pH 4	144.90 ± 25.08 ^{B}	455.67 ± 77.50 ^{B}	1,455.14 ± 151.03 ^{BC}
ZNP 48°C pH 4	66.47 ± 16.27 ^{C}	209.98 ± 55.25 ^{C}	786.49 ± 135.25 ^{BC}
ZNP 23°C pH 6.5	218.57 ± 58.62 ^{A}	668.05 ± 173.71 ^{A}	2,070.34 ± 371.47 ^{C}
ZNP pH 6.5 48°C	108.36 ± 34.39 ^{BC}	355.44 ± 113.92 ^{BC}	1,302.69 ± 284.93 ^{A}

The Effect of Carrageenan and pH on WVP (mg mm m^{-2} hr^{-1} $kPa^{-}1$) of Zein/MC Composite Films

	50 RH	70 RH	90 RH
MC 23°C pH 4	119.86 ± 28.50 ^{B}	357.31 ± 83.11 ^{B}	1,078.85 ± 236.36 ^{B}
MC 23°C pH 6.5	104.03 ± 15.54 ^{B}	314.89 ± 51.08 ^{B}	1,010.08 ± 244.18 ^{B}
MC Tween 23°C pH 6.5	115.13 ± 24.57 ^{B}	347.08 ± 73.19 ^{B}	1,046.81 ± 160.51 ^{B}
ZC Tween 23°C pH 4	117.74 ± 19.43 ^{B}	383.05 ± 69.41 ^{B}	1,337.49 ± 174.52 ^{B}
ZC Tween 23°C pH 6.5	124.40 ± 16.52 ^{B}	400.95 ± 48.69 ^{B}	1,328.46 ± 148.72 ^{B}
ZNP Tween 23°C pH 4	136.54 ± 17.86 ^{B}	417.37 ± 53.45 ^{B}	1,342.50 ± 111.56 ^{B}
ZNP Tween 23°C pH 6.5	205.48 ± 43.85 ^{A}	642.63 ± 151.19 ^{A}	2,001.90 ± 293.61 ^{A}

CHAPTER 5 CONCLUSIONS AND FUTURE WORK

When stabilizing ZNPs in aqueous dispersions, ι-CGN has been shown to be an effective stabilizer for ZNPs by coating the protein with an anionic outer layer. When a sufficient amount of ι-CGN is used, determined here to be at a ZNP:ι-CGN weight ratio of 10 or less, the hydrodynamic radius and dispersion turbidity of the stabilized particles remained consistent for up to 30 days. Addition of ι-CGN had no effect on elasticity of nanoparticles, but it was able to improve the resistance of ZNPs to aggregation from changes in pH and to sedimentation. Before CGN can be used as a viable stabilizer for ZNPs, future work must be done to improve yield when making the nanoparticles. There must also be more work on bringing these stabilizing effects to systems of higher nanoparticle concentration. Finally, further studies are warranted on the stability of ι-CGN-stabilized-ZNPs to high ionic strength media. Successful stabilization of these ZNPs will provide more conditions for their utility as potential encapsulating agents of bioactive compounds, adding value to these processed-corn byproducts.

Encapsulation of lutein into ZNPs was found to improve its digestive stability but reduced micellarization efficiency. The ion concentration relevant to physiological conditions caused ZNP to aggregate into relatively enzyme-inaccessible clusters during the simulated gastric conditions, so a significant fraction of ZNPs was not digested. All ZNP, including such aggregated clusters, were completely digested into shorter peptides in the simulated intestinal conditions, likely because the added bile salts, pancreatin, and lipase assisted the redispersion of ZNPs into the aqueous phase. Lutein was potentially protected within the ZNPs during the gastric phase because of the limited ZNP digestion, explaining the increased digestive stability. However, complete digestion of ZNP during the intestinal phase meant that the original capsule structure was lost. Decreased micellarization efficiency of lutein could then be attributed to favorable association between digested ZNP peptides and lutein, bile salts, or lipid components. The potential interactivity between zein-based peptides and these components needs to be investigated in future studies. Improvement in the micellarization efficiency and associated bioaccessibility of carotenoids entrapped in ZNPs must first be developed in order to utilize it as a delivery vehicle for hydrophobic bioactive compounds.

ZNPs have been found to improve the mechanical and moisture barrier properties of MC composite films. However, the phase separation of composite films is detrimental to both its

mechanical and moisture barrier properties. The drying temperature, pH, and composition of the solvent casting solution all affected the distribution of ZNPs dispersed in MC films. High temperature drying and low pH both improved ZNP distribution. This resulted in stronger and more elastic films as well as lower moisture permeability. The presence of CGN was also able to provide stabilize ZNPs at both pH 4 and 6.5, thus improving its mechanical and moisture barrier properties. There are many potential future steps in further improving the functional properties of this material. Further chemical modifications into nanoparticles such as cross-linking could improve mechanical strength of films. Different ZNP stabilizing agents could also be tested to improve affinity between the nanoparticle and the continuous phase.

Zein nanoparticles have many potential exciting applications for the food industry once a stabile colloidal dispersion is incorporating ZNPs are developed. As a hydrophobic prolamin, it would be an excellent candidate as an encapsulating agent for hydrophobic bioactive compounds such as carotenoids, flavors, or antimicrobials. ZNPs would also be a good encapsulating agent for functional or bioactive compounds such as. It can effectively allow for easy dispersion in water while controlling their release into the digestive system once consumed. ZNPs can then improve the stability or target the delivery of the functional ingredient. There is also potential to incorporate them into solvent cast packaging material to make nanocomposites. Nanocomposite materials can be stronger, have better barrier properties, or have active properties like deliver antimicrobials. However, there are many future challenges that must be overcome before commercializing zein for any of these applications.